The effect of hydrological events on stream nitrate dynamics at the catchment scale

Dissertation

vorgelegt von
Felipe Saavedra Melendez
aus

von der Naturwissenschaftlichen Fakultät III
der Martin-Luther-Universität Halle-Wittenberg
zur Erlangung des Akademischen Grades

Doktorgrades der Naturwissenschaften
-Dr. rer. nat.

Halle (Saale) 2025

1. Gutachter:	Prof. Ralf Merz
2. Gutachter:	Dr. Julia Knapp
Tag der Verteidigung:	10.12.2025

Zusammenfassung

Eine hohe Nitratbelastung in Gewässern stellt weltweit ein großes Problem dar und beeinträchtigt sowohl die Gesundheit aquatischer Ökosysteme als auch die Wasserversorgung für den Menschen. Um die Wasserqualität zu verbessern, ist ein besseres Verständnis der Nitratdynamik in Einzugsgebieten erforderlich. Trotz erheblicher Forschungsanstrengungen ist die Rolle hydrologischer Ereignisse für die Nitratdynamik über mehrere Einzugsgebiete hinweg bislang nicht vollständig geklärt. Ziel dieser Dissertation ist es daher, die Rolle hydrologischer Ereignisse für die Mobilisierung und den Transport von Nitrat, von der Quelle bis zum Fließgewässernetz, über eine große Anzahl von Einzugsgebieten hinweg zu beleuchten und die maßgeblichen Einflussfaktoren zu identifizieren.

Der erste Teil der Dissertation untersucht die Auswirkungen während und nach hydrologischer Dürren auf die Nitratkonzentration in 182 deutschen Einzugsgebieten. Dürreperioden und „Nach-Dürreperioden“ wurden identifiziert, charakterisiert und mit niederfrequenten Nitratmessungen am Auslass der Einzugsgebiete verknüpft, um Veränderungen der Nitratkonzentrationen zu quantifizieren. Die Ergebnisse zeigen, dass Dürren die Nitratkonzentrationen im Allgemeinen verringern; bei 40 % der Einzugsgebiete wurde eine signifikante Reduktion im Vergleich zu Zeiten ohne Dürre festgestellt. Während der „Nach-Dürreperioden“ zeigten 25 % der Einzugsgebiete ebenfalls eine verringerte Nitratkonzentration, was auf einen zusätzlichen verzögerten Effekt der Dürre hindeutet. Die Analyse saisonaler Muster ergab, dass während Dürren im Winter (Jahreszeit hoher Abflüsse) 25 % der Einzugsgebiete einen signifikanten Anstieg der Nitratkonzentration zeigten, während weitere 25 % einen Rückgang aufwiesen. Diese Unterschiede wurden durch klimatische Eigenschaften der Einzugsgebiete und ihre biogeochemische Retentionskapazität erklärt. Gebiete mit höheren jährlichen Niederschlägen und geringerer Retentionskapazität zeigten während Winterdürren einen Anstieg der Nitratkonzentrationen. Zudem wurde nach Dürren im Winter bei 19 % der Einzugsgebiete ein signifikanter Anstieg der Nitratkonzentration im Vergleich zu Zeiten ohne Dürre festgestellt, insbesondere in feuchten Einzugsgebieten mit hohem Stickstoffüberschuss. Dieser Überschuss, hauptsächlich bedingt durch Düngemitteleinsatz, stellt den entscheidenden anthropogenen Einfluss dar. Dieses Kapitel zeigt, wie klimatische Bedingungen und anthropogene Einträge (z. B. Düngung) die Nitratkonzentrationen während Winter-Nach-Dürreperioden beeinflussen und wie klimatische Faktoren sowie biogeochemische Retentionsprozesse die Nitratreaktionen während Dürren steuern.

Im zweiten Teil der Dissertation wird der Einfluss unterschiedlicher Abflussereignisse auf die Nitratkonzentration in 184 deutschen Einzugsgebieten anhand der Streuung in Konzentrations-Abfluss-Beziehungen (C-Q-Beziehungen) untersucht. Die Ereignisse wurden nach ihren Ursachen (Schneeschmelze, Regen und Regen-auf-Schnee) sowie der vorherigen

Bodenfeuchte klassifiziert. Ereignisse in Zusammenhang mit Schnee zeigten allgemein höhere Nitratkonzentrationen als durch C-Q-Modelle vorhergesagt, was auf eine verstärkte Nitratmobilisierung hinweist. Im Gegensatz dazu wiesen Regenereignisse bei trockenen Vorbedingungen negative Abweichungen von den C-Q-Prognosen auf, was auf eine reduzierte Nitratmobilisierung hindeutet. Zusätzlich wurde ein positiver Zusammenhang zwischen dem Ereignis-Abflusskoeffizienten (Anteil des abflusswirksamen Niederschlags) und den C-Q-Abweichungen festgestellt, was darauf hinweist, dass Abflussereignisse mit höherer hydrologischer Konnektivität die Nitratmobilisierung zusätzlich erhöhen. Abflussereignisse, die durch Regen auf geringer, heterogener Bodenfeuchte ausgelöst wurden, hingegen zeigten die niedrigsten Nitratkonzentrationen relativ zu den C-Q-Prognosen, vermutlich durch die Kombination von nicht ans Fließgewässernetz angeschlosssenen Nitratquellen und einer erhöhten biogeochemischen Retention in den Einzugsgebieten.

Der dritte Teil untersucht die Bedeutung räumlich verteilter Bodenfeuchte für die Nitratdynamik auf Einzugsgebietsebene. Mithilfe eines Multi-Branch Deep-Learning-Modells wurden die Nitratkonzentrationen in neun Einzugsgebieten in den USA vorhergesagt, mit Hilfe von täglichen Abflussdaten und einem hochaufgelösten satellitenbasierten Bodenfeuchteprodukt (SMAP-HydroBlocks). Das Modell reproduzierte die Nitratkonzentrationen erfolgreich mit einer Medianwert der Nash-Sutcliffe-Effizienz von 0,64. Räumliche Muster der Bodenfeuchte trugen zu 30 % der Modell-Feature-Importance bei. Ohne die Bodenfeuchte verringerte sich die Vorhersagekraft des Modells um 14 %. Beides hebt die Bedeutung der Bodenfeuchte insbesondere unter wechselhaften Bedingungen oder bei nahezu gesättigten Böden hervor. Mittels erklärbarer KI-Techniken (XAI) wurde festgestellt, dass Bodenfeuchte in Flussnähe besonders informativ für den Nitrat-Export waren. Dieser Abschnitt verdeutlicht das Potenzial der Integration von XAI und Fernerkundungsdaten zur Verbesserung der Vorhersagen von Nitratkonzentrationen und zur Identifizierung entscheidender Bereiche im Einzugsgebiet.

Diese Dissertation quantifiziert den Einfluss hydrologischer Ereignisse auf Nitratkonzentrationen in einer Vielzahl von Einzugsgebieten, betont die zentrale Rolle der hydrologischen Konnektivität und die Komplexität des Zusammenspiels von Transport und Transformationsprozessen insbesondere während Winterdürren und Abflussereignissen mit trockenen Vorbedingungen. Darüber hinaus wurden räumliche Muster der Bodenfeuchte mithilfe von Deep Learning und XAI-Techniken untersucht, wodurch deren Vorhersagekraft hinsichtlich der Nitratdynamik hervorgehoben wurde. Angesichts der prognostizierten Veränderungen hydrologischer Ereignisse und der Bodenfeuchte unter dem Einfluss des Klimawandels bieten die Ergebnisse dieser Dissertation wertvolle Erkenntnisse für ein optimiertes Wasserqualitätsmanagement und Monitoringstrategien.

Abstract

Nitrate contamination in fresh water systems remains a major concern worldwide, affecting aquatic ecosystems and human water supplies. Although significant efforts have been made to understand nitrate dynamics at the catchment scale, the role of hydrological events across multiple catchments is still not fully understood. This thesis summarizes three investigations about the role of hydrological events in nitrate mobilization across a large sample of catchments and the main factors controlling nitrate transport from sources to streams.

The first section of this thesis studies the impact of hydrological droughts and post-drought periods on nitrate concentration in 182 German catchments. Droughts and post-droughts were identified, characterized and linked to low-frequency nitrate observations at the catchment outlets to quantify changes in nitrate concentration. Results indicate that droughts generally decrease nitrate concentration, with 40% of the catchments showing a significant reduction compared to no-drought periods. For post-drought periods 25% of the catchments showed significant reduction of nitrate concentration, highlighting a delayed drought effect. Seasonal analysis revealed that during winter droughts (high-flow season), 25% of the catchments show a significant increase in nitrate concentration, while another 25% showed decreases. These differences during winter droughts were attributed to climatic characteristics and the biogeochemical retention capacity of the catchments. Catchments with higher annual precipitation and lower retention capacity tended to show increased nitrate concentrations during winter droughts. Moreover, during winter post-drought periods, 19% of the catchments showed a significant increase in nitrate concentration compared to no-drought conditions, primarily in wet catchments with excess of nitrogen input. This chapter demonstrates how climatic conditions and anthropogenic inputs interact to modulate nitrate responses during winter post-drought periods, and how climatic and biogeochemical retention processes influence nitrate responses during droughts.

The second section studies the effect of different types of runoff events on nitrate concentration across 184 German catchments by exploring scatter in concentration-discharge (C-Q) relationships. Events were classified based on their inducing conditions (i.e., snowmelt, rainfall, and rain-on-snow) and antecedent wetness. Results showed that snow-impacted events generally resulted in higher nitrate concentration than predicted by C-Q models, indicating enhanced nitrate mobilization. In contrast, rainfall events occurring under dry antecedent conditions showed negative deviations from the C-Q predictions, indicating reduced nitrate mobilization. Additionally, a positive relationship between event runoff coefficients and C-Q deviations was found, suggesting that runoff events with higher hydrological connectivity increase nitrate mobilization beyond C-Q predictions. Runoff events induced by rainfall on dry patchy soils (spatially heterogeneous moisture) exhibited the lowest nitrate concentration

relative to the C-Q predictions, likely due to the combined effects of nitrate sources disconnected from streams and enhanced biogeochemical attenuation within the catchments.

The third section examines the importance of spatially distributed soil moisture for nitrate dynamics at the catchment scale. A multi-branch deep learning model was developed to predict nitrate concentration in nine catchments in the United States, using streamflow and a high-resolution satellite-based soil moisture product (SMAP-Hydroblocks). The model successfully reproduced nitrate concentrations achieving a median Nash-Sutcliffe Efficiency of 0.64. Spatial patterns of soil moisture contributed 30% of model feature importance, and removing this information reduced the model performance by 14%, demonstrating its predictive power, especially under transitional wetness conditions or when the catchments were nearly saturated. Explainable AI (XAI) techniques revealed that near-stream areas were more informative regarding nitrate export. This section highlights the potential of integrating XAI with remote sensing data to improve nitrate prediction and identify key informative areas.

This thesis quantifies the effect of hydrological events on nitrate concentration across a large set of catchments, emphasizing the critical role of hydrological connectivity and complexity of the interplay between transport and transformation processes (in particular during winter droughts and runoff events with dry antecedent wetness conditions). Additionally, spatial patterns of soil moisture influencing nitrate concentration were explored using deep learning and XAI techniques, highlighting their predictive power for nitrate dynamics. Given the projected changes in hydrological events and soil moisture under climate change scenarios, the findings provide valuable insights for enhancing water quality management and monitoring strategies.

To my parents, whose constant encouragement taught me to always aim higher.

Acknowledgements

I would like to acknowledge every person who shared this journey with me during these PhD years. From both an academic and human perspective, I appreciate in the first place the exceptional supervision of Larisa Tarasova, who with empathy and motivation made this PhD a collaborative team effort, always pursuing academic excellence while also prioritizing work-life balance and mental health. I am grateful to Ralf Merz for his constant trust in my work, for his guidance, and for all the opportunities he continues to provide. Special thanks to Stefano Basso for his scientific and personal support, always offering kind advice during the challenges of research and foreign life in Germany. I also acknowledge Andreas Musolff for his impeccable scientific mentorship. Without his guidance, I would not have reached the level of scientific depth needed for this dissertation. Sincere thanks to Jana von Freyberg and Noemi Vergopolan for their warm welcome and support during my research stays in Switzerland and Princeton.

In my work environment, I thank the PhD and postdoc colleagues who shared this period with me. Some have been present for years: Sumra, Hsing-Jui, and Zhenyu, and others during shorter stays, like Deen, Pietro, Safae, Ying, Jia-Jui and Kerem. I feel fortunate to have shared time with such diverse and inspiring people. To our running group with Luis, Daniela, and others—thank you for so often helping me escape the stress of the PhD routine. I acknowledge the DYNAMO Cohort colleagues—Maria, Arianna, and Christina—for our constant meetings to release PhD stress, as well as our secretary Antje Heyne, and Sandra Hille, who were always supporting, and the big TRACER group of people, with whom I could share more than science.

On a personal note, I want to express my appreciation to my wife Evelyn, who came with me on this journey without knowing the challenges ahead. For constantly believe in me and for supporting me in her own unique psychological way. To the group of friends I made in Halle who gave meaning to my daily life—Antonio, Celia, Paul, and Mariana—thank you. To my music friends, a key outlet throughout this journey: Patrick, Max, Luis x2, Tomy, Lucas, Diego and Ale.

And to my parents in Chile, my sisters, uncles, and aunts, who always believed I would make it to the end—thank you for your unwavering support. Para mis tías y abuela tejedoras, Haydee, Brenda y Gilda, que con su lana combatí el frío alemán.

Table of Contents

List of Figures

List of Tables

Abbreviations

AI	Artificial Intelligence
C–Q	Concentration–Discharge relationship
C_{obs}	Observed solute concentration
ConvLSTM	Convolutional Long Short-Term Memory (deep learning model for spatio-temporal data)
DL	Deep Learning
HAND	Height Above Nearest Drainage (topographic index)
HB	HydroBlocks (satellite-derived soil moisture product)
GPU	Graphics Processing Unit, used for high-performance computing and deep learning
IQR	Interquartile Range
KGE	Kling–Gupta Efficiency
L1	L1 regularization (Lasso)
LASSO	Least Absolute Shrinkage and Selection Operator, a regression method with L1 regularization
LSTM	Long Short-Term Memory
Mix	Runoff event type: Mixture of rainfall and snowmelt
ML	Machine Learning
N_2	Atmospheric nitrogen (inert diatomic nitrogen gas)
N_2O	Nitrous oxide, a greenhouse gas from nitrification/denitrification processes
NASA	National Aeronautics and Space Administration
NH_3	Ammonia, a volatile nitrogen compound
NH_4^+	Ammonium, an ionized form of ammonia found in water and soil
NO_2^-	Nitrite, an intermediate nitrogen species in nitrification/denitrification
NO_x	Nitrate and nitrite collectively, nitrogen oxides contributing to reactive nitrogen
NO_3-*N*	Nitrate as nitrogen (dissolved inorganic nitrogen expressed in nitrogen mass units)
NSE	Nash–Sutcliffe Efficiency

p-val	p-value (statistical test probability)
P_{mm}	Daily precipitation in millimeters
PLAN	Conceptual framework: Proxies for inputs (People, Loads) and attenuation (Anthropogenic, Natural) to explain nitrate export
Q_{obs}	Observed stream discharge
QUADICA	Water QUAlity, DIscharge and Catchment Attributes for large-sample studies in Germany
REGNIE	German high-resolution gridded precipitation dataset
RMSE	Root Mean Square Error
SHAP	SHapley Additive exPlanations
SM	Soil Moisture
SM_{res}	Soil moisture spatial resolution
SMAP	Soil Moisture Active Passive (satellite mission)
UFZ	Helmholtz Centre for Environmental Research
WWTP	Wastewater Treatment Plant
XAI	Explainable Artificial Intelligence
Z-NO_3-N	Standardized nitrate concentration (Z-score)
Δres	Residual error between modeled and observed values
Δres_{50}	Median residual error (50th percentile)

1

Introduction

Nitrate (NO_3^-) is an inorganic nutrient, characterized by a high solubility in water and by a high biodegradability, and is an important compound in the nitrogen cycle [3]. Nitrate is a key nutrient for plants and microorganisms [4], and is widely used as a fertilizer worldwide. This ubiquitous compound is present in terrestrial, freshwater and marine environments [5, 6], while its excessive concentration, especially in aquatic environments poses a risk for human and ecosystem health [7, 8]. The excess of nitrate and phosphorus in water bodies in combination with light availability and warm temperatures can induce excessive algae growth in water bodies (i.e., algae blooms) reducing light penetration into the water column. Once these algae die their biomass is decomposed, leading to oxygen depletion, which causes severe harm to aquatic ecosystems [7, 9]. In addition, some of these algae, such as cyanobacteria and dinoflagellates, can be toxic, threatening the safety of human water supply chains and causing mass fish kills [10, 9].

1.1 Anthropogenic and natural nitrate sources

Nitrate is produced in the environment by natural and anthropogenic processes. The natural production of nitrate occurs in various compartments of terrestrial and aquatic environments. In the atmosphere nitrates (NO_x) are generated through chemical reactions that use lightning or other high energy processes. Nitrates are deposited to the land through rain, fog or snow (i.e., wet deposition), or they can simply adhere to surfaces (i.e., dry deposition). In wet and temperate climates, the episodic wet deposition typically exceeds dry deposition. Although atmospheric deposition of nitrate is a natural process, nitrates concentration in the atmosphere have significantly increased due to anthropogenic activities (e.g., fossil fuel combustion) increasing atmospheric nitrogen deposition in the last decades [11, 12, 13]. Nitrogen can also be incorporated into the landscape from the atmosphere through nitrogen fixation. This process is mediated by soil bacteria associated with the roots of plants (e.g., legumes) that convert atmospheric nitrogen N_2 to ammonia (NH_3) and then this ammonia is converted to nitrate by nitrification in the soils, with another type of bacteria mediating this biogeochemical

process [14, 15]. Another natural process of nitrate production is facilitated by biological decomposers, including fungi or bacterial communities. Decomposers can break down organic matter from soil or water and produce ammonium (NH_4^+), which can also be converted to nitrate through nitrification [16].

Anthropogenic nitrate production consists of two major sources: diffuse and point sources. Diffuse sources originate from synthetic fertilizer or manure applications to crop fields. Organic fertilizer and manure are decomposed through mineralization, a bacteria-mediated process that transforms organic compounds into ammonium, and can take days to weeks depending on soil oxygen, moisture, temperature, pH and carbon ratio [17, 18]. Typically, inorganic fertilizers are based on ammonium, and therefore immediately available for plants. However, ammonium from both inorganic and organic fertilizers can be quickly transformed to nitrate (i.e., from hours to days) through nitrification [19, 5]. The application of fertilizer varies in amount and frequency according to the land characteristics, crops and environmental factors. Since the Green Revolution in the 1970s, the amount of fertilizer application has increased exponentially in the world [20]. This excess fertilizer application remains in the soil in organic forms at depths beyond root uptake zone, producing a pool of organic nitrogen that can eventually be mineralized and leached to groundwater or delivered directly to streams [21, 22].

Anthropogenic point sources, in contrast, correspond to effluents of industries or cities. These effluents are often treated with nitrogen removal techniques in wastewater treatment plants (WWTP). Water from WWTP still contains considerable amounts of ammonium, nitrite (NO_2^-) and nitrate, especially when treatment plants lack advanced nutrient removal processes [23, 24]. Although some water treatment plants are influenced by heavy rainfall, point source loads are more constant throughout the year, compared to diffuse sources [25, 26]. Hence, point sources are particularly important during low-flow periods, when there is less water in the stream to dilute resulting nitrate concentrations in the receiving streams [25, 27].

From the available nitrate sources, the anthropogenic ones are the most important in anthropogenically-affected catchments [25, 28]. In Europe, regulation of fertilizer application in the 1990s and the considerable improvement of water treatment technologies sharply decreased the annual nitrogen surplus in the catchments, however, responses are often delayed by decades in some cases, as nitrate is still present in the soil and groundwater as a legacy [29, 21].

1.2 Nitrate dynamics: transport and transformation

From sources to stream, nitrate travels through different pathways depending on the location of sources and prevailing environmental conditions. While point sources directly release nitrate to the streams, nitrate from diffuse sources reaches streams through a variety of hydrological pathways that are activated under different hydrological conditions [30]. Nitrate dynamics comprise two main components: transport and transformation. Due to its high solubility, the transport of nitrate generally follows the same trajectory as water. During wet conditions (e.g., after heavy rainfall) different water pathways from land to streams are activated. This dynamic process is referred to as hydrological connectivity and is crucial for understanding nitrate dynamics [30, 31, 32]. The heterogeneous activation of hydrological pathways interacts with the spatially heterogeneous distribution of nitrate sources in the landscape, posing a

significant challenge for identifying which sources are the ones contributing to stream nitrate [33, 34].

Moreover, while nitrate transits from land to stream it undergoes biogeochemical transformations. Nitrate can be reduced to harmless N_2 gas through the action of denitrifying bacteria and associated enzymes. This biogeochemical process is defined as denitrification, and it is the most important process for nitrate removal [35, 36]. Denitrification needs anaerobic conditions and electron donors such as organic matter or pyrite, typically found in waterlogged soils, deep groundwater, or in the hyporheic and riparian zone of the rivers [37]. In some cases, incomplete denitrification can also produce nitrous oxide (N_2O), an alarming greenhouse gas [36]. Quantifying nitrate transformation at the catchment scale is challenging and relies on modeling or isotopic analyses that are not available in most catchments [38, 39].

1.2.1 C–Q relationships to understand nitrate dynamics

Concentration–discharge (C–Q) relationships are a common tool to study these processes at the catchment scale as they use discharge as a catchment-average proxy of hydrological connectivity to understand different solute dynamics. C–Q relationships at the outlet of catchments are commonly represented as a power law [40] and the shape of the C–Q plots encode export regimes of critical substances such as nutrients delivered to streams [34, 41]. Basu et al. [42] introduced a theoretical framework which considers the fraction of soil volume of a catchment that is able to load solutes relates to the ratio between actual discharge and a maximum discharge when the entire catchment is contributing water. Assuming an infinite concentration of sources and a homogeneous precipitation, a power law C–Q relationship can be theoretically obtained. Nevertheless, there are various factors that can induce a different behavior. Some of these factors are the spatial distribution of sources, nitrate removal in wetlands or artificial drainage of agricultural land can affect C–Q predictions [43]. In addition, rainfall events are not homogeneously distributed across time and space, and this spatiotemporal heterogeneity is not considered in the theoretical C–Q framework proposed by [42].

Studies based on C–Q analyses have found that nitrate dynamics at the catchment scale depend on the type of nitrate sources and their location in the catchment, hydrological connectivity, hydrogeological characteristics and the capacity of the catchment to retain nutrients [44, 43, 45]. The contrasting behaviors of nitrate in different catchments highlight the complexity of understanding the nitrate dynamics in better detail, e.g., at finer temporal resolutions. Although C–Q relationships are a powerful tool to study the aggregated nitrate dynamics at the catchment scale, there is often visible scatter that is not fully understood and may reflect anomalous hydrological conditions as hydrological events [46, 47, 48].

C–Q relationships use discharge as a proxy for hydrological connectivity, however the spatiotemporal variability of hydrological processes occuring at the catchment scale may not be captured by this aggregated metric. Hydrological connectivity is the movement of water across the landscape and is influenced by rainfall, evapotranspiration, and static landscape features such as land cover, topography, and soil properties [49, 50]. This dynamic concept modulates the connection of diffuse nitrate sources from the landscape with streams through the activation of flowpaths in the catchment. Other proxies for hydrological connectivity include event runoff coefficients [51, 52], average groundwater levels [53, 54], and spatially averaged soil moisture

[55]. Nevertheless, aggregated proxies do not consider the spatial heterogeneity of hydrological pathways, which is crucial to understand nutrient hotspots [56].

Spatial patterns of soil moisture can also serve as indicators of hydrological connectivity [57, 58, 59]. As connectivity increases, so does the spatial variability of soil moisture, driven largely by lateral water flows along topographic convergence zones [60, 61]. These spatial patterns highlight active areas where water is redistributed and nutrients are transported. Shifts between wet and dry conditions cause temporal changes in soil moisture patterns that may also provide insight about solute transport processes through subsurface flow [61, 62].

While C–Q relationships have advanced our understanding of aggregated nitrate export, a key knowledge gap persists regarding the role of individual hydrological events and spatially variable runoff generation in shaping nitrate dynamics at the catchment scale.

1.2.2 Hydrological events and nitrate dynamics

Hydrological events are occurrences within the water cycle that alter water availability, thereby altering nutrient pathways within catchments and impacting ecosystems and human water supply [63, 64].

1.2.2.1 Hydrological droughts

Hydrological droughts are defined as continuous deficit in discharge in a stream, and are normally triggered by lack of precipitation or snowmelt [65]. The persistent deficit in water in catchments comes often together with a general reduction of soil moisture that changes the hydraulic properties of the soil. When catchments are dry most of the rainfall will infiltrate directly into deeper soil layers [66]. However, for some expansive soils, the lack of moisture can reduce infiltration capacity leading to surface runoff [67]. This alteration between vertical and horizontal fluxes of water in the soil is spatially heterogeneous and difficult to measure at the catchment scale.

The lack of moisture and recharge, lowers the groundwater table, affecting the water supply, agriculture and ecosystems [65, 68]. Nevertheless, as groundwater has a slower response compared to more superficial flows, the contribution of groundwater to streamflow continues over longer periods. In such conditions, groundwater becomes a major source of streamflow during prolonged dry periods [69, 70].

The lowering of the water table decreases horizontal water fluxes in the soil, disconnecting hydrological pathways that supply surface and subsurface flows in the catchments [54, 71]. This hydrological disconnection affects the transport and transformation of nutrients from the landscape to the streams [72]. During drought conditions, fertilizers applied on agricultural soils may accumulate in the soil due to the lack of transport and the reduced capability of plants to uptake nitrate during water stress periods. Stored in organic form in soils, nitrogen can be mobilized to the rivers in the post-drought period if catchment wetness increases.

On the other hand, wastewater treatment plants can supply an important fraction of streamflow during droughts [e.g., 70% in South Carolina, United States 27], increasing the concentrations of nutrients and pharmaceuticals due to lack of dilution.

The responses of nitrate during droughts across catchments might then depend on the distribution of nitrate sources on the landscape, their spatial connectivity with streams, the

catchment properties that affect retention and the activation of flowpaths (e.g., geology and geomorphology of the catchments), and the drought properties (e.g., duration, severity). However, there is a lack of studies exploring these factors in a large number of catchments.

1.2.2.2 Runoff events

Conversely, runoff events are episodes in which excess water reaches streams typically through faster pathways, such as shallow subsurface or surface flow [32]. During events, subsurface flow can easily transport mineralized nitrate from diffuse sources [73]. However, nitrate C–Q relationships during runoff events often exhibit considerable scatter [47, 48].

Leveraging high-frequency sensors, various studies have investigated nitrate dynamics during events in single or few catchments, revealing distinct long-term C–Q relationships compared to the event C–Q relationships (i.e., C–Q plots during single runoff events). The varying event C–Q relationships observed over time within catchments can vary according to dominant flow sources, such as groundwater and shallow subsurface flow. During runoff events the proportion of surface and subsurface flow relative to total discharge may increase and therefore the concentration of the solutes transported through fast hydrological pathways. Transport through faster pathways is enhanced by wet antecedent moisture conditions, that can increment catchment hydrological connectivity from sources to streams during runoff events [74, 48, 75]. The timing of fertilizer application is often unknown and can also trigger rapid nitrate transport when it is close enough in time to the occurrence of runoff events [76, 77, 72]. Moreover, biogeochemical cycling processes might also influence the response during events, particularly when analyzed at subdaily timescales [46]. Finally, the characteristics or types of runoff events can play a role as catchment hydrological connectivity may respond differently for different event types [78, 79, 80].

The diverse factors playing a role in nitrate dynamics during runoff events make it difficult to disentangle the physical mechanisms that modulate nitrate transport at the catchment scale and there is a lack of large sample studies comparing responses across diverse catchments.

1.2.3 Objectives

The objectives of this work are summarized as follows:

- Investigate the effect of droughts on nitrate dynamics across numerous catchments.
- Identify and analyze controls of nitrate dynamics during runoff events across multiple catchments.
- Investigate the role of spatial patterns of hydrological connectivity on nitrate dynamics during dry and wet periods.

This research is structured into three main chapters, each addressing a distinct aspect of nitrate dynamics and hydrological behavior in catchments. Chapter 2 investigates how drought events, followed by wet winter periods, intensify nitrate concentrations in German rivers. It highlights the role of post-drought mobilization and delayed hydrological responses in shaping nitrate extremes. Chapter 3 analyzes the variability in nitrate concentration-discharge (C–Q) relationships across different runoff events. By categorizing event types,

it provides a clearer understanding of the factors contributing to observed scatter and the challenges in trend detection. Finally, Chapter 4 presents a novel application of explainable artificial intelligence to model nitrate dynamics based on spatial soil moisture data, focusing on hydrological connectivity patterns and their implications for nutrient transport. This research was conducted in the United States, where high-frequency nitrate measurements and high-resolution soil moisture products are available.

2

Winter Post-Droughts Amplify Extreme Nitrate Concentrations in German Rivers

Hydrological droughts, characterized by periods with a shortage of surface or subsurface water supply, can alter runoff generation processes and nutrient dynamics at the catchment scale [70, 81]. This is particularly concerning because the frequency of droughts is expected to increase in Germany with advancing climate change [82, 83]. Droughts and post-drought conditions potentially intensify nitrate fluxes from land to streams, threatening aquatic ecosystems and potable water supplies [84, 85].

Anthropogenic pollution is the main trigger of high levels of nitrate contamination in aquatic systems in Europe [86, 39] and worldwide [12, 13]. While point source contamination (e.g., wastewater) is often diluted by discharge into streams, nitrate from diffuse sources such as agriculture is mobilized through fast and shallow hydrological pathways that are activated under wet soil conditions [87]. In addition to transport, interactions between sources and biogeochemical processes in the soil and streams that remove nitrate can lead to diverse concentration-discharge relationships [45]. In German agricultural catchments, out-of-phase seasonal variations of catchment wetness and biogeochemical processes of nitrate removal often result in high nitrate concentrations in winter and low concentrations in summer [88, 89, 2].

During hydrological droughts, nitrate dynamics can be altered by changes in both transport and biogeochemical processes [90]. In catchments dominated by point sources, nitrate concentrations generally increase because of the lack of dilution, which can mask in-stream retention processes [70]. However, in agricultural catchments, the responses can vary. Reduced hydrologic connectivity between sources and streams reduces transport [87, 88] and enhances the biogeochemical removal of nitrate owing to longer subsurface residence times in the soil [91, 27] and streams [38], promoting lower nitrate concentrations. Changes in runoff generation processes can also alter nitrate concentrations during drought. Zhou et al. [87] demonstrated that within a catchment with mixed land use during droughts, enhanced instream removal

processes, combined with a more pronounced contribution of runoff from forested upland areas with a lower nitrate influx, led to a decrease in nitrate concentrations at the catchment outlet. Conversely, lower nitrate dilution in catchments with contaminated groundwater during droughts can increase the concentration of nitrate in streams [70, 92, 93]. Dry conditions during drought can also limit denitrification rates and nitrogen consumption by plants, increasing nitrogen storage in the soil [94, 95, 96].

The lack of transport from diffuse sources to streams, potential reduction in denitrification, and reduced nitrogen uptake by water-stressed vegetation can lead to the additional accumulation of nitrogen in the soil during dry conditions [97, 98]. During the post-drought period (i.e., the period after the end of a hydrological drought), the excess stored nitrogen can be mineralized and then consumed by plants or mobilized once the moisture levels in the catchments recover from drought [18]. Several studies have reported post-drought flushes of nitrate in individual streams, often with exceptionally high nitrate concentrations [92, 99, 100]. Morecroft et al. [99] found higher stream nitrate concentrations in agricultural and forest areas in the UK, with only forest areas showing enhanced nitrification and mineralization processes. Jutglar et al. [101] also observed a post-drought flush in 90% of 41 spring sampling locations in a southwest region of Germany after the severe drought of 2003. However, post-drought nitrate flushes do not always occur. Jarvie et al. [92] found a post-drought increase in nitrate concentrations only in the upland sites of the Wye catchment in England, and not in the lowlands where agricultural activity is concentrated. In contrast, Van Metre et al. [102] showed that agricultural areas in the Midwest US produced exceptionally high nitrate concentrations after the 2011 drought in zones with high post-drought precipitation. Moreover, Lee et al. [18] found in their global analysis that 43% of the 118 study catchments exhibited higher post-drought nitrate transport and this effect mainly occurred in warm regions with anthropogenic modifications of the landscape. Despite these findings, a full understanding of the conditions under which a post-drought flush of nitrate occurs remains challenging.

Contrasting findings from single- or few-site observations and model-based studies indicate a knowledge gap regarding the primary drivers of high nitrate concentrations during and after droughts. In our analysis, we offer a large-scale and large-sample assessment of the impact of hydrological droughts and post-droughts on nitrate concentrations at the outlets of 182 German catchments with diverse land-use, climatic, and topographic features. We aim to (i) quantify the differences in nitrate concentrations under drought, post-drought, and no-drought conditions in our study catchments, and (ii) estimate the likelihood of extremely high nitrate concentrations during these hydrological conditions and their correspondence with nitrate loads. With climate change altering the frequency of droughts in the future, we aim to provide insights for water managers regarding hotspots of post-drought nitrate pollution, helping to mitigate adverse impacts on riverine, lake, and coastal environments.

2.1 Methods

We used stream water nitrate concentration data (NO_3-N) obtained from federal state monitoring programs in Germany at the outlets of 182 mesoscale catchments [103] and mean daily discharge measurements from the same locations. Nitrate data were available at

biweekly or monthly intervals with a median time span of 21 years (ranging from 5 to 40 years between 1980 and 2020). Catchment sizes varied from 95 to 23 600 km^2, with minimum mean elevations (30 m a.s.l.) in the North German Plain region and the highest elevations in the alpine catchments (1180 m a.s.l.). The predominant land use is agriculture, ranging from 11% to 84% (median 50%) of the catchment area.

2.1.1 Identification of droughts

We identified hydrological droughts using daily discharge data from 1978 to 2020 and a variable threshold level approach [65]. We computed a variable threshold for each station using the 80th percentile of the flow duration curve (i.e., 80% of the flow values are excluded) of the smoothed discharge time series for each day of the year. We smoothed the discharge time series over a time window of 30 d to reduce the number of dependent events [104]. Drought was defined as a period of 30 or more consecutive days with smoothed discharge values below the threshold. The post-drought period was defined as the 100 d period after the end of the drought. If another drought occurred during a post-drought period, the corresponding nitrate samples were considered drought samples. We based our selection of 100 d on covering typical response periods [101, 105]. Furthermore, we tested different thresholds for defining droughts (figures 2.5 and 2.6) and post-droughts (figures 2.7(b) and 2.8) to ensure the suitability of our selections for the diverse catchments in the study area. We found that catchments with a significant difference (p-value ≤ 0.05) in nitrate anomalies between post-drought and drought, and no-drought periods remained consistent across a wide range of possible threshold values.

2.1.2 Data analysis

Our first goal was to quantify nitrate concentrations during drought and post-drought periods in different seasons. We observed a decreasing trend in nitrate concentrations since the 1990s in many of the studied catchments because of changes in European fertilizer application regulations. To isolate the effect of hydrological droughts from the potential trends and the intrinsic seasonality of the observed nitrate time series, we removed the long-term trend by subtracting a simple moving average method with a 5-year time window (figure 2.9). We then subtracted the seasonal mean (i.e., the mean value of the samples collected on the day of the year within a 30 d window) from each detrended nitrate sample to obtain nitrate concentration anomalies (Z-NO_3-N).

Each identified nitrate anomaly was attributed to drought or post-drought conditions. In the subsequent analyses, we only considered catchments with at least 15 nitrate samples collected during both the drought and the post-drought periods. For each catchment and season, we computed the differences in median anomaly values between drought and post-drought compared to no-drought conditions and tested the significance of these differences using the Kruskal–Wallis nonparametric test with a significance level of 5% [106].

We linked the spatial variability of median nitrate anomalies during the drought and post-drought periods to the spatial variability of catchment descriptors that characterize the main aspects of nitrate export in German catchments. The catchment descriptors were obtained from the QUADICA dataset [103]. We tested the main drivers of nitrate dynamics at the long-term catchment scale using the PLAN framework [24], which incorporates anthropogenic inputs

(i.e., the proportion of agricultural land or the number of people, P, weighted by the specific nitrate load, L) and catchment attenuation (artificial and natural attenuation, A and N). For anthropogenic inputs, we analyzed the fraction of agricultural areas in the catchment, which is the primary source of nitrate in our study domain [2]; the total nitrogen input from wastewater treatment plants per unit of area, which is particularly important during low-flow conditions [70]; and the mean annual nitrate surplus between 1991 and 2015 that includes fertilizer surplus and atmospheric deposition. We characterize the natural attenuation using three proxies: mean annual nitrate retention (i.e., the difference between mean annual nitrogen surplus and mean annual load) that also accounts for a potential biogeochemical removal of nitrate [107], fraction of water-impacted soils (stagnosols, semi-terrestrial, semi-subhydric, subhydric, and moor soils) as a proxy of riparian areas and wetlands where nitrate is often removed [108], and soil thickness which is related to transit times, with thicker soils characterized by longer residence times and hence more biogeochemical retention [109]. In addition to the PLAN framework, we consider climatic descriptors that may affect the temporal variability of nitrate dynamics [110]. We used the mean annual precipitation, mean annual temperature, and mean annual frequency of runoff events, identified using an automatic runoff event identification method as climatic descriptors [51].

Finally, we define seasonal extremes as nitrate anomalies that exceeded the 85th percentile of all anomalies in a given catchment and season (i.e., calendar winter, spring, summer, and autumn). We further computed the frequency of occurrence of these seasonal extremes during drought and post-drought conditions (figure 2.10) and compared this occurrence frequency to the expected frequency, assuming a uniform distribution of seasonal extremes for each hydrological condition (i.e., 15%). We quantified the effect of selecting different thresholds to define seasonal extremes on their likelihoods by comparing them with the corresponding expected frequencies (figure 2.11).

2.2 Results

2.2.1 Drought and post-drought nitrate anomalies

The observed median nitrate anomalies during drought and post-drought exhibited varied responses compared to the no-drought conditions (figures 2.1e and 2.1j). During droughts in any season, 60% of the catchments exhibited lower and 40% significantly lower nitrate anomalies (median difference of $-0.59\,\mathrm{mg\,l^{-1}}$ of NO_3-N, p-value ≤ 0.05) compared to no-drought conditions (figure 2.1e). However, this was reversed in winter, the most critical season of nitrate export from catchments (figures 2.1a, 2.1e, table 2.1 and figure 2.12). During winter droughts, we observed higher nitrate concentrations compared to no-drought conditions in 49% of the catchments, with 25% of the catchments showing a positive significant difference (median difference of $0.57\,\mathrm{mg\,l^{-1}}$ of NO_3-N, p-value ≤ 0.05) regardless of the drought definition (figures 2.5 and 2.6), primarily in Southern Germany (figure 2.1a).

Similarly, during post-droughts at any season, 63% of all catchments showed lower and 25% significantly lower nitrate anomalies (median difference of $-0.34\,\mathrm{mg\,l^{-1}}$ of NO_3-N, p-value ≤ 0.05) compared to no-drought conditions (figure 2.1i). However, during winter post-drought conditions, we observed higher nitrate concentrations compared to no-drought conditions in

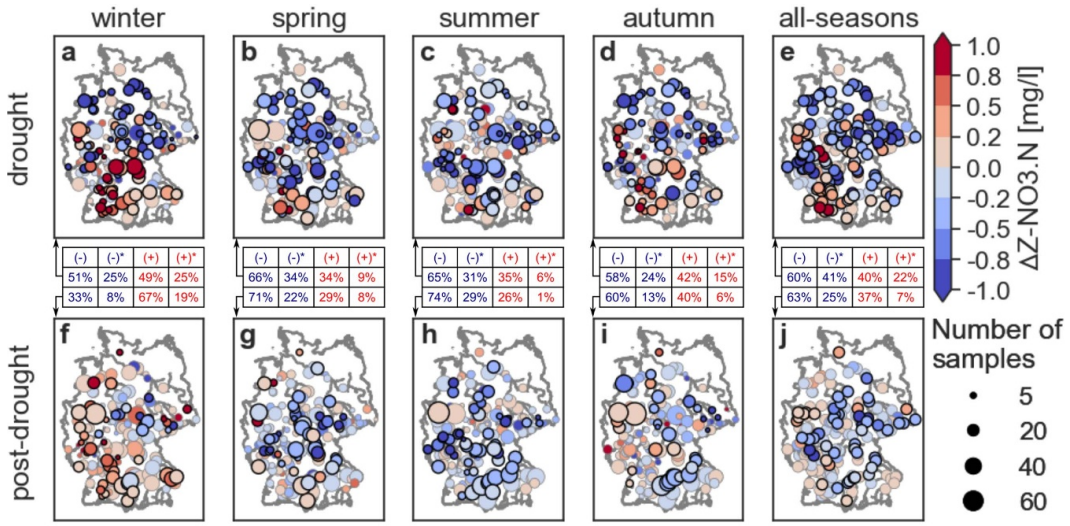

Figure 2.1: Difference between median values of nitrate anomalies (ΔZ-NO_3-N) for drought (a)–(e) and post-drought (f)–(j) groups of samples when compared to no-drought conditions (i.e., baseline for ΔZ-NO_3-N estimation) for different seasons. The size of the circles represents the sample size used to compute median values except in all-seasons (e), (j), where the circle size is set constant for better visualization. The black outline of the circles shows a statistically significant difference compared to the no-drought group (Kruskal–Wallis test, $p \leq 0.05$). Tables between panels show the number of catchments with negative (−), significant negative (−)*, positive (+), and significant positive (+)* differences in nitrate anomalies (ΔZ-NO_3-N) when compared to no-drought conditions.

67% of the catchments, with 19% of the catchments showing significantly higher concentrations (median difference of 0.41 mg l^{-1} of NO_3-N, p-value ≤ 0.05) irrespective of the post-drought definition (figure 2.18), particularly in Western Germany (figure 2.1e).

In spring, summer, and autumn, nitrate concentrations were lower during drought and post-drought periods than under non-drought conditions. In fact, we found lower nitrate anomalies in 65% of the catchments in spring (figure 2.1b, 31% of which decrease significantly, p-value ≤ 0.05), 66% of the catchments in summer (figure 2.1c, 31% of the catchments show a significant decrease, p-value ≤ 0.05), and 58% of the catchments in autumn (figure 2.1d, 24% of the catchments show a significant decrease, p-value ≤ 0.05). The median magnitude of nitrate reduction during droughts in the catchments with significantly lower nitrate anomalies varies from 0.55 to 0.73 mg l^{-1} of NO_3-N in these seasons (table 2.1). Furthermore, during post-droughts, nitrate concentrations are lower compared to no-drought conditions in 71% of the catchments in spring (figure 2.1f, 22% of the catchments show a significant decrease, p-value ≤ 0.05), 74% of the catchments in summer (figure 2.1g, 29% of the catchments show a significant decrease, p-value ≤ 0.05), and 60% of the catchments in autumn (figure 2.1h, 13% of the catchments show a significant decrease, p-value ≤ 0.05). The median magnitude of reduction in nitrate anomalies during spring, summer and autumn in catchments with significantly lower nitrate anomalies ranges between 0.4 and 0.45 mg l^{-1} of NO_3-N (table 2.1).

2.2.2 Seasonal nitrate extremes during droughts and post-droughts

We extend our analysis to explore the impact of hydrological droughts on the likelihood of extremely high nitrate anomalies in each season. Differences in the likelihood of observed seasonal extremes during droughts compared to the expected likelihood (i.e., 15%) were

consistent with median differences in nitrate anomalies during droughts compared with non-drought conditions (figures 2.1a–2.1d). In catchments where nitrate anomalies were significantly higher during droughts (red dots, figure 2.2a), the likelihood of seasonal extremes was the highest, with a median increase in the likelihood of seasonal extremes of 23% (table 2.2). Nevertheless, the nitrate load during these events was lower than the median values of winter loads (point sizes figures 2.2a and 2.13) owing to low discharges during droughts.

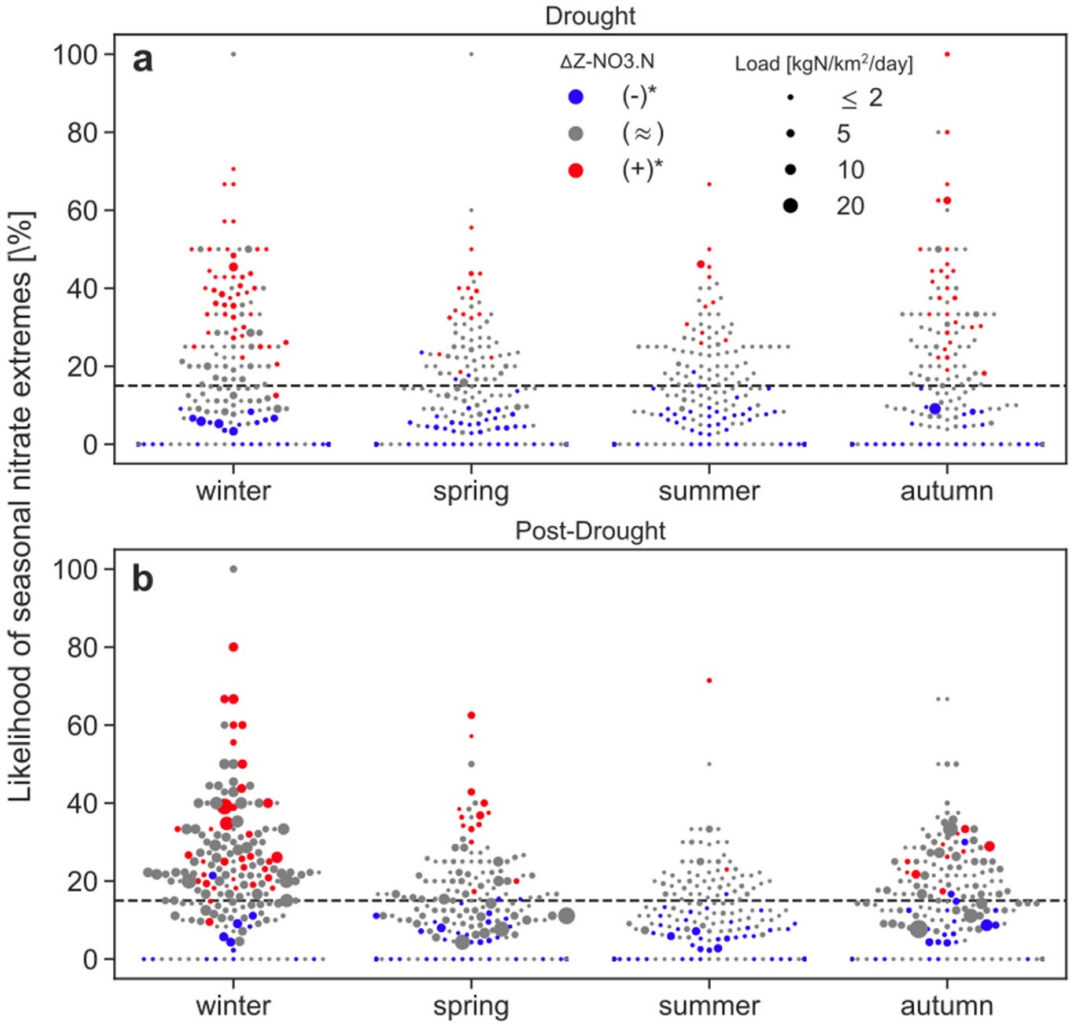

Figure 2.2: The likelihood of seasonal nitrate extremes during drought (a) and post-drought (b) conditions. Catchments are sorted according to their differences in median nitrate anomalies (ΔZ-NO_3-N) during droughts (a) or post-droughts (b) compared to no-drought conditions: significant negative difference $(-)$*, no significant difference ($\approx$), and significant positive difference $(+)$* (see figure 2.1a). Seasonal nitrate extremes are defined as the nitrate anomalies exceeding the 85th percentile of all anomalies for a given catchment and season (figure 2.7). The black dashed line corresponds to the expected frequency of seasonal extremes (i.e., 15%). The size of the circles shows the median value of NO_3-N specific load of all seasonal extremes taken during drought or post-drought conditions of the corresponding season.

Seasonal extremes during winter post-drought were generally more likely to occur than the expected value (median increase of 6% in the likelihood). In particular, catchments with higher median nitrate anomalies (red dots, figure 2.2b) have a median increase in the likelihood of extremes of 11% (table 2.2), and catchments with no significant differences in median nitrate anomalies compared to non-drought conditions (gray dots, figure 2.2b) in winter, have a median increase in the likelihood of seasonal extremes of 5%. In both groups of catchments,

the combined effect of seasonal extremes of nitrate anomalies and recovered winter levels of streamflow (which were the highest in winter in the majority of the study catchments) led to higher specific loads than the median winter specific loads, amplifying the hazard of extreme nitrate concentrations and nitrate loads (figure 2.13c).

2.3 Discussion

Nitrate anomalies displayed pronounced spatial heterogeneity, particularly in winter during drought and post-drought periods (figure 2.1). Winter was the most critical season for delivering nitrate downstream at our study sites. In winter, we observed a higher mean nitrate concentration and discharge, and hence higher loads, compared with the other seasons (figure 2.12). Additionally, we observed that extreme nitrate concentrations (i.e., the 15th highest 15th) mainly occur in this season. Consequently, the following analyses attempt to disentangle the spatial variability of nitrate concentrations, particularly during winter droughts and post-droughts, by exploring and discussing the differences in catchment descriptors following the PLAN framework by characterizing anthropogenic nitrogen inputs (PL), catchment natural attenuation (N), and climatic conditions for catchments with contrasting directions of nitrate anomalies.

2.3.1 Spatial variability of nitrate export during winter droughts

We found that the groups of catchments that exported significantly higher (25% of the catchments, figure 2.1, table 2.1 (+)*) and significantly lower (25% of the catchments, figure 2.1, table 2.1 (-)*) nitrate concentrations in streams compared with non-drought conditions did not differ in their anthropogenic inputs (PL, figures 2.3a, d, and g). Although we found differences in the proportion of agricultural land between catchments with different nitrate concentrations during winter droughts, the mean annual nitrogen surplus, which is a more precise indicator of diffuse nitrogen sources, did not show any significant differences between these catchments. Moreover, the fraction of wastewater nitrogen contribution to annual nitrogen sources was not significantly different between catchments with significantly higher and lower nitrate concentrations during winter droughts, indicating that anthropogenic sources were not the main drivers of spatial variability. During spring and autumn droughts, when runoff rates were lower than during winter droughts, catchments with more wastewater contribution showed significantly higher nitrate anomalies (figures 2.14 and 2.15), which is in agreement with previous studies reporting high nitrate concentrations from point sources during drought conditions due to a lack of dilution [70, 92]. However, the fraction of wastewater input did not affect summer droughts (figure 2.16). During the warm summer months, biogeochemical removal in the soil and streams increases, which might obscure the effects of wastewater sources [87].

Natural attenuation (N) is a main driver of spatial variability in nitrate responses during winter droughts. Catchments with increasing nitrate concentrations during winter droughts had lower mean annual nitrogen retention and a reduced abundance of water-impacted soils (figure 2.3c), illustrating the importance of natural retention and transformation in the catchment, specifically in riparian wetlands during winter droughts compared to non-drought

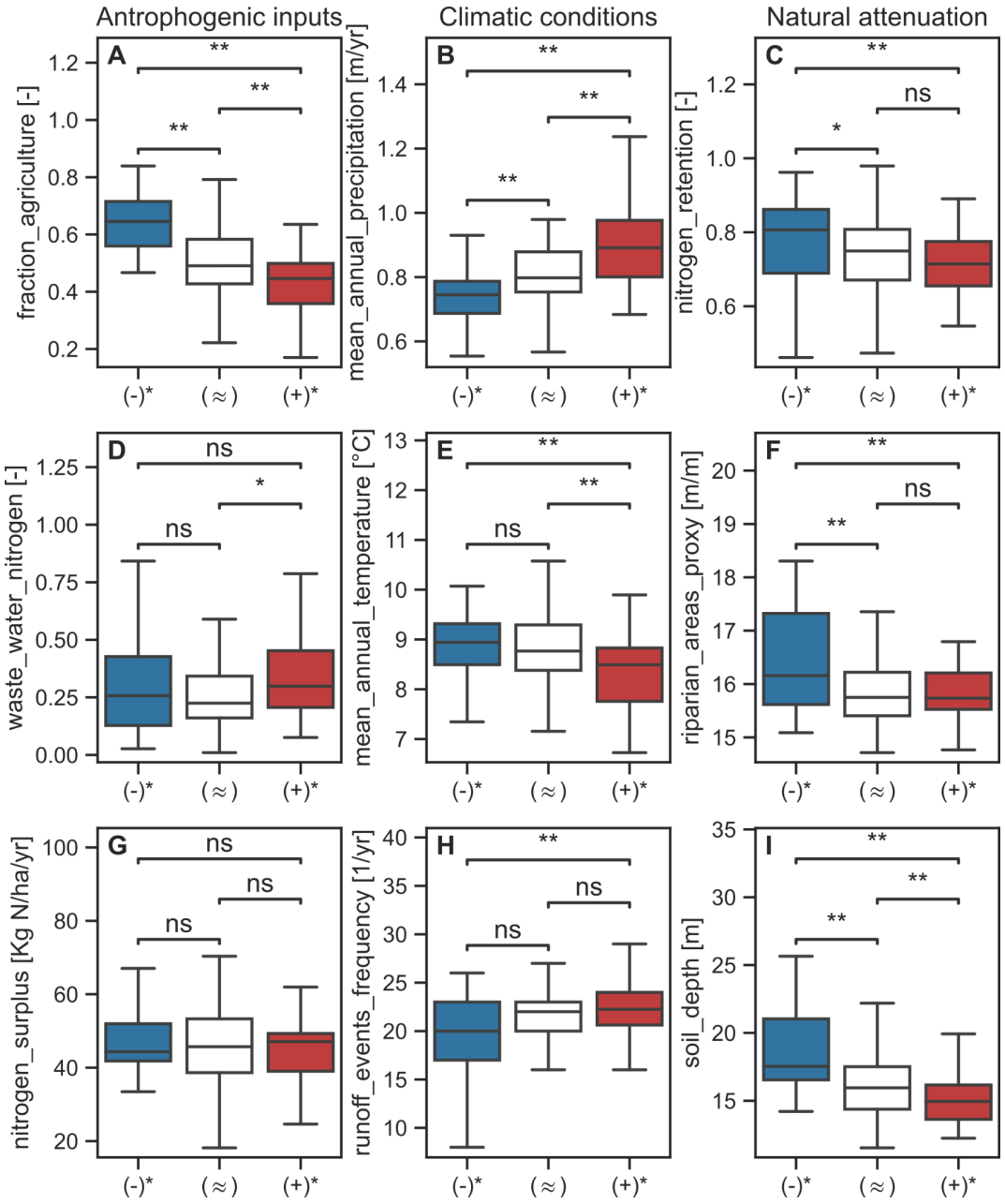

Figure 2.3: Catchment characteristics linked to anthropogenic inputs (a), (d), (g), climatic conditions (b), (e), (h), and natural attenuation (c), (f), (i) for catchments exhibiting significant negative anomalies (-)*, no significant anomalies (≈), and significant positive nitrate anomalies (+)* during winter drought periods (see figure 2.1a). The Kruskal–Wallis test was used to determine significant differences between the groups (ns: pval $>$ 0.05, *: pval $\leq$ 0.05, **: pval $\leq$ 0.01).

conditions. Furthermore, catchments with shallower soils correspond to smaller subsurface storage and are potentially associated with shorter transit times, which might lead to less efficient nitrogen removal from soils [109].

Catchments with significantly higher nitrate concentrations during winter droughts had higher mean annual precipitation and lower mean annual temperatures. Diffuse sources may be less disconnected in wetter catchments than in drier catchments, even during winter droughts. Therefore, the expected reduction in nitrate transport due to source-stream disconnection might be less pronounced. In contrast, warmer and drier catchments with higher annual nitrogen retention exhibit lower nitrate concentrations during winter droughts than during non-drought periods, suggesting that climatic conditions and natural nitrogen attenuation are the primary drivers of spatial variability in nitrate export during winter droughts.

Additionally, we examined all descriptors available from the QUADICA dataset relevant for our study period (i.e., 1978–2020) and normalized per unit area to complement our analysis and uncover any potential drivers beyond the PLAN framework (table 2.3). Catchments with relatively higher nitrogen abundance in the groundwater than in the topsoil (lower vertical nitrogen heterogeneity, het_v in table 2.3) also showed increased nitrate concentrations during winter droughts, possibly due to the contribution of contaminated groundwater [111]. These catchments often have a higher fraction of fissured aquifers, which are known for their low nitrogen retention (table 2.3) [112], highlighting the importance of natural retention in aquifers. Although instream processes can increase nitrogen removal, especially during low flows [38], we did not identify descriptors that specifically pinpointed these processes (e.g., drainage density) as primary drivers of the spatial variability of nitrate responses during winter droughts, possibly because of lower instream removal during winter [87].

We checked the overlap of catchments with significantly higher nitrate anomalies during winter drought and post-drought compared to non-drought conditions (figure 2.17). We found that only 9% of the catchments showed significantly higher nitrate anomalies during both winter drought and post-drought. This suggests that the observed spatial heterogeneity during winter droughts and post-droughts was driven by different processes.

2.3.2 Spatial variability of nitrate export during winter post-droughts

During winter post-droughts, we found that catchments exhibiting higher nitrate anomalies compared to non-drought conditions (19% of the catchments, figure 2.1f, (+)*) were mainly located in West and Southeast Germany. Catchments with a higher nitrogen surplus exhibited significantly higher stream nitrate concentrations during winter post-droughts than during non-drought periods (figure 2.4g). Catchments with higher fertilizer applications, represented by a higher nitrogen surplus [113], are prone to nitrogen accumulation in the soil during droughts because of reduced plant uptake and less nitrate export from the soils during dry periods. Thus, after the drought ends, these catchments can export anomalously high nitrate concentrations [102]. Instead, the natural attenuation of nitrate in catchments does not considerably affect the spatial patterns of winter post-drought export of nitrate to streams (figure 2.4c, f, and i), which is in line with Jutglar et al. [101], who did not find a relationship between soil types associated with different denitrification potential, and the magnitude of the post-drought flush [114].

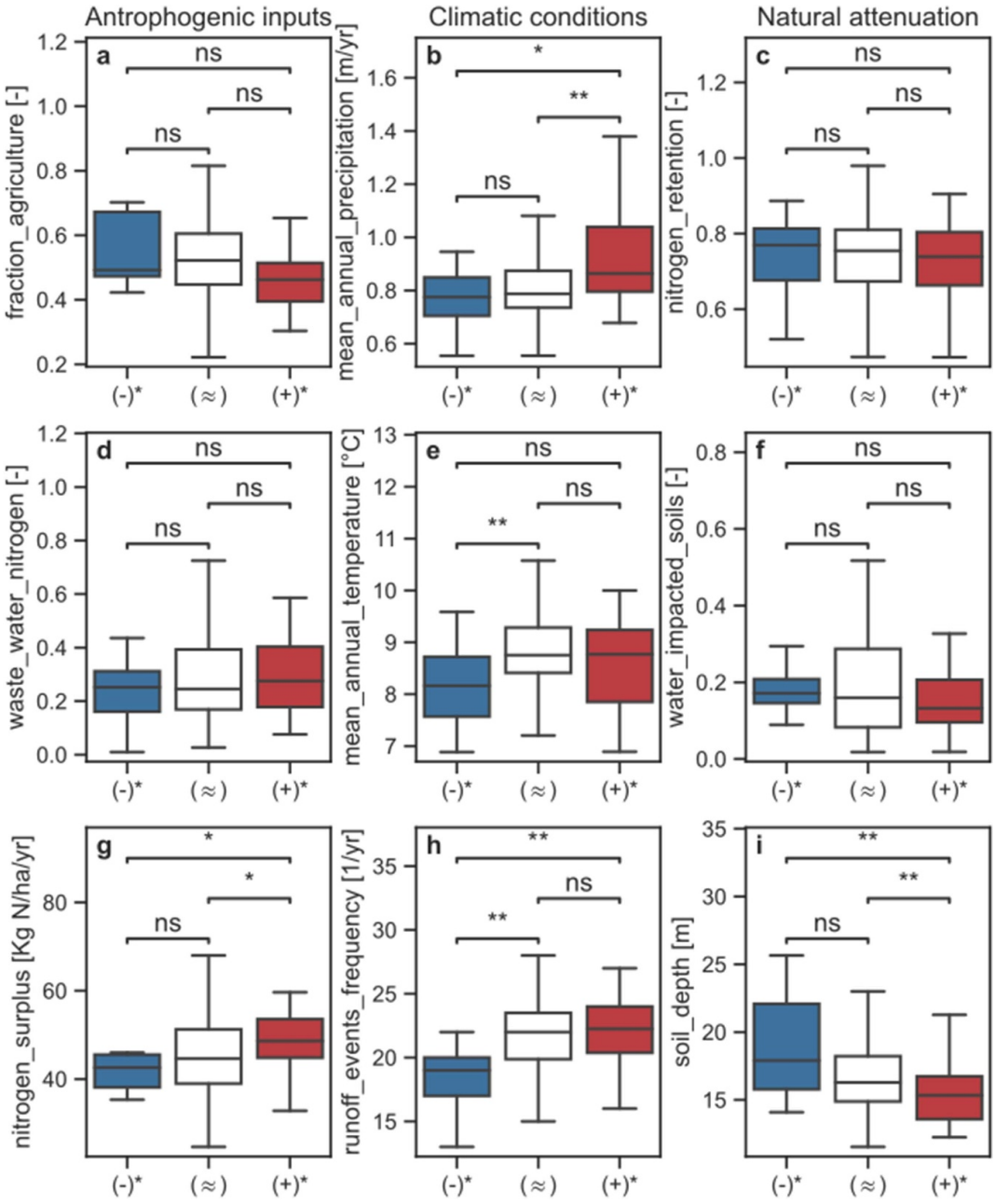

Figure 2.4: Catchment characteristics linked to anthropogenic inputs, climatic conditions, and natural attenuation for catchments exhibiting significant negative anomalies (-)*, no significant anomalies (≈), and significant positive anomalies (+)* during winter post-drought periods (see figure 2.1b). The Kruskal–Wallis test was used to determine significant differences between the groups (ns: pval $>$ 0.05, *: pval $\leq$ 0.05, **: pval $\leq$ 0.01).

We found that catchments with significantly higher nitrate concentrations during post-drought winter had higher mean annual precipitation and a higher frequency of runoff events (figure 2.4b, h). Wetter conditions can enhance the transport of accumulated nitrogen from the soil to streams, leading to higher nitrate concentrations. In addition, in catchments with a higher frequency of runoff events, faster pathways from sources to streams are more likely to be activated, thereby mobilizing the stored nitrogen in the soil under dry conditions [115, 48]. Conversely, the post-drought nitrate anomalies in winter were lower than those in drier catchments, with a generally low frequency of runoff events and a low nitrogen surplus. In drier catchments, we expect a slower reconnection of hydrological pathways after droughts and therefore reduced nitrate transport from diffuse sources during the post-drought period [116]. Similarly, we found lower nitrate anomalies during drier seasons under post-drought conditions in most catchments, suggesting that during these periods, though discharge levels are recovered, nitrate transport between diffuse sources and streams is lower than that under normal hydrological conditions [105]. Although there is evidence that post-drought nitrate flashes are related to episodes of fast rewetting conditions [117], we found no consistent relationship between the magnitude of post-drought flashes and the runoff magnitude or rewetting speed during the post-drought period (figures 2.18d, e). Similarly, we found no consistent relationship between the post-drought nitrate responses and drought characteristics (duration, severity, and intensity, figures 2.18a–c).

2.3.3 Implications

Our results revealed that the winter season exhibited the most distinct disparities between drought, post-drought, and no-drought conditions. Winter is the most critical season for high nitrate concentrations and loads in the streams (figure 2.12). Notably, winter nitrate contamination can be particularly impactful on water bodies, such as lakes and estuaries, exacerbating the risk of eutrophication in subsequent periods [84, 7]. Moreover, more frequent drought events are likely to occur in the future due to climate change [82, 83], potentially increasing the threat of harmful episodes of high nitrate concentrations in streams.

Our analysis indicates that wetter catchments generally display higher nitrate concentrations during winter droughts and post-droughts than under non-drought conditions. In addition, during winter droughts, natural attenuation is a major driver of spatial variability in nitrate responses. These findings indicate that during winter droughts, the interplay between transport and biogeochemical retention processes at the catchment scale becomes particularly sensitive, which highlights the importance of protecting and expanding nitrate retention zones, such as riparian wetlands, to mitigate the environmental challenges associated with high nitrate concentrations during winter droughts [118, 119]. Furthermore, climatic characteristics and anthropogenic inputs of the catchments shaped the spatial variability of nitrate responses during winter post-droughts. We observed that catchments limiting fertilizer application in recent decades were less prone to experience winter post-drought flushes of nitrate (negative relationship with reduction in nitrogen surplus in the last few decades, table 2.4), evidencing that at large scale it is important to curtail fertilizer application [114]. Additional measures, such as tile drain management, might also be beneficial at the local scale to limit rapid nitrate transport from agricultural land to streams [73].

The likelihood of seasonal extreme nitrate concentrations was 24% higher during winter droughts compared to the expected levels in catchments with significantly higher nitrate anomalies than during non-drought conditions (i.e., catchments with wetter conditions and low nitrogen retention capacity). Regardless of the load levels, elevated nitrate concentrations in streams can alter nutrient stoichiometry and affect aquatic ecosystems that are sensitive to variations in nutrient ratios [120]. Moreover, the frequency of seasonal extremes was 11% higher during winter post-drought in catchments exhibiting significantly higher nitrate concentrations compared to no-drought conditions, leading to high levels of loads (figure 2.2b). More frequent seasonal nitrate extremes during winter post-drought can have adverse ecological effects on downstream estuaries and lakes. Nitrates can persist for extended periods in water bodies, increasing the risk of eutrophication [84, 6, 9]. Moreover, the excessive transport of nitrate from diffuse sources during post-drought periods affects groundwater even for longer periods, which could jeopardize current attempts to improve groundwater quality [86, 101].

2.4 Chapter conclusions

In this study, we conducted a large-scale analysis to examine the effects of hydrological drought and post-drought conditions on the nitrate concentrations in streams across a diverse set of catchments in Germany. Generally, we found that 40% and 25% of the catchments during seasonal droughts and post-droughts, respectively, show significantly lower nitrate anomalies. However, during winter, the most critical season for nitrate concentrations and loads, nitrate anomalies showed more pronounced spatial variations, with more catchments showing higher nitrate anomalies, particularly during the post-drought period. Specifically, we find that 25% of the catchments exhibited significantly higher median nitrate concentrations during winter droughts than during non-drought periods. On average, these catchments are characterized by wetter conditions and higher nitrogen retention capacities. During winter post-droughts, 20% of the study catchments exported significantly higher nitrate concentrations than during non-drought conditions. Catchments with significantly higher nitrate concentrations during the winter post-drought had wetter conditions and higher nitrogen surpluses. During the winter post-droughts period, we observed an increase in the frequency of seasonal nitrate extremes in our study catchments, which, combined with high winter discharge levels, can result in exceptionally high nitrate loads. Our study highlights the diverse responses of nitrate concentrations to drought and post-drought conditions across catchments and seasons, indicating that most catchments are likely to exhibit higher nitrate concentrations during extreme hydrological events. As the frequency of droughts is expected to increase under climate change conditions, these insights are crucial for targeted adaptation in the future. The main findings of this study can be summarized as follows:

1. During hydrological droughts, 40% of catchments showed significantly lower nitrate concentrations, and during post-drought periods, 25% exhibited significant reductions compared to no-drought conditions.

2. Considerable spatial variability was observed, especially in winter droughts and post-droughts where 25% and 19%, respectively, of the catchments exhibited higher nitrate concentrations compare to no-drought conditions in winter.

3. Catchments with higher annual precipitation and lower retention capacity exhibit increased nitrate concentrations during winter droughts, whereas catchments with higher annual precipitation and high nitrogen surplus show increased nitrate concentrations during winter post-drought periods.

4. Nitrate seasonal extremes increased by 6% during winter post-droughts, posing a risk to aquatic environments.

2.5 Chapter statement

This chapter presents a formatted version of the original paper by Saavedra, Felipe, Andreas Musolff, Jana Von Freyberg, Ralf Merz, Kay Knöller, Christin Müller, Manuela Brunner, and Larisa Tarasova. 2024. "Winter Post-Droughts Amplify Extreme Nitrate Concentrations in German Rivers.", published in Environmental Research Letters, 19(2)024007, (https://doi.org/10.1088/1748-9326/ad19ed), reproduced here with permission.

Author contributions: Felipe Saavedra Melendez drafted the manuscript and performed the formal analyses. Larisa Tarasova and Andreas Musolff contributed to the conceptualization. Felipe Saavedra Melendez prepared the manuscript with input from all co-authors.

Acknowledgements: The authors acknowledge the two anonymous reviewers for their valuable suggestions that helped to improve the original manuscript. Larisa Tarasova was supported by the German Research Foundation ('Deutsche Forschungsgemeinschaft', DFG) in terms of the research group FOR 2416 'Space-Time Dynamics of Extreme Floods (SPATE)'. Jana von Freyberg was supported by the Swiss National Science Foundation SNSF (Grant PR00P2_185931).

Data availability statement: The data that support the findings of this study are openly available at the following URL/DOI: `https://doi.org/10.4211/hs.0ec5f43e43c349ff818a8d57699c0fe1`, `https://doi.org/10.4211/hs.88254bd930d1466c85992a7dea6947a4`.

2.6 Supporting Information

Table 2.1: Median difference in Z-NO_3.N between drought and post-drought conditions compared to no-drought conditions for each season and in catchments with significant positive (+)* and significant negative (-)* differences.

ΔZ-NO3.N [mg/l]		winter	spring	summer	autumn	all-seasons
Drought	(+)*	0.57	0.55	0.40	0.50	0.29
	(-)*	-0.86	-0.62	-0.55	-0.73	-0.59
Post-drought	(+)*	0.41	0.27	0.60	0.23	0.21
	(-)*	-0.48	-0.45	-0.45	-0.40	-0.34

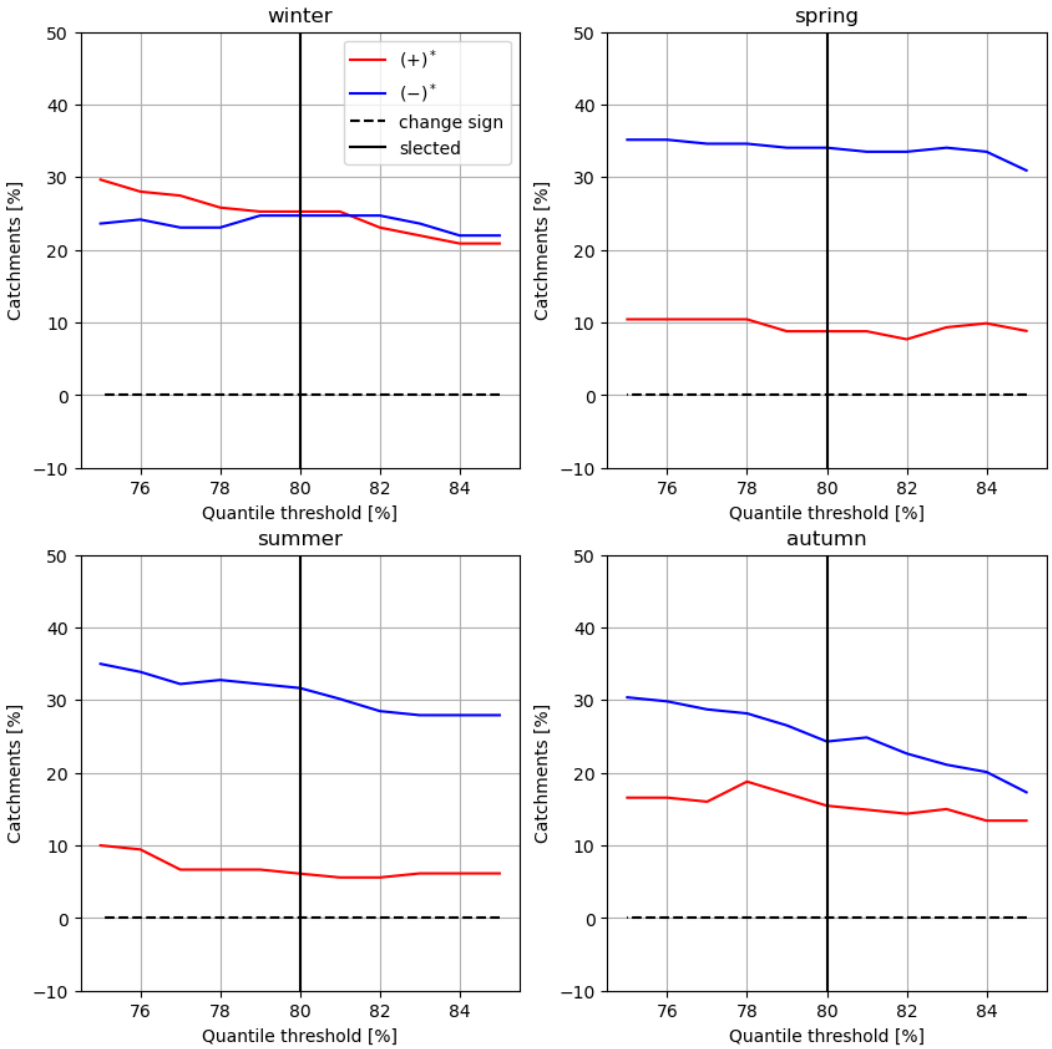

Figure 2.5: The fraction of catchments exhibiting significantly higher (+)* or lower (–)* nitrate anomalies during droughts when compared to no-drought conditions corresponding to different values of quantile threshold used for drought definition (see the Method section of the main manuscript for details). The black dashed line represents the percentage of catchments changing their responses from (+)* to (–)* or from (–)* to (+)* when compared to the selected threshold (vertical black line).

Table 2.2: Frequency of seasonal extremes during drought and post-drought conditions for each season and in catchments with significant positive (+)*, negative (-)* and non significant (≈) differences compared to no-drought conditions (see figure 1).

Frequency extremes [%]		winter	spring	summer	autumn
drought	(-)*	0%	0%	1%	0%
	(≈)	15%	14%	17%	13%
	(+)*	39%	36%	36%	39%
postdrought	(-)*	1%	0%	2%	5%
	(≈)	20%	14%	13%	16%
	(+)*	26%	37%	47%	27%

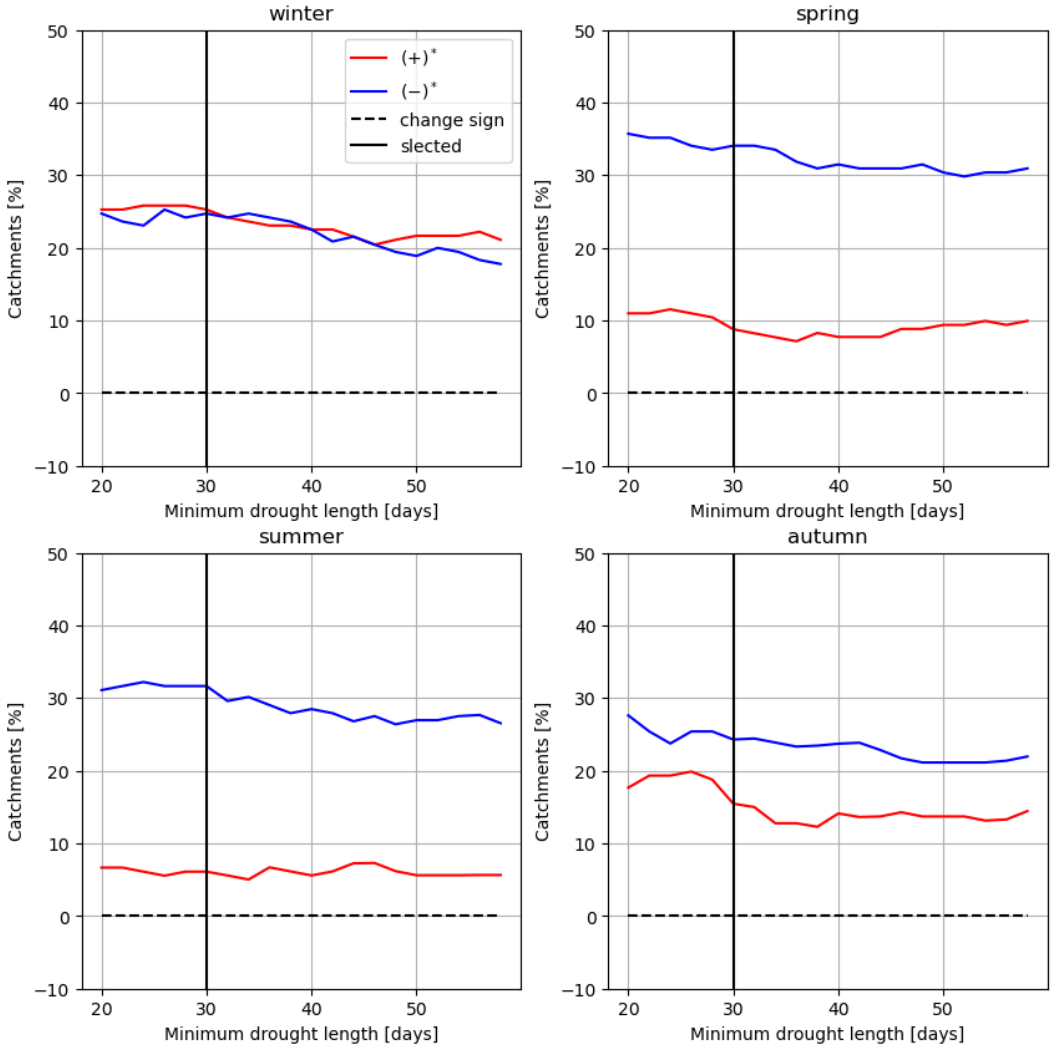

Figure 2.6: The fraction of catchments exhibiting significantly higher (+)* or lower (−)* nitrate anomalies during droughts when compared to no-drought conditions corresponding to different values of the minimum drought duration criteria used for drought definition (see the Method section of the main manuscript for details). The black dashed line represents the percentage of catchments changing their responses from (+)* to (−)* or from (−)* to (+)* when compared to the selected threshold (vertical black line).

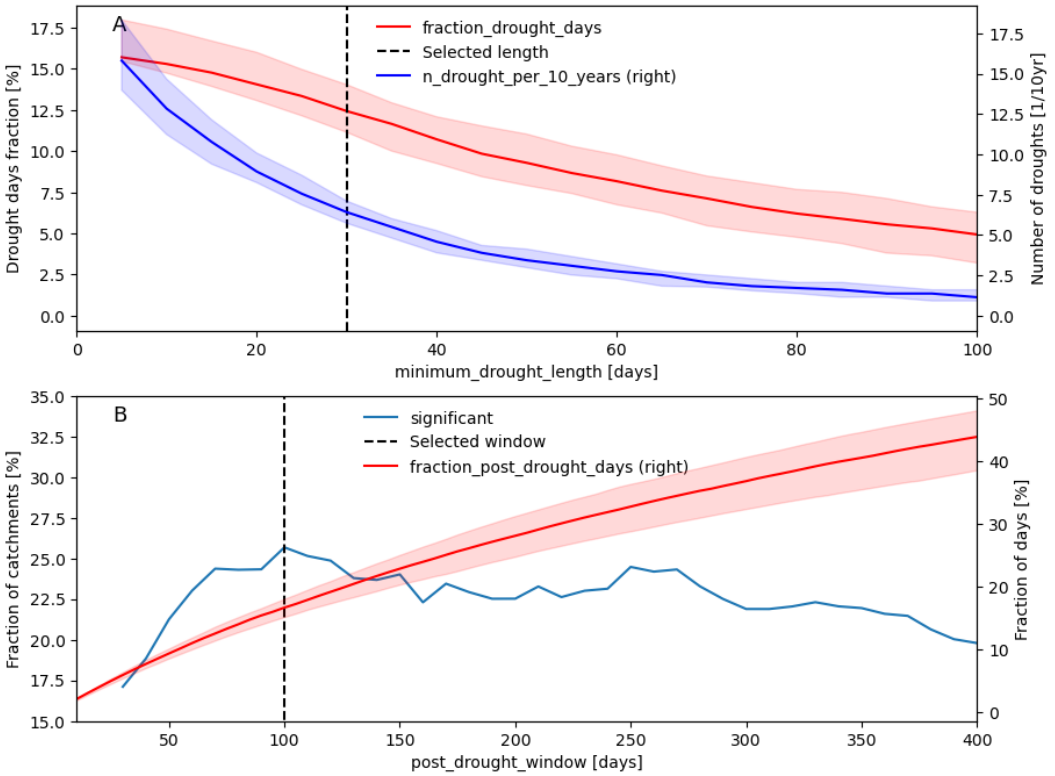

Figure 2.7: Median fraction of drought days of the discharge time series across catchments and number of droughts for different drought minimum lengths (5 to 100 days with 5 days intervals) (A). The average number of catchments exhibiting significant difference (Kruskal–Wallis test, p-value<0.05) between post-drought and no-drought periods across seasons and the fraction of post-drought days for different post-drought lengths (30 to 400 days with 5 days intervals). The colored bands show the interquartile range (IQR) across catchment for each variable.

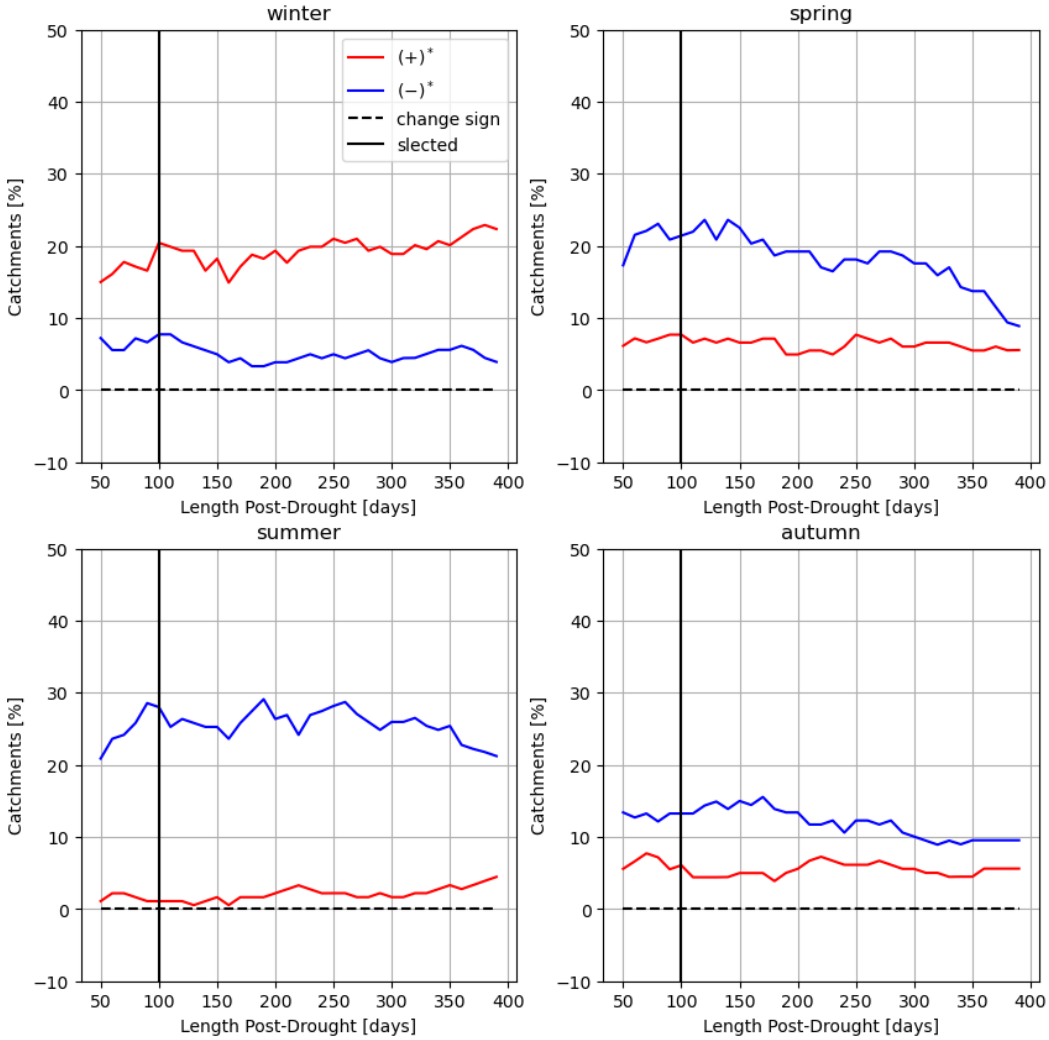

Figure 2.8: The fraction of catchments exhibiting significantly higher (+)* or lower (–)* nitrate anomalies during post-droughts when compared to no-drought conditions corresponding to different lengths of the post-drought period (see the Method section of the main manuscript for details). The black dashed line represents the percentage of catchments changing their responses from (+)* to (–)* or from (–)* to (+)* when compared to the selected threshold (vertical black line).

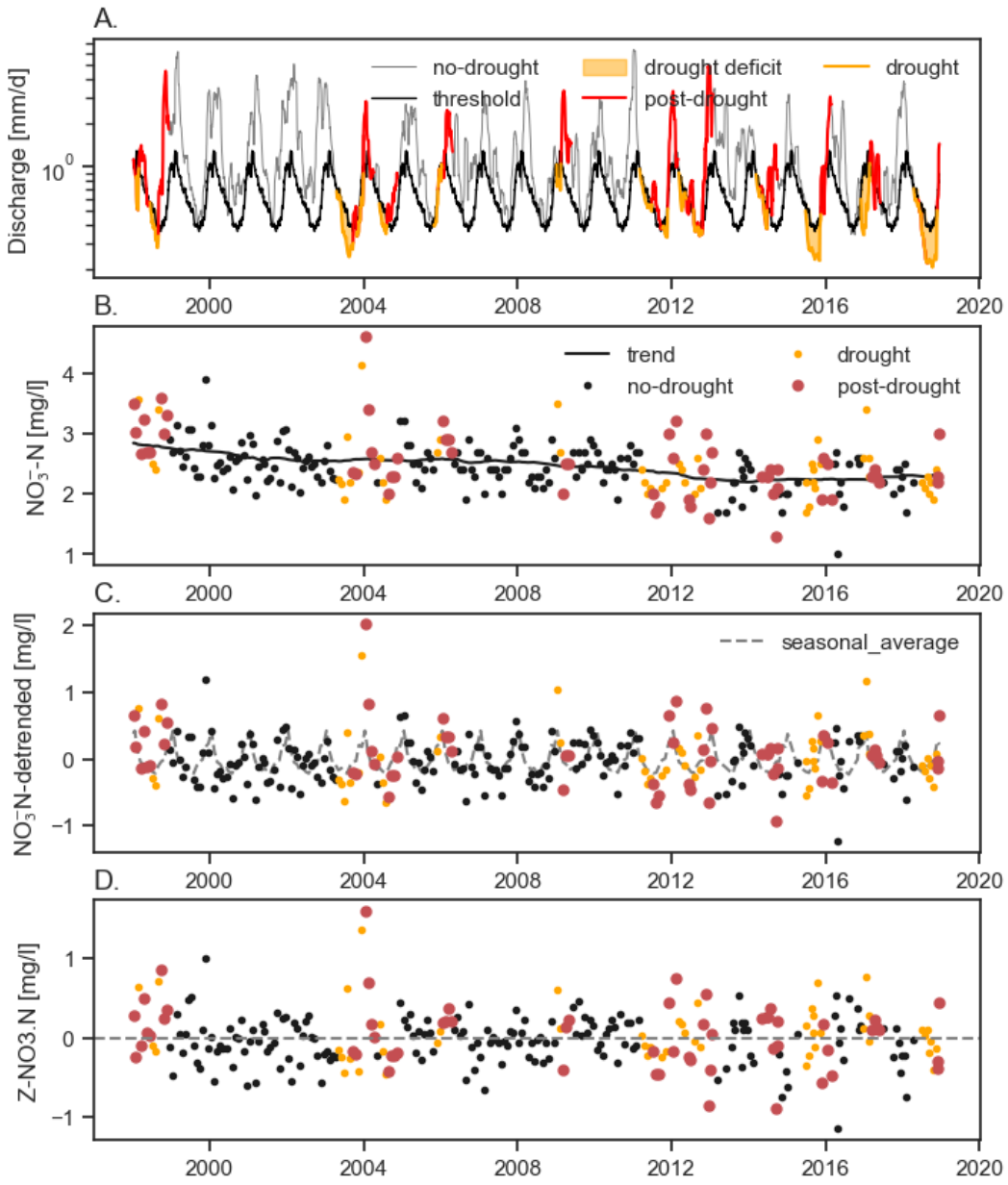

Figure 2.9: Example of drought definition and nitrate time series decomposition, station the Stör River at Willenscharen (Schleswig-Holstein). Discharge time series during droughts, post-droughts and no-drought, and variable threshold (A). Raw nitrate data and long-term trend (B), detrended nitrate time series and seasonal mean (C), nitrate anomalies (Z-NO3.N) after subtracting the seasonal average (C).

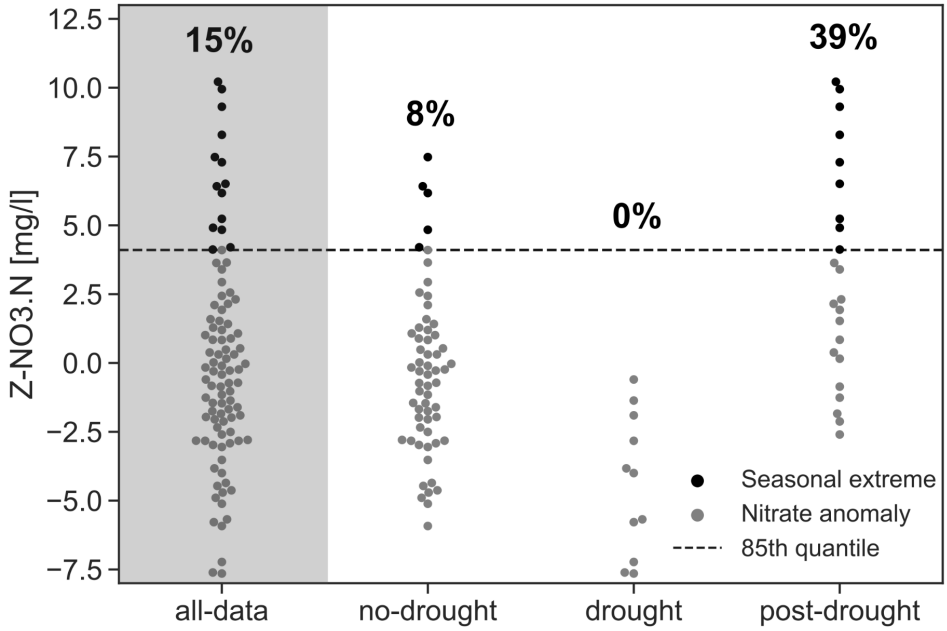

Figure 2.10: Nitrate anomalies (Z-NO3.N) and their seasonal extremes (nitrate anomalies above the 85th percentile for each season) for the Lager Hase River at Uptloh (North Rhine-Westphalia) during winter sorted according to hydrological conditions (i.e., drought, post-drought, and not a drought). The frequency of seasonal extremes for each hydrological condition is shown in blue text above the samples.

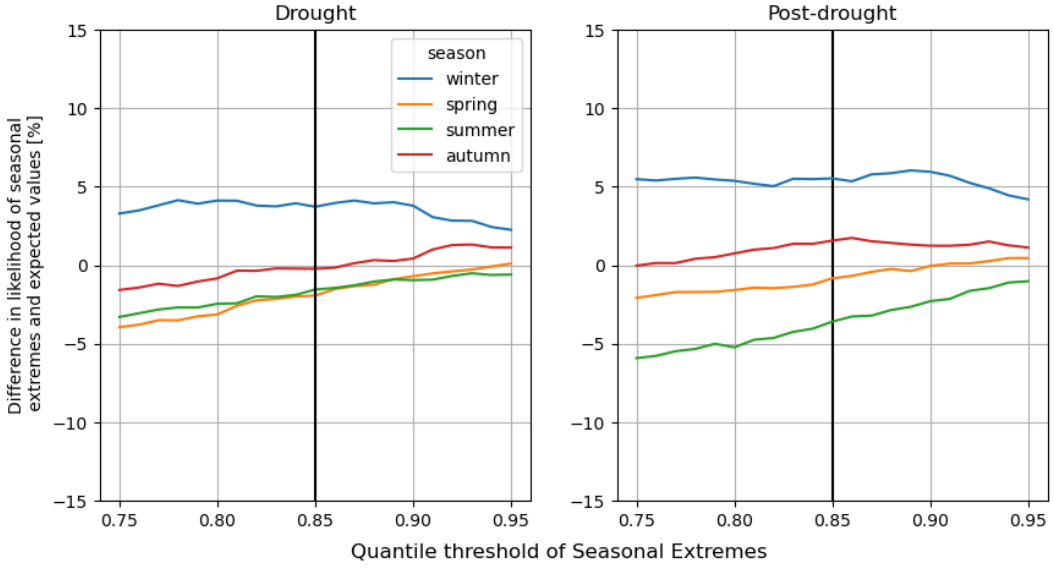

Figure 2.11: Differences in the likelihood of nitrate seasonal extremes and the expected value (see the Method section of the main manuscript) for different quantile thresholds of the definition of seasonal extremes. The selected threshold is shown with a vertical black line.

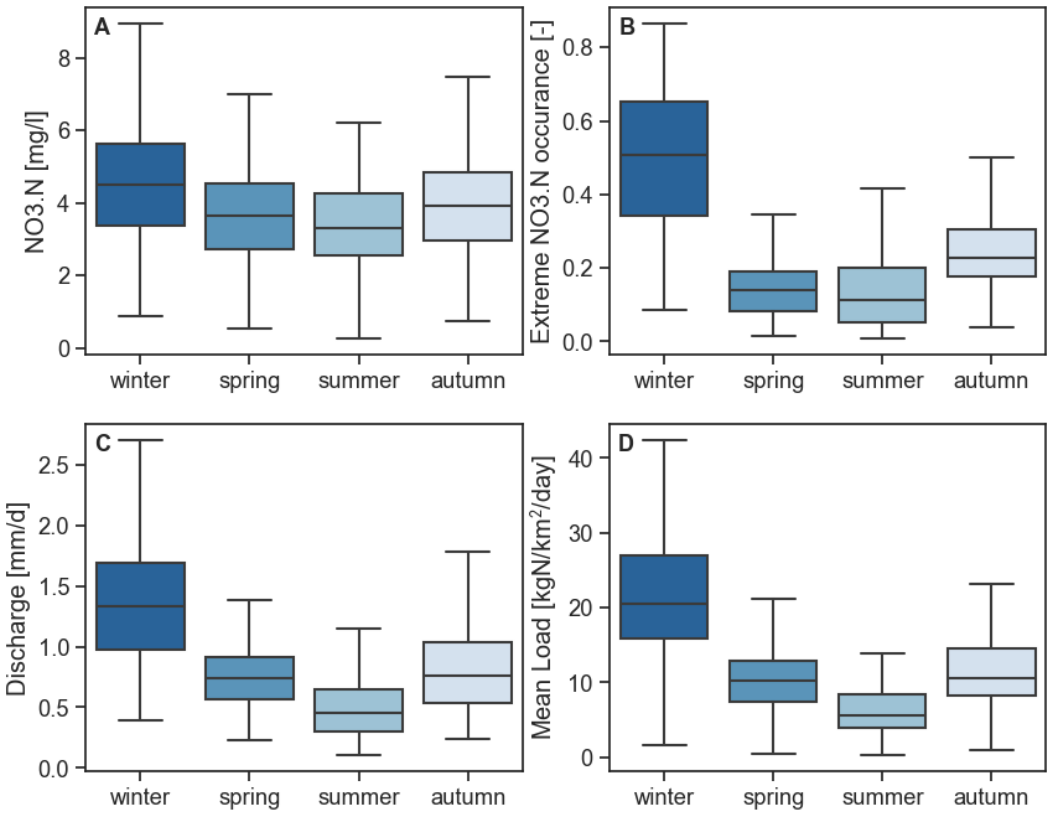

Figure 2.12: Mean nitrate concentration (a), the proportion of highest 15th nitrate concentrations (b), mean discharge (c), and mean load (d) during different seasons among study catchments.

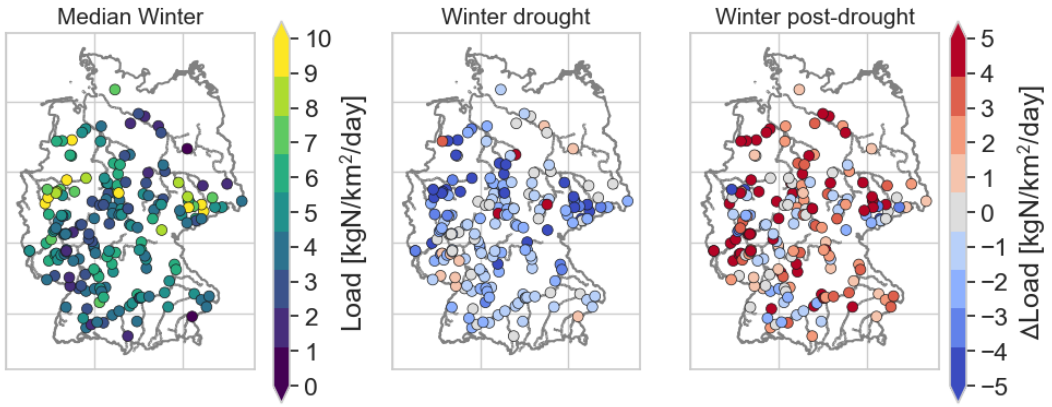

Figure 2.13: Median value of NO3.N specific load of all winter samples (A). Differences of median values of NO3.N specific load during winter seasonal extremes under drought (B) and post-drought conditions (C) compared to median values of all winter samples (A).

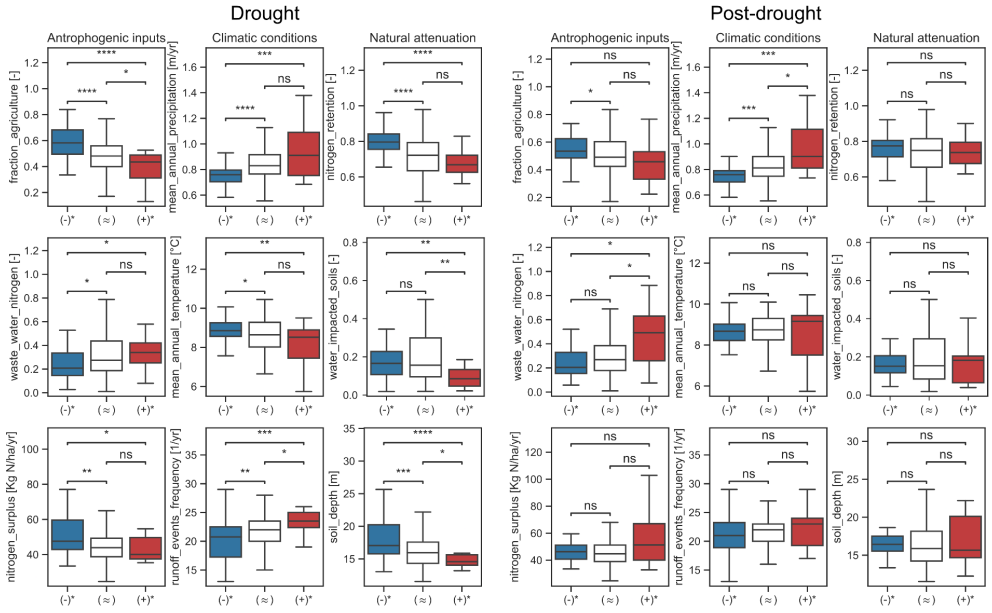

Figure 2.14: Catchment characteristics linked to anthropogenic inputs, climatic conditions, and natural attenuation for catchments exhibiting significant negative anomalies (–), no significant anomalies (≈), and significant positive anomalies (+) during spring drought (left panels) and post-drought (right panels) periods. The Kruskal–Wallis test was used to determine significant differences between boxplots (ns: pval >= 0.05, *: pval < 0.05, **: pval < 0.01).

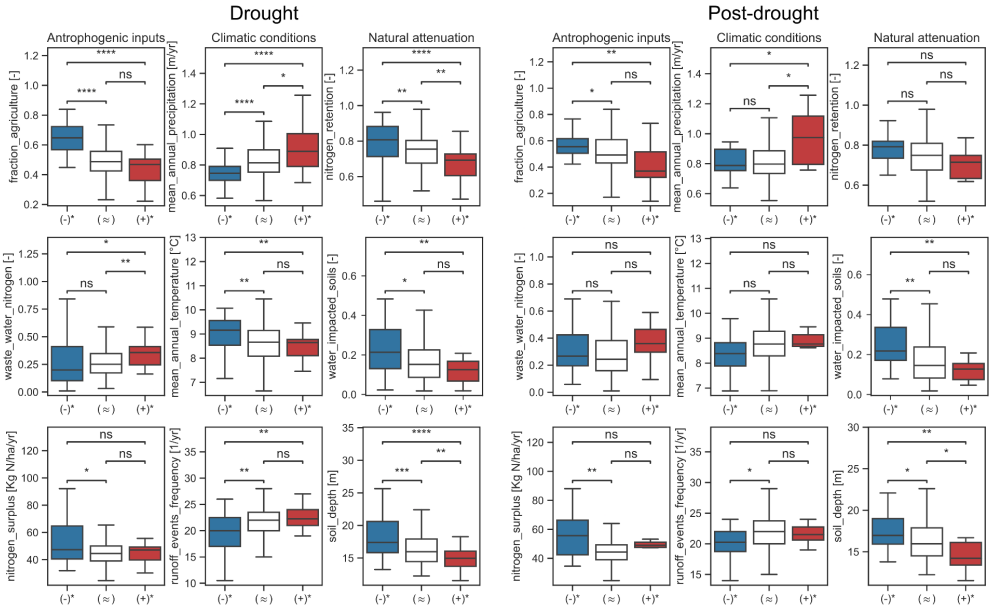

Figure 2.15: Catchment characteristics linked to anthropogenic inputs, climatic conditions, and natural attenuation for catchments exhibiting significant negative anomalies (–), no significant anomalies (≈), and significant positive anomalies (+) during autumn drought (left panels) and post-drought (right panels) periods. The Kruskal–Wallis test was used to determine significant differences between boxplots (ns: pval >= 0.05, *: pval < 0.05, **: pval < 0.01).

Table 2.3: A list of catchment descriptors from the QUADICA dataset [103] that are significantly different in catchments with significantly higher (*+) and significantly lower (*-) nitrate anomalies during winter droughts compared to no-drought conditions. The sign next to the descriptor shows the direction of the relationship (e.g., P_mm (+): catchment anomalies are higher in catchments with higher mean annual precipitation). We used only descriptors normalized by catchment area (i.e., to facilitate comparability between catchments of diverse sizes in our dataset) representative for the study period (i.e., 1980–2020).

Category	Descriptor	Description	Sign of correlation
CLIMATIC AND TOPOGRAPHIC	P_mm	Mean annual precipitation	+
	P_lambda	Mean precipitation frequency λ	+
	P_alpha	Mean precipitation depth	+
	PET_mm	Mean annual potential evapotranspiration	+
	AI	Aridity index as AI=PET_mm/P_mm	-
	T_mean	Mean annual air temperature	-
	dem.mean	Mean elevation of catchment	+
	dem.median	Median elevation of catchment	+
	slo.mean	Mean topographic slope of catchment	+
	slo.median	Median topographic slope of catchment	+
	twi.mean	Mean topographic wetness index	-
	twi.med	Median topographic wetness index	-
BIOGEOCHEMICAL RETENTION	twi.90p	90th percentile of the TWI	-
	f_calc	Fraction of calcareous rocks	+
	f_fissured	Fraction of fissured aquifer	+
	f_fiss1	Fraction of fissured aquifer (code 3)	+
	f_fiss2	Fraction of fissured aquifer (code 4)	+
	dtb.median	Median depth to bedrock in the catchment	-
	f_gwsoils	Fraction of water-impacted soils	-
	f_clay	Mean fraction of clay in top soil	+
	f_clay_agri	Mean fraction of clay in top agricultural soil	+
	WaterRoots	Mean available water content in the root zone	+
ANTHROPOGENIC INPUTS	soilP.mean	Mean top soil P in catchment	-
	soilN.mean	Mean top soil N in catchment	+
	f_artif	Fraction of artificial land cover	+
	f_agric	Fraction of agricultural land cover	-
	f_forest	Fraction of forested land cover	+
	f_urban	Fraction of urban land cover	+
	f_industry	Fraction of industrial land cover	+
	f_arable	Fraction of arable land	-
	f_pastures	Fraction of pastures	+
	f_agri_hetero	Fraction of heterogeneous agricultural areas	+
	f_fores	Fraction of forested land cover	+
	f_scrub	Fraction of scrubland	+
	f_sarea	Fraction of source areas	-
	pdens	Mean population density	+
	N_WW	Sum of N input from point sources including waste water treatment plants	+
	P_WW	Sum of P input from point sources including waste water treatment plants	+
	dNsurp71_91	Change in mean N surplus between the periods 1971-1990 and 1991-2015	-
	het_v	Mean ratio between potential seepage and groundwater NO3-N concentrations	-

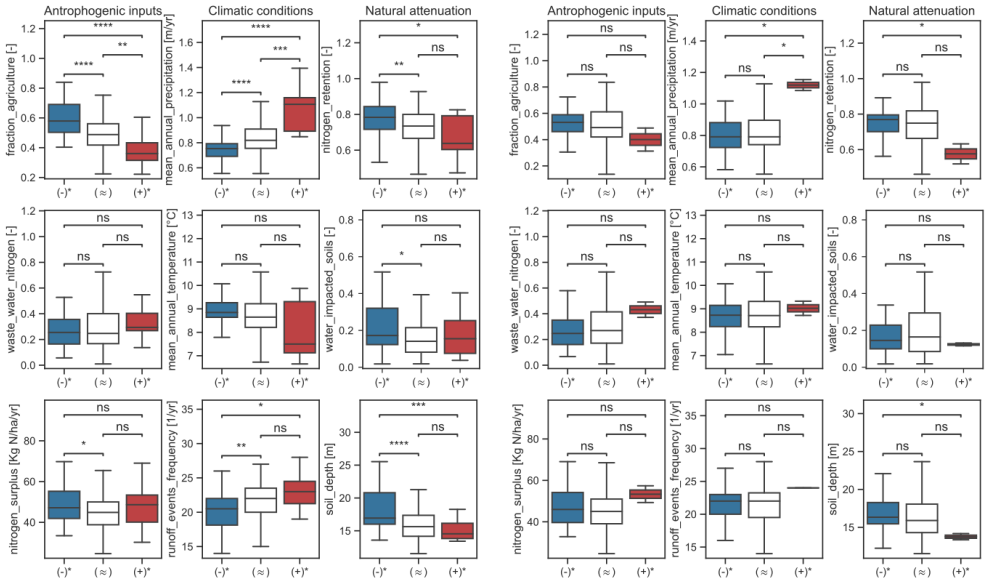

Figure 2.16: Catchment characteristics linked to anthropogenic inputs, climatic conditions, and natural attenuation for catchments exhibiting significant negative anomalies (–), no significant anomalies (≈), and significant positive anomalies (+) during summer drought (left panels) and post-drought (right panels) periods. The Kruskal–Wallis test was used to determine significant differences between boxplots (ns: pval >= 0.05, *: pval < 0.05, **: pval < 0.01).

Table 2.4: A list of catchment descriptors from the QUADICA dataset [103] that are significantly different in catchments with significantly higher (*+) and lower (*-) nitrate anomalies during winter post-droughts compared to no-drought conditions. The sign next to the descriptor shows the direction of the relationship (e.g. P_mm (+): catchment anomalies are higher in catchments with higher mean annual precipitation). We used only descriptors normalized by catchment area (i.e., to facilitate comparability between catchments of diverse sizes in our dataset) representative for the study period (i.e., 1980–2020).

Category	Descriptor	Sign of correlation
BIOGEOCHEMICAL RETENTION	dtb.median	-
CLIMATIC AND TOPOGRAPHIC	P_WW	+
	P_alpha	+
	P_lambda	+
	P_mm	+
ANTHROPOGENIC INPUTS	f_artif	+
	f_industry	+
	N_WW	+
	pdens	+
	Nsurp91_15	+
	DNsurp71_91	-

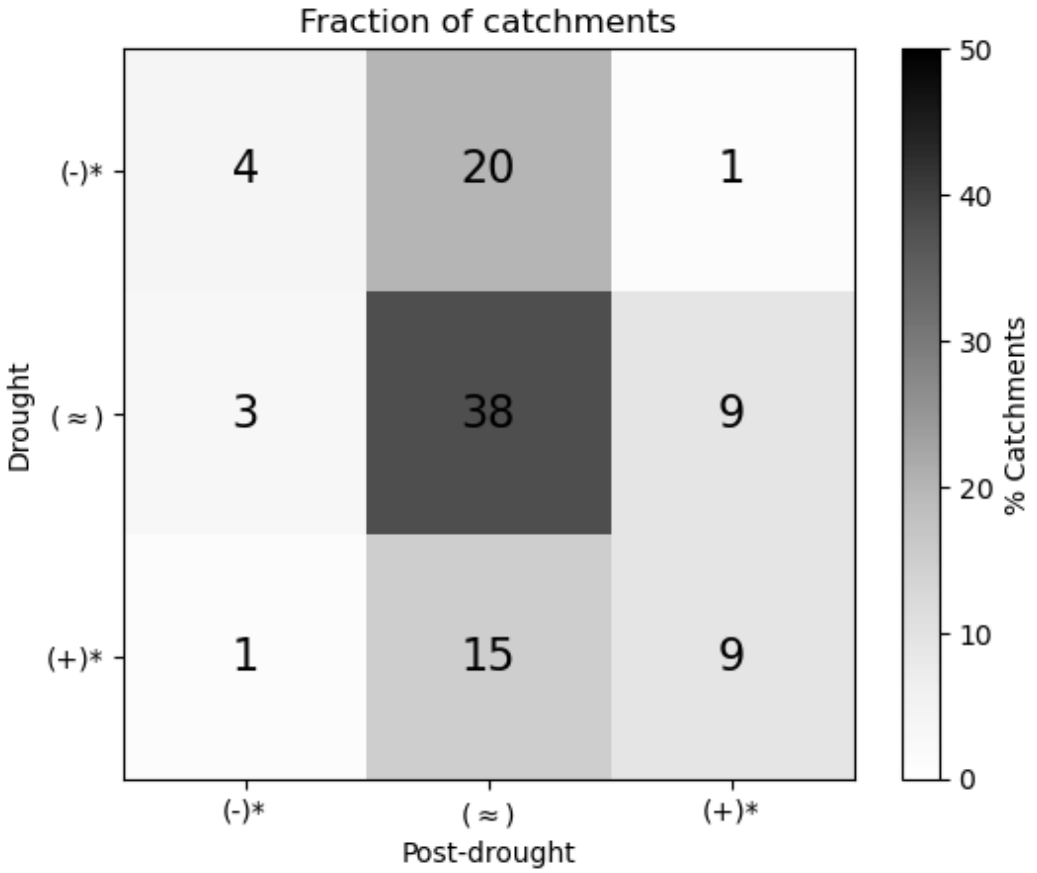

Figure 2.17: Fraction of catchments with significant positive (+)*, negative (–)* and non significant (≈) differences compared to no-drought conditions (refer to figure 1) during winter droughts and post-droughts, and their correspondence to each other (e.g., only 3% of the catchments exhibit significantly lower nitrate anomalies during winter post-drought and non-significant nitrate anomalies during winter droughts compared to no-drought conditions).

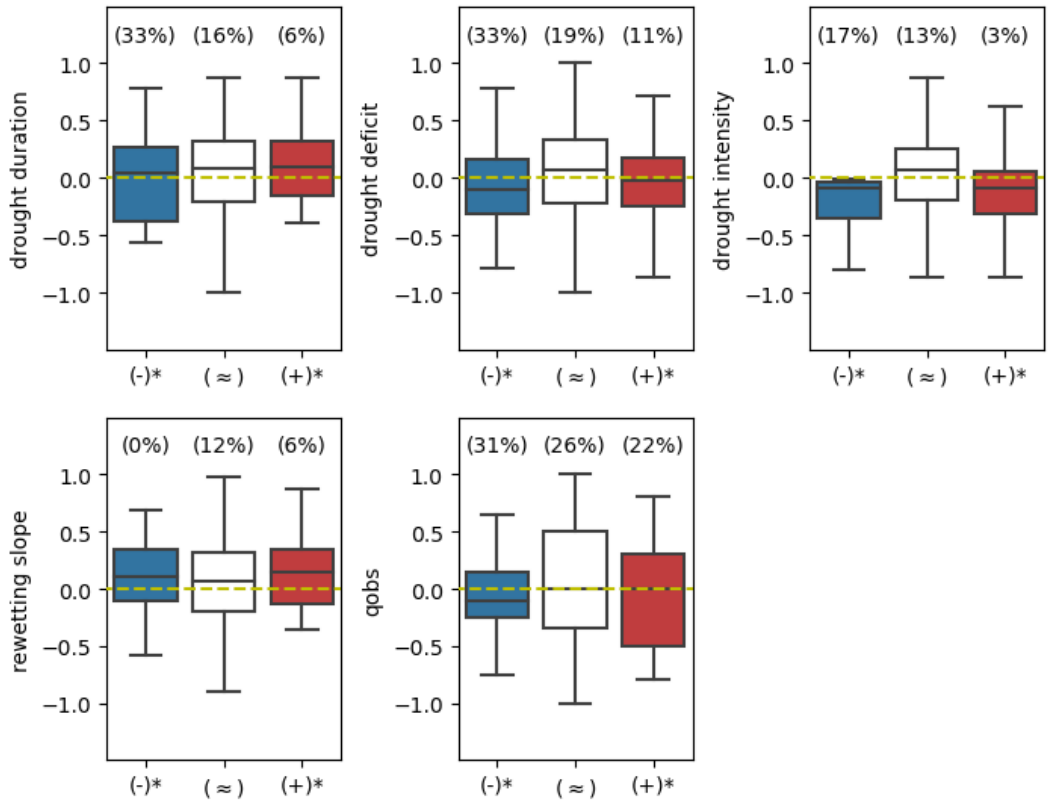

Figure 2.18: Spearman correlations between the magnitude of nitrate anomalies and drought characteristics (duration, deficit and intensity) and post-drought hydrological conditions (rewetting slope and specific discharge, qobs) across individual catchments. Catchments are categorized into three groups: catchments with significant negative (–)*, significant positive (+)* and no significant (≈) differences in nitrate anomalies (ΔZ-NO3.N) during winter post-droughts when compared to no-drought conditions (refer to figure 1, main Manuscript). Drought duration represents the length in days of each drought. Drought deficit indicates the accumulated difference between smoothed streamflow time series and the variable threshold (please refer to the Method section in the main Manuscript for details). Drought intensity is a ratio of the drought deficit and duration. The rewetting slope represents the speed of wetness recovery from droughts and is computed as the slope of the linear regression between daily discharge and time during the period of 15 days prior to and 15 days after the end of the corresponding drought event. qobs represents the daily mean specific discharge of the sample day in mm/day.

3

Disentangling Scatter in Long-Term Concentration–Discharge Relationships: The Role of Event Types

Fertilizer application on agricultural land remains the main source of nitrate contamination in human-impacted catchments, despite regulations of the past decades that stimulated a reduction of fertilizer application in Europe [121]. Moreover, due to longlasting legacy effects, a delay in the reduction of riverine nitrate concentration (C) was reported in many catchments [122, 25, 123, 23].

Long-term concentration–discharge (C–Q) relationships are a valuable tool for analyzing water quality gradients and trends, and for developing water management strategies [124]. The shape of C–Q relationships encodes export patterns and reflects the temporally varying quantities of critical substances such as nutrients delivered to streams [125, 40, 41]. Depending on the slope of the log–log linear dependency of concentrations from discharge (Q), three different export patterns [125] can be defined: dilution (negative slope), enrichment (positive slope) and neutral (no relationship between C and Q or slope close to 0). Differences in long-term C–Q-relationships among catchments can be associated with differences in availability and spatial distribution of solute sources [43, 126, 127, 33], their hydrologic connectivity [128, 77, 30] and biogeochemical processes within the soil and stream that can retain or permanently remove nitrate from stream water [129, 77, 45, 130].

Biogeochemical processes that affect nutrient cycles in soil and water might add variability to long-term C–Q relationships. The effectiveness of the denitrification process, which removes nitrate from the soil, depends on periodic environmental factors such as temperature and soil moisture and the availability of electron donors [131, 132]. Instream removal processes are also more efficient during low flows and higher temperatures, adding more variability to the low-flow portion of the longterm C–Q relationships [38, 45]. Moreover, the availability of nitrate sources is balanced by fertilizer application and mineralization of organic nitrogen compounds and hence varies in time, adding temporal variability to C–Q relationships. Timing

of fertilizer application is often unknown, and the mineralization processes depend on chemical soil conditions and environmental factors (e.g., soil moisture and temperature) that mediate communities of microorganisms [133, 17]. Average residence times of nitrate in agricultural catchments can last for decades, producing a legacy in soil [22, 29, 122, 134] that can buffer the periodic effect of biogeochemical processes which reduces the variability in the concentration of nitrate [21, 123, 135].

The scatter of C–Q relationships might also be related to hydrologic conditions at the time of sampling [48, 136], which are investigated for a large number of catchments only by a few recent studies [47, 137]. Minaudo et al. [47] showed that in most of the 219 French catchments, nitrate samples taken during baseflow conditions exhibit an enrichment export pattern, while during runoff events, a neutral or opposite pattern (dilution) prevails, generating scatter in the combined long-term C–Q relationships. The cause of this scatter can be also traced to a variety of responses observed at the event scale in several studies with high-frequency data in single or a few catchments [e.g., 76, 138, 115, 139].

Our study relies on low-frequency nitrate data, which are often used to build long-term C–Q relationships [e.g., 140, 141]). However, studies with high-frequency data found large variability in the C–Q patterns during events [event C–Q relationship; e.g., 48, 77, 75]) that might add scatter to the long-term C–Q relationship. Disparate event C–Q relationships in a catchment over time are mainly attributed to varying dominant flow sources (e.g., groundwater, shallow subsurface flow), antecedent wetness conditions [74, 48, 75], time of fertilizer application [76, 77, 72], biogeochemical cycling [46] and runoff event characteristics or types [78, 79, 80, 48]. For example, Winter et al. [96] showed that in a few catchments located in Central Germany, runoff events generated by rainfall with dry antecedent conditions export lower nitrate concentrations due to lower hydrologic connectivity but exhibit a high variability of event C–Q slopes. In contrast, Knapp et al. [48] showed that using high-frequency concentration and discharge observations from one small forested catchment located in Switzerland during larger runoff events with dry antecedent conditions the slopes of the event C–Q relationships are more positive due to the accumulation of nitrate in the soil during dry periods by atmospheric deposition and the subsequent mobilization by event water. Moreover, in several catchments in USA and Europe, snowinduced events were found to export high nitrate concentration [115, 74, 142]. Similarly, in the previously mentioned Central German catchments, Winter et al. [96] found high nitrate concentrations and flat event C–Q slopes during snow-impacted events, indicating that sufficient nitrate sources are available and most of the relevant flow paths are activated and connected to the stream during such events.

It was shown that hydrologic connectivity as a portion of the catchment connected to the stream via surface or subsurface pathways increases according to the wetness state of the catchment [31, 53] and modulates export of nutrients at different scales. At seasonal scale, nutrient transport to streams can be increased with higher hydrologic connectivity in catchments with abundant sources [143, 144, 145]. At event scale, the activation of different flow paths during different levels of hydrologic connectivity evaluated using shallow wells or models can partially explain changes in nitrate concentration during events [146, 147, 148]. However, at the larger scale, such observations are not available.

At catchment scale, soil moisture or discharge rates are often used as proxy of hydrologic connectivity [e.g., 32, 53]). The event runoff coefficient (i.e., a volumetric ratio of quick flow and input precipitation or snowmelt), which represents how efficiently streamflow responds to catchment water inputs, can also be considered as its proxy [e.g., 149, 72, 146]). Higher runoff coefficients are associated with wetter antecedent catchment states, indicating that such conditions favor a more efficient rainfall–runoff response [51, 72] and possibly activation of more surface and subsurface hydrologic flow pathways that facilitate fast transport of water and nutrients from the landscape to the stream [31, 66, 148].

New approaches to characterize and classify runoff events according to hydrologic conditions offer a possibility to efficiently aggregate information about the antecedent wetness state of catchments and characteristics of inducing events (e.g., rainfall, snowmelt) and to distinguish events with contrasting hydrological responses for a large number of catchments [1]. Such classification of event types combined with concentration of nitrate in stream water might unravel scatter in long-term C–Q relationships as exemplified in Fig. 3.1. In Fig. 3.1a, biweekly nitrate data are associated with the event type at the time of stream water sample collection. When these data are plotted in the log–log C–Q space (Fig. 3.1b), some event types exhibit positive (higher concentration) or negative (lower concentration) deviations from the long-term C–Q relationship.

Our study aims for the first time to investigate the presence of systematic deviations in long-term C–Q relationships produced by different runoff event types for a large dataset of catchments. We hypothesize that these deviations are related to the differences in nitrate transport during these event types and we investigate such deviations from the long-term C–Q relationships in 184 German catchments. Specifically, our goal is to examine the effect of runoff event types on the observed scatter in C–Q relationships by addressing the following research questions:

1. Do samples collected during different event types deviate differently from the long-term C–Q relationships observed at the catchment outlets?
2. Which climatic and landscape characteristics explain differences in the observed C–Q deviations among German catchments?
3. Which are the potential mechanisms that explain the direction and magnitude of C–Q deviations for different event types?

Understanding the nature of nitrate deviations from the long-term C–Q relationships might provide useful information for water quality managers to reduce the risk of extreme nitrate loads to water bodies, as well as improve sampling campaigns to better capture nitrate C–Q scatter.

3.1 Methods

3.1.1 Study catchments and data

In this study, we analyzed low-frequency (biweekly to monthly) nitrate concentration data from 184 mesoscale catchments in Germany for the period from 2000 to 2015. The data were

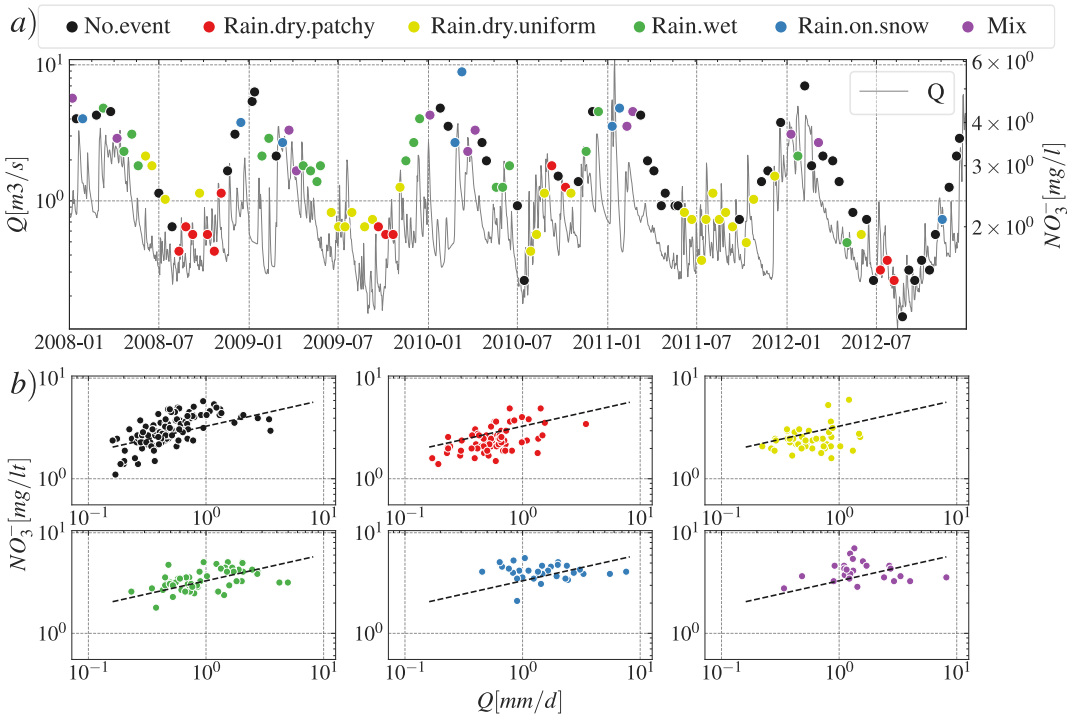

Figure 3.1: (a) Time series of daily discharge and biweekly grab sample nitrate concentrations during event and no-event conditions in the Naab River at the gauge of Unterköblitz, Bavaria over a period of 5 years. Event types are differentiated by colors (see Fig. 3.3 for details). (b) Double logarithmic plot of C–Q pairs for samples (from 2000 to 2012) taken during different event types and no-event conditions. Dashed black lines show the long-term C–Q relationships (same line in each subplot) obtained from linear regression in a double logarithmic plot of C–Q values for all available samples.

obtained from the water quality and quantity database of Germany [150, 2] in combination with a recently developed classification framework of runoff events [1]. Similar to Ebeling et al. [2], we exclude the data prior to the 2000s to avoid impacts of improved wastewater treatment technologies in Germany. In total, we considered 33 713 nitrate samples.

Sizes of study catchments range from 95 to 23 615 km^2 (with a median size of 704 km^2 and cover all four main German natural regions: the North German Plain, Central Uplands, South German Scarplands and Alpine Foreland (Fig. 3.2a). The climate varies from temperate oceanic to temperate continental from west to east. Mean annual precipitation ranges from 567 mm in the lowland northeastern catchments up to 1379 mm in the alpine catchments in the south. The predominant land use in the study catchments is agriculture, with a median coverage among catchments of 50 % and a range from 13 % to 84 %. The median portion of catchment area covered by forest is 41 % of the catchment area (Fig. 3.2b).
The runoff event classification framework of Tarasova et al. [1] considers runoff events identified from daily discharge data in catchments with no major flow regulations. The location of the discharge stations does not always coincide with water quality stations in the dataset of Ebeling et al. [2]. Both datasets are linked by pairing stations that are located on the same stream and differ less than 20 % in their drainage areas. These were considered as identical outlets, similar to Guillemot et al. [145]. The mean overlap between drainage areas of the corresponding outlets from the two datasets is 95 % with a standard deviation of 5 %.

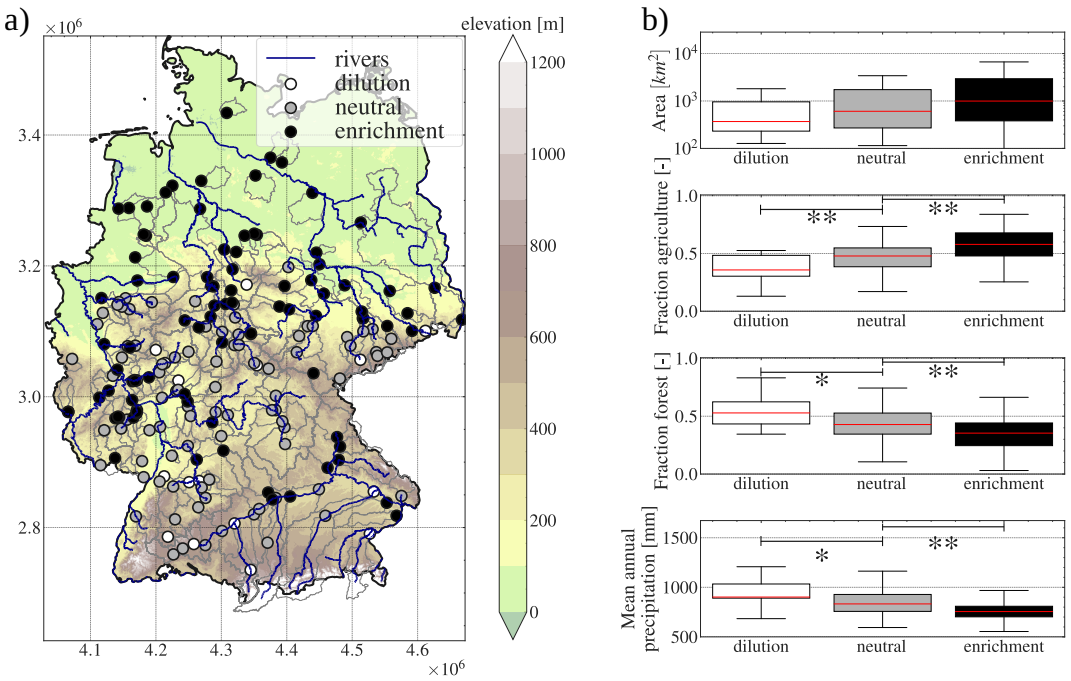

Figure 3.2: (a) Study area and stations of nitrate concentration measurements in stream water. Gray lines show catchment boundaries. Catchment outlets (points) are color-coded according to the long-term export pattern (dilution, neutral and enrichment). Blue lines show the main rivers. The background color map corresponds to the elevation. Purple labels indicate German natural regions. (b) Area, fraction of agriculture, fraction of forest and mean annual precipitation of study catchments grouped according to export patterns (dilution, neutral and enrichment). Red lines show medians of boxplots and significance of median differences between adjacent boxplots was estimated using the Kruskal–Wallis test (displayed as $*$ for $p < 0.05$ and $**$ for $p < 0.01$).

3.1.2 Identification and classification of hydrological events

Runoff events and corresponding precipitation events were separated using an automated time-series approach developed by Tarasova et al. [51]. The method was applied to daily discharge and precipitation data obtained from the REGNIE dataset [151]. The method includes baseflow separation, precipitation attribution (i.e., corresponding inducing events (rainfall and/or snowmelt) are linked to runoff events) and an iterative procedure to adjust site-specific thresholds for the refinement of multi-peak events. The median event duration is 12 d with a standard deviation of 7.7 d. The shortest event duration is 1 d, however, 95 % of the identified events exhibit a duration of 3 or more days. Each identified runoff event was then classified in the first place by considering the nature of inducing events (rainfall, mixture of rainfall and snowmelt or rain-on-snow) (Fig. 3.3a) using the proportions of rainfall and snowmelt in the total volume of precipitation events (Table 3.1 in the Supplement). In the second step, we considered the antecedent wetness state (wet or dry) by accounting for the catchment-averaged soil moisture state prior to the event. Catchment-average snow water equivalent and soil moisture were simulated by the mesoscale hydrological model [152, 153] and provided in Zink et al. [154]. Additionally, the classification considers spatial organization of soil moisture within the catchment using the spatial coefficient of variation of soil moisture, classifying events as uniform or patchy, with the latter corresponding to highly variable soil moisture within the catchment. A more detailed description of the classification framework is provided in Tarasova et al. [1].

Each nitrate sample was linked to either no event (No.event), or to one of the five event types (Fig. 3.3a): rain-on-snow (Rain.on.snow), mixture of rainfall and snowmelt (Mix), rainfall during wet antecedent conditions (Rain.wet), rainfall during dry antecedent conditions with spatial uniform distribution of soil moisture (Rain.dry.uniform) and rainfall with dry antecedent conditions with heterogeneous spatial distribution of soil moisture (Rain.dry.patchy). Note that we simplified the event types to increase the number of nitrate samples of each event type.

3.1.3 Long-term C–Q export patterns

For each catchment, the long-term C–Q relationship was derived as a linear regression between nitrate concentration (C) and discharge (Q) in the log–log space (Fig. 3.3b). Based on the slope of the long-term C–Q relationships (b), we grouped all study catchments according to three different long-term C–Q export patterns: dilution ($b < 0.1$) refers to a limitation of sources during high flows, enrichment ($b > 0.1$) is related to a transport limitation with abundant sources or solute uptake during low flows [45], and neutral ($b \sim 0$) indicates no monotonic relationship between C and Q. As stated by Ebeling et al. [44], this latter group exhibits largely invariable concentration with low ratios of coefficients of variation (CVc/CVq). Three different catchments are shown as an example of each export pattern in Fig. 3.3c.

3.1.4 Quantifying the deviations from long-term C–Q relationship

For each catchment, we want to quantify whether samples taken at a specific event type show systematic deviations from the long-term C–Q regression compared to all samples. We

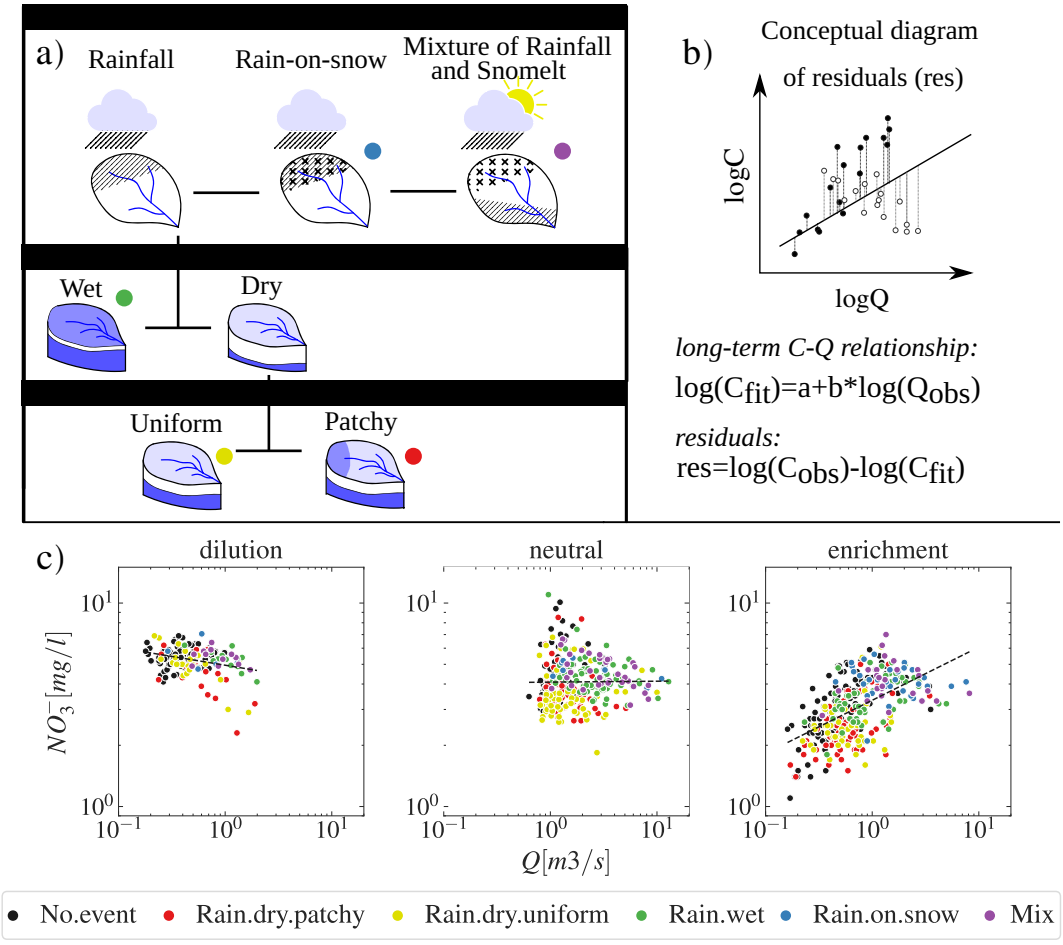

Figure 3.3: (a) Hierarchical scheme for event classification (modified from Tarasova et al. [1]; classification criteria are provided in Table 3.1). Colored dots located next to the five different event types indicate their markers. (b) C_{obs} and Q_{obs} are observed concentration and discharge, C_{fit} is the nitrate concentration estimated from fitting the long-term C–Q relationship with a linear relation in log–log space, and res is the residual value. (c) C–Q plots for three different catchments attributed to different long-term nitrate export patterns based on the logC–logQ slope b, i.e., dilution ($b < -0.1$, the Würm River in Pforzheim), neutral ($b \sim 0$, the Wupper River in Opladen) and enrichment ($b > 0.1$, the Naab River in Unterköblitz).

quantified the deviation of each grab sample from the long-term C–Q relationship for each catchment by computing the corresponding residual concentration from the long-term C–Q linear regression line (Fig. 3.3b). Resulting residuals were subsequently grouped according to the hydrological event type at the time of sampling.

Due to the variable number of grab samples attributed to different event types (Fig. 3.8 in the Supplement), for each catchment, we performed a bootstrapping procedure that can explicitly handle unbalanced data by iteratively comparing two random subgroups of samples with the same size [undersampling method, e.g., 155]). The procedure is implemented in the following way for each catchment: n nitrate samples of a certain event type and the same number of nitrate samples from all samples (general pattern) are chosen randomly with replacement (i.e., each data point can be chosen more than once, following bootstrapping procedure). The difference of median residuals of an event type and residuals of the general pattern is then the measure of deviation of a corresponding event type from the long-term C–Q relationship (Δres). We obtained this measure 10 000 times to robustly compute its distribution (Fig. 3.9) and median value (Δres50). The number of samples n was chosen for each catchment and event type according to the number of nitrate samples available for the corresponding event type. For each catchment, event types with less than 10 nitrate samples are excluded from the analysis. The median number of nitrate samples among all study catchments and event types is 27. For each catchment and from all the iterations, we obtain the median deviations between event types and the general pattern (Δres_{50}). In order to evaluate the persistence of C–Q deviations across catchments, we tested the significance of Δres_{50} across catchments for each event type using the non-parametric Kruskal–Wallis test [106] at the significance level $\alpha = 0.05$.

Low-frequency datasets such as the one used in our study might contain samples collected during different phases of the event hydrograph (e.g., falling or rising limb). This might hamper the interpretability of the results due to possible bias in observed nitrate concentration linked to the time of sampling and the hysteresis effect revealed in high-frequency observations [e.g., 138, 75]). In fact, Pohle et al. [137] showed systematic differences in nitrate concentration between samples collected during rising and falling limbs for numerous catchments in Scotland. To understand the potential effect of the hysteresis on the deviations from long-term C–Q (Δres_{50}), we repeat the bootstrapping procedure described above considering samples collected during the rising limb, falling limb and near the event peak (near-to-peak). The rising limb of a runoff event starts at the beginning of the event and finishes 1 d before the day of the peak discharge. The falling limb starts 1 d after the day of the peak discharge and finishes at the end of the runoff event. In addition, we defined near-to-peak as samples collected from 1 d before to 1 d after the day of the peak discharge. Of the total samples taken during runoff event types, 34 % correspond to the rising limb, 55 % to the falling limb and 30 % to near-to-peak. Notice that the definition of near-to-peak samples allows some overlap with the other two groups of samples to use a more balanced number of samples than considering samples collected on the day of the peak of discharge only (11 % of the samples were collected during the day of the peak discharge).

3.1.5 Catchment descriptors and relationships to C–Q deviations

In order to explore the differences of deviations from the long-term C–Q relationships across the catchments, we examined the Spearman rank correlation of median residuals for each catchment with various catchment descriptors. Here, we only examine catchment descriptors that were previously identified as primary controls of the nitrate C–Q export patterns in Germany [2]. This includes topographic descriptors (median topographic wetness index, median slope and area); land cover descriptors (fraction of agriculture, forest and artificial surface); soil and aquifer descriptors (median soil depth and fraction of sedimentary aquifer); nitrate sources descriptors (nitrate surplus, agricultural horizontal heterogeneity, nitrate vertical ratio); and hydrometeorological descriptors (aridity index, mean annual potential evapotranspiration, precipitation and temperature) (Table 3.2). Detailed derivations of the above-mentioned catchment descriptors are provided in Ebeling et al. [2].

3.2 Results

3.2.1 Frequency of runoff event types

Stream water samples taken during runoff event conditions account for 58 % of all samples. These samples are classified to one of the five event types as follows: 18 % – Rain.dry.patchy, 11 % – Rain.dry.uniform, 15 % – Rain.wet, 7 % – Rain.on.snow and 7 % – Mix.

On average across catchments, the fraction of samples taken during each event type vary at different discharge rates. Above median discharge rate, 74 % of all samples correspond to an event and the event types Rain.wet, Rain.on.snow and Mix occur more frequently (Fig. 3.4a). In contrast, only 49 % of samples below median discharge rate were taken during an event and most of these grab samples correspond to Rain.dry.patchy and Rain.dry.uniform types.

The frequency of event types also varies seasonally (Fig. 3.4b). In winter, most of the grab samples were taken during Rain.on.snow, Mix and Rain.wet event types. In the spring months, Rain.dry events become more frequent than Rain.on.snow, Mix and Rain.wet event types. During summer, most of the samples were taken either under No.event conditions or during Rain.dry.uniform and Rain.dry.patchy events. In autumn, the frequency of grab samples taken during Rain.wet, Rain.on.snow and Mix event types increases.

3.2.2 Long-term C–Q relationships and deviations during event types

We computed long-term nitrate C–Q relationships for the 184 catchments, obtaining slopes (b) from -0.6 to 1.48, with a mean of 0.13. In total, 88 study catchments exhibit neutral patterns, 80 catchments are characterized by enrichment patterns and only 16 catchments show dilution patterns. Across all catchments, the median R^2 value of the long-term C–Q relationship was low (0.14), indicating the presence of considerable scatter in the regressions.

We explored the residuals (res) of all nitrate data from all catchments and found that 65 % and 68 % of the samples taken during Rain.on.snow and Mix event types, respectively, have positive residual values, indicating that concentrations were higher than the long-term log–log linear C–Q regressions. In contrast, 69 % and 60 % of the samples during Rain.dry.patchy and Rain.dry.uniform events, respectively, have negative residuals values. We found a less clear

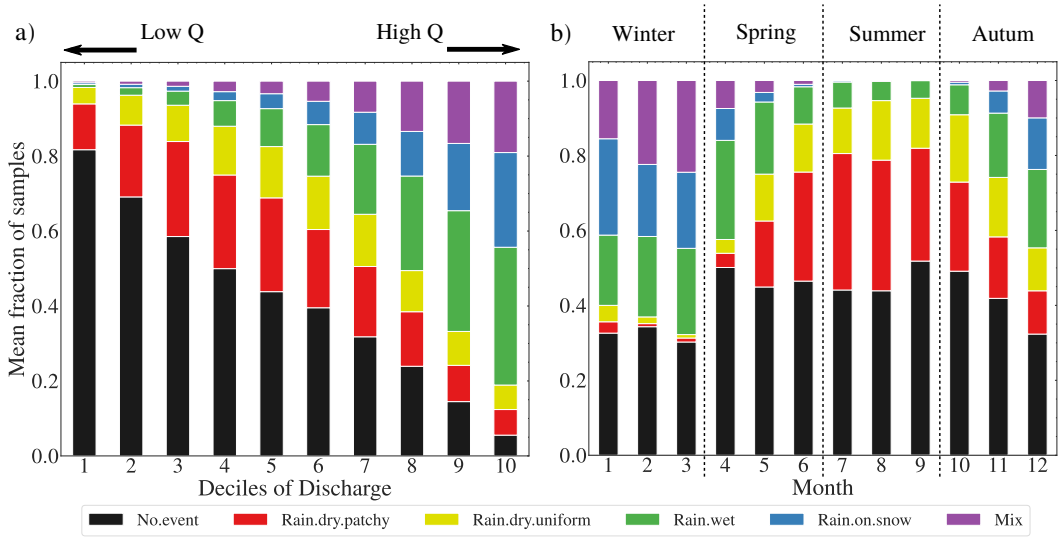

Figure 3.4: (a) Mean fraction of samples linked to each event type according to each catchment decile of discharge, and (b) seasonal distribution of mean fraction of samples linked to each event type in the study catchments.

picture for samples taken during Rain.wet events and No.event conditions with 53 % and 56 % of positive residuals, respectively (Fig. 3.10).

We found strong differences in median deviations from the long-term C–Q relationships (Δres_{50}) among different event types (Fig. 3.5a). Rain.on.snow and Mix event types often have more positive Δres_{50} values (79 % and 93 % of the study catchments correspondingly) (Fig. 3.5b) when compared across catchments. Contrastingly, Rain.dry.patchy and Rain.dry.uniform event types show negative values of Δres_{50} more often (96 % and 61 % of the study catchments), with Rain.dry.patchy events showing stronger deviations. Contrasting behavior between snow-impacted events (i.e., Mix and Rain.on.snow) and rainfall events with dry antecedent wetness conditions (Rain.dry.patchy and Rain.dry.uniform) occurs across most of the study catchments independently of their long-term export pattern (Fig. 3.5b). For Rain.wet events, deviations can be negative as well as positive (52 % and 48 % of study catchments, respectively) with a median of Δres_{50} across catchments close to zero (Fig. 3.5a). For samples that were taken during No.event conditions, the Δres_{50} value is slightly positive in 85 % of all catchments.

The sign of C–Q deviations are in line with observed nitrate concentration during different event types (Fig. 3.11). Negative residuals during Rain.dry.patchy and Rain.dry.uniform events coincide with lower nitrate concentrations for most of the catchments, independent of the long-term C–Q pattern. Similarly, during Rain.on.snow and Mix events, positive C–Q deviations correspond to nitrate concentrations higher than median for most of the catchments with a neutral or enrichment C–Q pattern. For catchments with the dilution export pattern, nitrate concentration for Rain.on.snow and Mix events is similar to the average, however higher discharge generates positive residuals in this case.

We analyzed the influence of the sampling time within runoff events separating samples taken during the rising limb, near-to-peak and falling limb. Although there are certain data limitations for a few groups of samples (gray tiles in Fig. 3.12b), we are able to reproduce the analyses for most of the cases. Similar to the case when using all samples (Fig. 3.5b), the values of Δres_{50} for samples taken during the rising limb, near-to-peak and falling limb

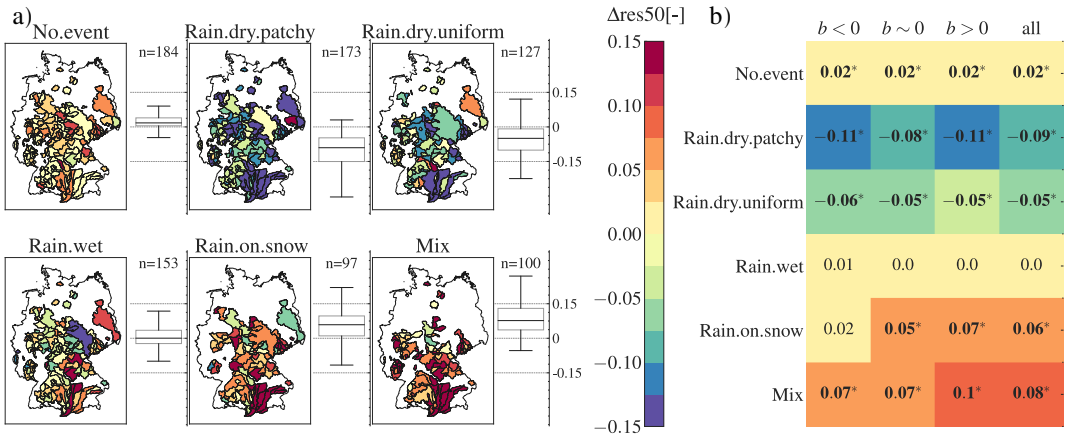

Figure 3.5: Median deviations of nitrate concentrations from the long-term C–Q relationships (Δres_{50}). (a) Δres_{50} values of different event types for each catchment. On the right-hand side of each map, boxplots show the distribution of Δres_{50} values across catchments for each event type (box limits represent the interquartile range and whiskers correspond to the 5th and 95th percentiles). (b) Heatmap of Δres_{50} values averaged across different groups of catchments, considering all nitrate data for each event type and No.event. The first three columns of the heatmap correspond to one of the long-term export patterns (i.e., dilution, slope $b < 0$, neutral, slope $b \sim 0$, and enrichment, slope $b > 0$) and the fourth column corresponds to all study catchments. Bold font and $*$ indicates significant differences (Kruskal–Wallis test, $p < 0.05$) between median deviations across catchments for each event type and median deviation across catchments of all nitrate samples.

are mostly positive for Rain.on.snow and Mix events and negative for Rain.dry.patchy and Rain.dry.uniform. Our results confirm that the time of sampling during runoff events does not affect our findings regarding median C–Q deviations for different types of runoff events.

Although the sign of C–Q deviation is consistent across catchments for most of the event types, the magnitude of deviation varies across catchments (Fig. 3.5a). The variability of Δres_{50} expressed as interquartile ranges across catchments (boxplots in Fig. 3.5a) is the lowest for the samples taken during No.event conditions (0.03) and Rain.wet events (0.06). The largest variability was detected for Rain.dry.patchy events (0.1), followed by Mix (0.09) and Rain.dry.uniform events (0.09).

3.2.3 Variability of C–Q deviations across German catchments

We analyzed the spatial variability of C–Q deviations for different event types (Fig. 3.5a) computing Spearman rank correlations between deviations and catchment descriptors. We found significant correlations between Δres_{50} for each event type and catchment descriptors. Topographic properties (i.e., median slope and topographic wetness index) have the strongest correlation to the Δres_{50} values of almost all event types (Fig. 3.6). Specifically, flatter catchments (low median topographic slope) with greater soil depths that are mostly located in the North German Plain and Alpine Foreland tend to exhibit more positive residuals for Rain.wet, Rain.on.snow and Mix events, and more negative residuals for Rain.dry.patchy events and samples taken during No.event conditions (Fig. 3.5a). Catchments with these characteristics often show high agricultural land cover (Fig. 3.13), however the fraction of agriculture shows less significant correlations with Δres_{50} than topographic descriptors. Moreover, in catchments with larger fractions of water-impacted soils (e.g., stagnosols, semi-terrestrial, semi-subhydric, subhydric and moor soils), we found more positive residuals for

snow-impacted events (Rain.on.snow, Mix) and more negative residuals for Rain.dry.patchy events. These catchments are often located in Central East or North-West Germany.

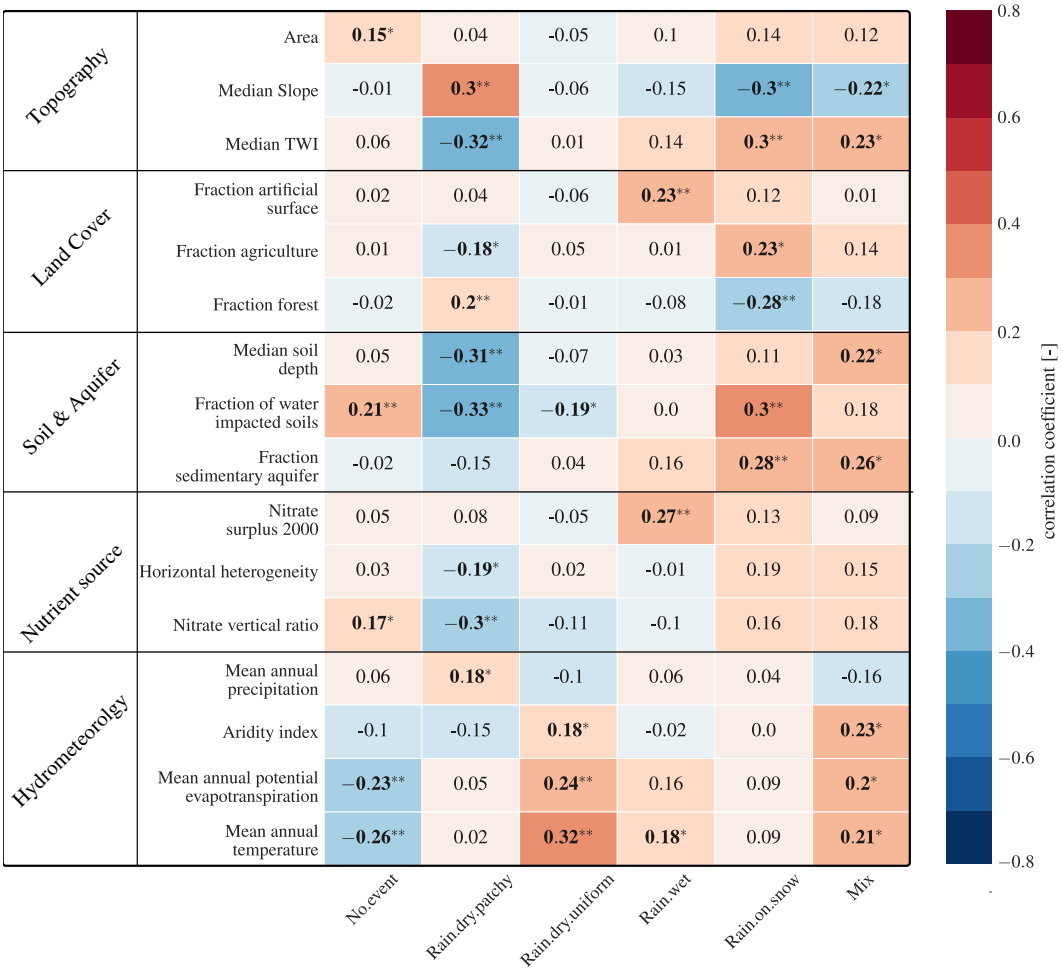

Figure 3.6: Spearman rank correlation coefficient between deviations of nitrate concentrations from the long-term C–Q relationships (Δres_{50}) of a particular event type across study catchments and catchment descriptors. Significant correlations are indicated by bold font and $*$ for $p < 0.05$ and $**$ for $p < 0.01$.

Correlations between Δres_{50} and fraction of agriculture in the catchments are less significant than those with topographic descriptors (Fig. 3.6). Instead, we observed strong correlations between Δres_{50} and the fraction of forest ($p < 0.01$). Forested catchments show less positive Δres_{50} values for Rain.on.snow events and less negative values for Rain.dry.patchy events. However, we also noticed that the fraction of forest is positively correlated with topographic slope and negatively correlated with soil depth and the fraction of agriculture (Fig. 3.13).

Nutrient source descriptors were also significantly correlated with Δres_{50}. Horizontal heterogeneity of agricultural sources correlates negatively with Rain.dry.patchy residuals and the vertical concentration ratio of nitrate correlates negatively with Δres_{50} values of Rain.dry.patchy and No.event conditions. Nitrate surplus is significantly related only to Rain.wet residuals.

3.2.4 Relationship between hydrologic connectivity and event type variations in residuals

We examined event runoff coefficients corresponding to different catchments and event types to link the relation between hydrologic connectivity for these event types and corresponding deviations of their samples from the long-term C–Q relationships (Fig. 3.7a). Catchment median event runoff coefficients exhibit a coefficient of variation of 41 % across catchments. Nevertheless, variability of median runoff coefficients across event types for single catchments is larger in most of the cases, with coefficients of variation from 12 % to 118 % and a median value of 67 % across catchments. We found that event types with significantly higher median runoff coefficients also exhibit significant differences in Δres_{50} values (Fig. 3.7b and c). Only Mix and Rain.on.snow events have similar runoff coefficients and similar Δres_{50} values.

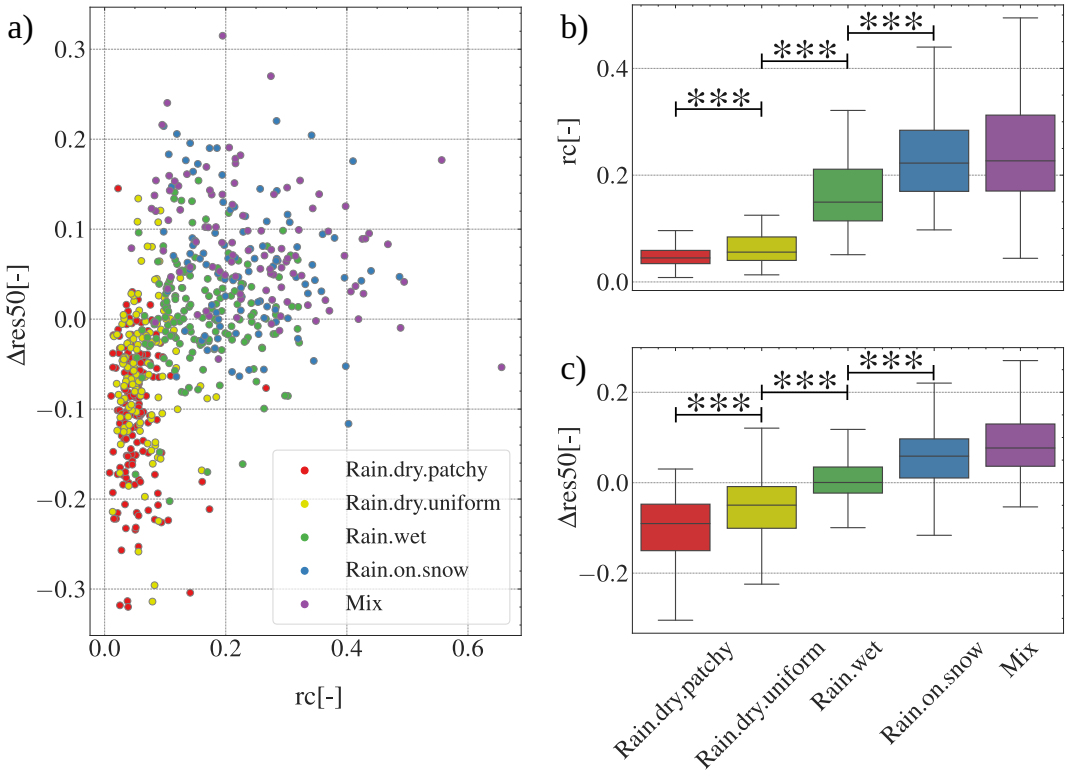

Figure 3.7: (a) Relationship between Δres_{50} for each catchment and event type and median runoff coefficient (rc); runoff coefficient is not defined for No.event. (b) Variability of runoff coefficients (rc) for each event type and (c) median residuals for each event type. Significance of median differences between adjacent boxplots was estimated using the Kruskal–Wallis test ($p < 0.001$).

3.3 Discussion

3.3.1 Direction and magnitude of C–Q deviations for different event types

We found systematic differences in the direction and magnitude of deviations of nitrate concentrations (Δres_{50}) from the long-term C–Q relationships during different types of runoff events despite the large variety of study catchments (Fig. 3.5). In the following paragraphs, we will discuss potential mechanisms that can explain the variability of C–Q deviations across event types.

Positive deviations for nitrate concentrations during snow-impacted events (i.e., higher nitrate concentration compared to the general C–Q pattern) are in line with previous studies that have shown an increase of nitrate concentration in stream water during snow-impacted events in forested and agricultural catchments [74, 142, 115]. This is in line with Winter et al. [96], who showed using high-frequency data that snow-induced events export the highest nitrate concentration compared to other event types in six German catchments with mixed land use. Our results clearly show that snowmelt does not generate lower concentration of nitrate compared to the long-term C–Q relationship, although this might be expected due to lower nitrate concentration in snowfall than in stream water from agricultural catchments [5]. Instead, higher concentration indicates enhanced nitrate transport from soil sources with no source limitation during these types of events. We argue that during snow-impacted events, hydrologic connectivity is high between nitrate sources and streams due to elevated wetness conditions [148], which is consistent with previously reported high nitrate concentration during the winter period [143, 147, 156]. Due to excessive catchment wetness during snow-impacted events, a high amount of new water transported by faster and shallower pathways can reach the stream (a so-called inverse storage effect; [157]), mobilizing large amounts of nitrate available in the soil [156]. In addition, during these events, the mobilized water is less affected by biogeochemical processes due to lower microbial activity induced by low temperature during snow-impacted events [5].

Furthermore, our analysis shows that Rain.dry.uniform and Rain.dry.patchy events generate lower nitrate concentrations compared to the other types of events or No.event conditions (Fig. 3.11), producing strong negative C–Q deviations (Fig. 3.5). Along the same lines, Winter et al. [96] showed that runoff events with dry antecedent conditions exhibit lower concentration compared to other event types in six German catchments with mixed land use. There are two possible explanations for the occurrence of this phenomenon. On the one hand, Rain.dry.uniform and Rain.dry.patchy events occur more often during the dry season, when nitrate concentrations are reported to be lower [19, 145] due to a hydrological disconnection between agricultural sources and streams under dry conditions, as well as higher biogeochemical nitrate removal processes, including biotic uptake and denitrification [129, 35, 158, 5]. On the other hand, during runoff events with dry antecedent conditions, nitrate concentrations can be diluted below pre-event concentration levels. This is shown by high-frequency observations in agricultural catchments that report more frequent negative event C–Q slopes during the dry season [159, 96, 3, 115]. In such cases, nitrate concentration decreases compared to pre-event concentrations due to hydrologic disconnection between streams and agricultural land, and the growing importance of runoff generated from riparian zones [157, 61, 160], which are known to buffer nitrate inputs due to high denitrification potential [147, 119, 161]. Our results show that the combined effect of lower pre-event concentration and further decrease in concentrations due to runoff events magnifies the observed negative deviations of nitrate samples from the long-term C–Q relationships. Nevertheless, the data available for this study do not allow us to quantify the contribution of individual effects of these two factors on the scatter of long-term C–Q relationships of nitrate. On the contrary, studies in pristine headwaters and forested catchments found that rainfall events with dry antecedent conditions can mobilize large amounts of nitrate, increasing the concentration in streams [48, 115]. Since these findings

are based on the observations in a single or only a few catchments with limited agricultural activity, different nitrate sources, such as atmospheric deposition or nitrate fixation and nitrate accumulation in soil between events, might be more relevant. Agriculture is a dominant land use type in the catchments used in this study (median fraction of agricultural land is 50 %), therefore a considerable nitrate accumulation in soil as the result of fertilization dominates over any other nitrate source [28, 14], explaining the discrepancy between our findings and the results from pristine headwaters and forested catchments on the role of rainfall events with dry antecedent conditions for nitrate mobilization.

Different from runoff events with dry antecedent conditions, we found that nitrate grab samples taken during No.event conditions exhibit slightly positive deviations, indicating higher concentrations compared to the long-term C–Q relationships. No.event samples also exhibit higher nitrate concentrations (Fig. 3.11) compared to Rainfall events with dry antecedent conditions (i.e., Rain.dry.patchy and Rain.dry.uniform), with both groups of samples being collected during relatively low discharge conditions (Fig. 3.4a). This suggests that the lack of dilution during No.event conditions might produce more positive residuals.

3.3.2 The role of hydrologic connectivity between different event types

The hypothesized role of hydrologic connectivity on shaping nitrate deviations during runoff events is supported by the relation between event runoff coefficients and the deviation of nitrate concentrations from the long-term C–Q relationships for different event types (Fig. 3.7). Higher runoff coefficients indicate a more efficient rainfall–runoff response, either due to the activation of stored water or the fast runoff of rainwater or snowmelt into the stream. Across all studied catchments, the highest runoff coefficients are consistently found for snow-impacted events (Rain.on.snow and Mix) (Fig. 3.7). High values of runoff coefficients were connected to highly positive residuals, indicating that compared to the C–Q relationship, more nitrate was mobilized during high levels of hydrologic connectivity. Studies using high-frequency data show that during runoff events in wet seasons, when catchments are hydrologically more connected, shallow flow paths are activated transporting greater amounts of nitrate [74, 72, 162]. Similarly, Von Freyberg et al. [146], Ocampo, Sivapalan, and Oldham [147] and Stieglitz et al. [148] showed that upland zones are more efficiently connected to riparian zones by shallow pathways during wet months, permitting effective transport of nutrients to the stream.

There are no significant differences in event runoff coefficients between two types of snow-impacted events (i.e., Mix and Rain.on.snow) (Fig. 3.7), despite possible differences in their characteristic snowmelt intensities [1]. While the melting of the snowpack is only induced by temperature increase during Mix events, additional portions of snowpack might be melted by additional energy brought by rainfall during rain-on-snow events [163]. However, in both cases, event runoff coefficients are similarly high (Fig. 3.7b), suggesting similar hydrologic connectivity [31]. This, in turn, results in similar deviations of nitrate concentrations from the long-term C–Q relationships for these two snow-impacted event types, reemphasizing the primary role of hydrologic connectivity on the observed deviations of C–Q relationships.

In contrast to snow-impacted events, lower runoff coefficients typical for rainfall events with dry antecedent conditions (i.e., Rain.dry.patchy and Rain.dry.uniform) indicate that a small portion of event water can reach the stream, which means that distant zones from

the stream network associated with longer pathways exhibit lower or lack of connection during these types of runoff events. Moreover, the overall dry antecedent conditions with a heterogeneous spatial distribution of soil moisture indicate a potential disconnection of runoff generation zones, and therefore the hydrologic connectivity might be lower during such events (i.e., Rain.dry.patchy) than during events with uniform spatial distribution of soil moisture (i.e., Rain.dry.uniform) as shown by lower event runoff coefficients of the former (Fig. 3.7). Differences in the connectivity of these two types of events are also in line with differences in residuals with the strongest negative residuals observed for Rain.dry.patchy events. Similarly, Outram et al. [72] showed that lower event runoff coefficients during runoff events with dry antecedent conditions mobilize only a small quantity of nitrate due to the inactive subsurface pathways. Studies using high-frequency nitrate and discharge data showed that during dry periods, upland and riparian zones are usually disconnected [147, 148, 146]. This evidence from single catchments are in line with our results across a large set of German catchments, suggesting a crucial role of hydrologic connectivity for nutrient transport.

During Rain.wet events, runoff coefficients are between those of snow-impacted events and rainfall events with dry antecedent conditions (Fig. 3.7) which indicate an intermediate level of hydrologic connectivity between sources and streams, and thus both positive and negative C–Q deviations (Fig. 3.5).

3.3.3 Climatic and landscape controls of the variability of C–Q deviations across Germany

Despite systematic differences of C–Q deviations for different event types, we found considerable spatial variability in the magnitude of these deviations across German catchments (Fig. 3.5a). In the next paragraphs, we discuss how catchment characteristics may control deviations of concentrations taken during events from the long-term C–Q relationship (Δres_{50}).

The correlation of C–Q deviations during snow-impacted events with topographic and soil properties (Fig. 3.6) indicates that in flatter catchments with thick soils and a high fraction of sedimentary aquifers, these types of events generate higher nitrate concentrations compared to the average long-term behavior. Contrarily, C–Q deviations during Rain.dry.patchy events are more negative, indicating that nitrate concentrations during these events tend to be smaller than the long-term average in catchments with these characteristics. Previous studies have shown how these characteristics are able to promote nitrate removal in catchments. Deep sedimentary aquifers have a high potential of denitrification due to a great availability of electron donors, longer transit times and more anoxic conditions due to sufficient reduction capacity [164, 165, 37], generating a lower nitrate supply in deeper soils compared to shallow soil [77]. In addition, flat catchments (low topographic slope, higher topographic wetness index) tend to have a higher portion of riparian wetlands [108] that can reduce nitrate concentrations from stream water. During snow-impacted events, fast flow pathways between nitrate sources and the stream are activated and nitrate stored in shallow soils can be mobilized, bypassing the denitrification attenuation of the soil and the riparian zone, which is also largely suppressed during low temperatures in winter [5, 158], resulting in higher nitrate C–Q deviations. In contrast, Rain.dry.patchy events might mobilize water from connected near-stream source zones, where riparian wetlands from flatter areas contribute water with low nitrate concentration [166,

158], generating more negative C–Q deviations. In addition, deviations during these events might be associated with longer transit times due to thicker soil and less hydrologic connectivity [156] which can reduce nitrate concentrations in streams. Instead, steeper catchments with shallow soils during Rain.dry.patchy events show less nitrate attenuation due to shorter flow paths and less favorable conditions for denitrification, generating relatively higher stream water nitrate concentrations during these events and therefore decreasing the magnitude of C–Q deviations.

We acknowledge that some catchment characteristics are highly correlated (Fig. 3.13). Flatter catchments often exhibit higher fractions of agriculture, therefore more diffuse source availability. Although the correlation of the fraction of agriculture and C–Q deviations during Rain.on.snow events was less significant than topographic descriptors, a potential increment of diffuse sources in flatter catchments might also enhance the mechanism of nitrate bypassing the buffer capacity of catchments during Rain.on.snow events, generating higher C–Q deviations. For most of the event types, we found that the fraction of agriculture itself is not sufficient to explain the differences in nitrate deviations from the long-term C–Q relationships between catchments (Fig. 3.6). However, the vertical ratio of nitrate between topsoil and groundwater and the horizontal spatial distribution of agricultural land within the catchment (i.e., horizontal heterogeneity) were strongly correlated with C–Q deviations for Rain.dry.patchy events (Fig. 3.6). During Rain.dry.patchy events, the mobilization of distant nitrate sources (horizontally and vertically) is reduced due to the low hydrologic connectivity, resulting in lower nitrate concentration of stream water and more negative deviations in catchments with top-loaded nitrate profiles as well as more distant agricultural lands from streams. The high spatial variability of agricultural nitrate sources, expressed as horizontal heterogeneity and vertical ratio of nitrate, and the temporal variability of sources possibly induced by elevated subsurface and riparian zone removal during different levels of hydrologic connectivity, promote deviations of nitrate concentrations from the long-term C–Q relationships.

3.3.4 Implications of this study

In this study, we performed the first large-scale analysis of long-term nitrate C–Q relationships, differentiating runoff event types. We show that flatter catchments with soil conditions favorable for denitrification or distant nitrate sources are prone to generate disproportional loads during runoff events with high levels of hydrologic connectivity, presenting an ecological risk for aquatic ecosystems. These findings can be instructive for implementing more effective water quality management strategies to prevent extreme nitrate loads from reaching water bodies in such catchments during events associated with high levels of hydrologic connectivity (i.e., snow-impacted events).

The connection between nitrate concentrations and different types of runoff events shown in our study indicates that possible changes in the occurrences of different event types due to the ongoing climate change might in turn affect the dynamics of nutrient exports in the catchments. With advancing climate change, air temperature is projected to increase further, leading to a substantial decline in seasonal snowpack accumulation and earlier snowmelt onset in Central Europe [167]. Several studies reported a reduction in snow accumulation in Germany over the last decades [168, 169, 170], with a consistent reduction in the frequency of Rain.on.snow

events [163], suggesting that the corresponding positive deviations from the long-term nitrate C–Q relationships are likely to occur less often in the future. Less frequent snow-impacted events would reduce nitrate mobilization from the soil under these critical event conditions. Consequently, more nitrate may remain in the soil sources. A fraction of this soil nitrate is expected to be removed by denitrification, whereas another fraction may last longer as soil nitrate legacy [107, 22], thus generating unknown long-term effects in the nitrate dynamics during future runoff events. On the other hand, higher temperatures lead to a decrease of soil moisture [171], propitiating dry conditions and reducing hydrologic connectivity. An increase in frequency of rainfall events with dry antecedent conditions observed in several German catchments [96] indicates that negative deviations might become even more frequent during warm seasons in the future.

By using low-frequency, long-term nitrate data, we were able to provide information about characteristic nitrate transport during different types of events and identify hydrologic connectivity associated with these types as a critical control of nitrate dynamics in German catchments. Our findings using low-frequency data are largely supported by the detailed analysis of high-frequency data in individual catchments from previous studies; but thanks to the large number of analyzed catchments, we were able to provide a more comprehensive analysis of systematic deviations of nitrate concentrations during events of different types and provide valuable insights on the origins of the scatter in C–Q relationships. The abundance of low-frequency data worldwide and transferable nature of the applied event classification framework provide the means of further applications in contrasting environments to better understand long-term nitrate C–Q relationships across contrasting environments. Moreover, our results suggest that sampling campaigns should be designed specifically to capture runoff events with different levels of hydrologic connectivity in order to better explain the scatter in long-term C–Q relationships and better isolate the role of singular processes (i.e., nitrate uptake, denitrification).

Although the presence of the event-scale hysteresis effect might considerably affect nitrate concentration during rising and falling limbs of the event hydrograph in some catchments [137], we found a similar direction of deviations from the long-term C–Q relationships when we considered samples taken during rising limb, falling limb and near-to-peak (Fig. 3.13b). Hence, our results suggest that the variability, potentially added by the presence of hysteresis patterns, is lower than the deviations observed for different event types from the long-term C–Q relationships. Increasing availability of high-frequency datasets coupled with new statistical modeling approaches might be used in the future to evaluate hysteresis-related effects in the existing long-term C–Q datasets to further disentangle inter- and intra-event variability of nitrate dynamics at larger scales.

3.4 Chapter conclusions

We analyzed for the first time the effect of different runoff event types on the scatter observed in concentration–discharge (C–Q) relationships across 184 German catchments. Specifically, we examined the deviations of the concentration of nitrate samples collected during different runoff event types from the long-term C–Q relationships. Our results highlight pronounced

deviations in most of the catchments, regardless of their overall long-term C–Q export patterns (dilution, neutral, or enrichment). Thus, scatter apparent in long-term C–Q relationships can indeed be partially explained by different types of runoff event conditions.

We found that nitrate transport is enhanced during snow-impacted events compared to long-term C–Q relationships. On the other hand, nitrate concentrations tend to be lower than the long-term C–Q relationships when rainfall coincides with dry antecedent conditions. The C–Q relationships during rainfall on wet antecedent conditions were not significantly different from the long-term relationships. We argue that hydrologic connectivity to the nitrate sources, here represented by the values of event runoff coefficients, is crucial to explain deviations from the long-term C–Q relationship during different event types.

Finally, we found that flatter catchments with high denitrification potential (i.e., deep soils, presence of sedimentary aquifers), as well as catchments with agricultural areas located farther from the stream or with top-loaded nitrate profiles, exhibit an enhanced nitrate transport during snow-impacted events and lower nitrate concentrations during events induced by rainfall with dry antecedent conditions compared to the long-term C–Q relationships. Catchments with these characteristics are prone to generate disproportional loads during snow-impacted events, exacerbating ecological risk for receiving water bodies. Findings from this study improve our understanding of the effects of runoff event types on nutrient dynamics and provide valuable insights for optimizing water quality management and monitoring. The main findings of this study can be summarized as follows:

1. Snow-impacted runoff events frequently lead to positive deviations in nitrate concentrations, suggesting enhanced mobilization of nitrate during these periods.

2. Rainfall events preceded by dry antecedent conditions generally exhibit negative deviations in nitrate concentrations, meaning nitrate levels during these events tend to be lower than C–Q preditions.

3. Variability in event runoff coefficients among different runoff event types reveals contrasting levels of hydrological connectivity, which plays a critical role in controlling nitrate transport. Runoff events with higher event runoff coefficients correspond to more connected flow paths, facilitating nitrate export to streams.

3.5 Chapter statement

This chapter presents a formatted version of the original paper by Saavedra, F. A., Musolff, A., von Freyberg, J., Merz, R., Basso, S., and Tarasova, L. (2022), entitled “Disentangling scatter in long-term concentration–discharge relationships: The role of event types,” published in Hydrology and Earth System Sciences, 26(23), 6227–6245 (https://doi.org/10.5194/hess-26-6227-2022), reproduced here with permission.

Author contributions: Felipe Saavedra Melendez drafted the manuscript and performed the formal analyses. Larisa Tarasova and Andreas Musolff contributed to the conceptualization. Felipe Saavedra Melendez prepared the manuscript with input from all co-authors.

Acknowledgements: We thank Camile Minaudo and two anonymous reviewers for their valuable suggestions that improved the manuscript. Larisa Tarasova was supported by the German Research Foundation ("Deutsche Forschungsgemeinschaft", DFG) via research group FOR 2416 "Space–Time Dynamics of Extreme Floods (SPATE)". Jana von Freyberg was supported by the Swiss National Science Foundation (SNSF grant PR00P2_185931).
This research was funded by the Helmholtz-Zentrum für Umweltforschung under the DYNAMO Cohort.

Data availability statement: Water quality dataset is available online at: `https://doi.org/10.4211/hs.a42addcbd59a466a9aa56472dfef8721` [150]. Runoff event classification is available upon request at: `https://doi.org/10.5281/zenodo.3575024` [172]. Catchment characteristics dataset is available at: `https://doi.org/10.4211/hs.82f8094dd61e449a826afdef820a2c19` [103].

3.6 Supporting Information

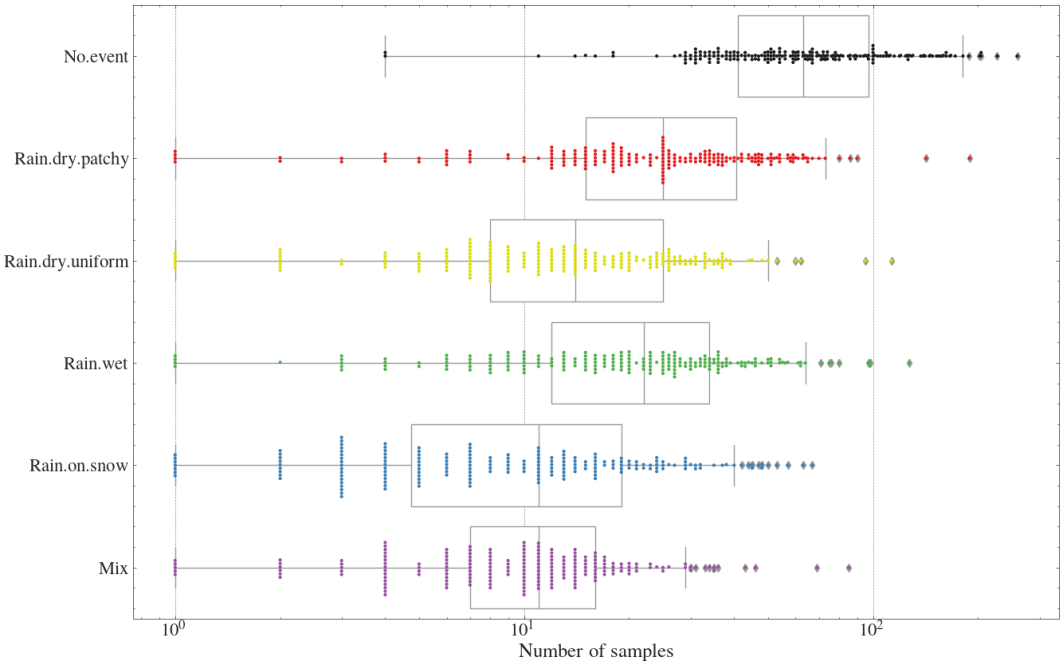

Figure 3.8: Number of samples in all 184 catchments attributed to each event type. Vertical lines show medians, 5th and 95th percentiles of boxplots.

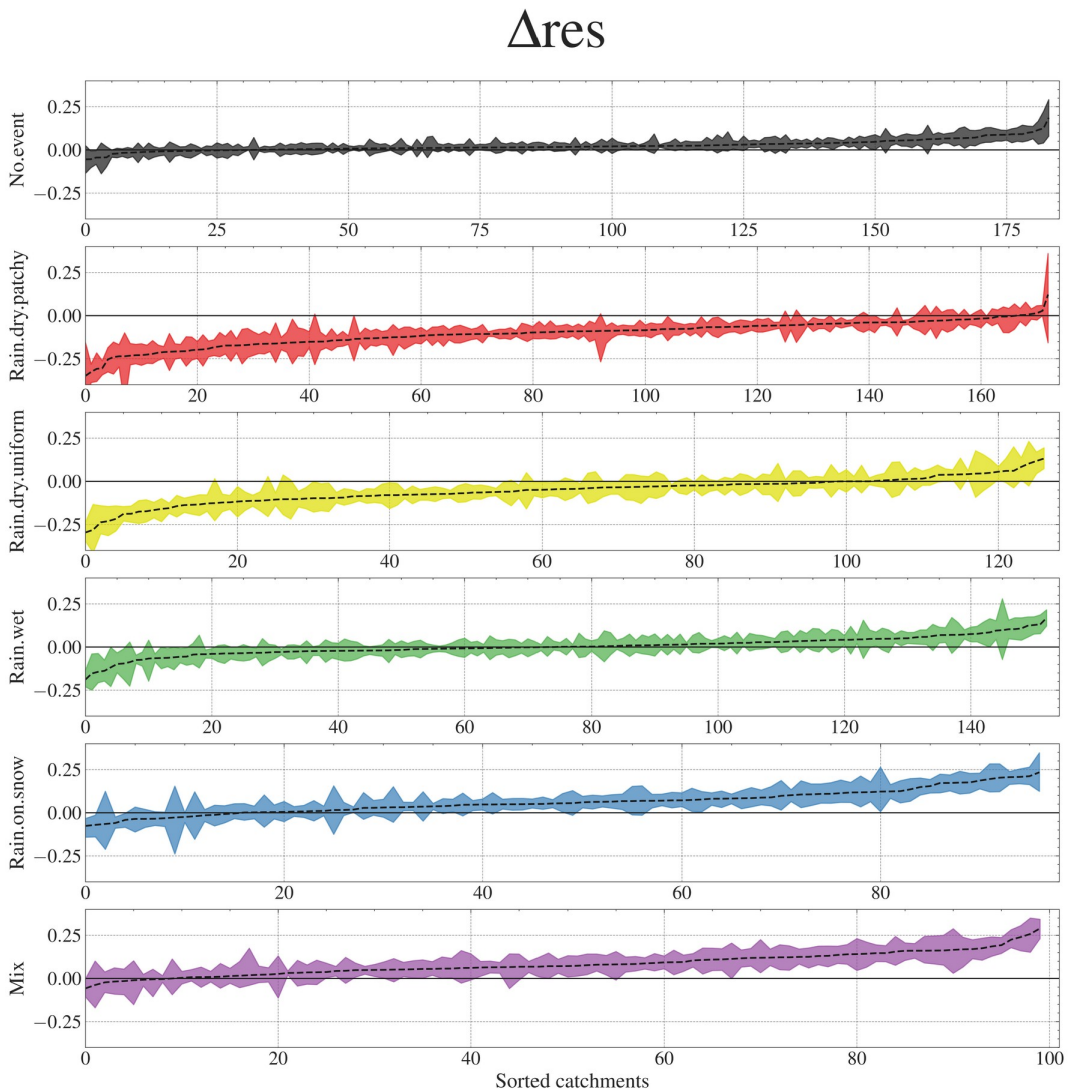

Figure 3.9: Results of bootstrapping differences of C–Q residuals for different event types and all samples (Δres) 10000 times. Dashed lines show the median bootstrapped differences of residuals (Δres_{50}), and colored bands represent the 25% and 75% percentiles of bootstrapped differences. Catchments are sorted in each subplot based on Δres_{50} values for better visualization.

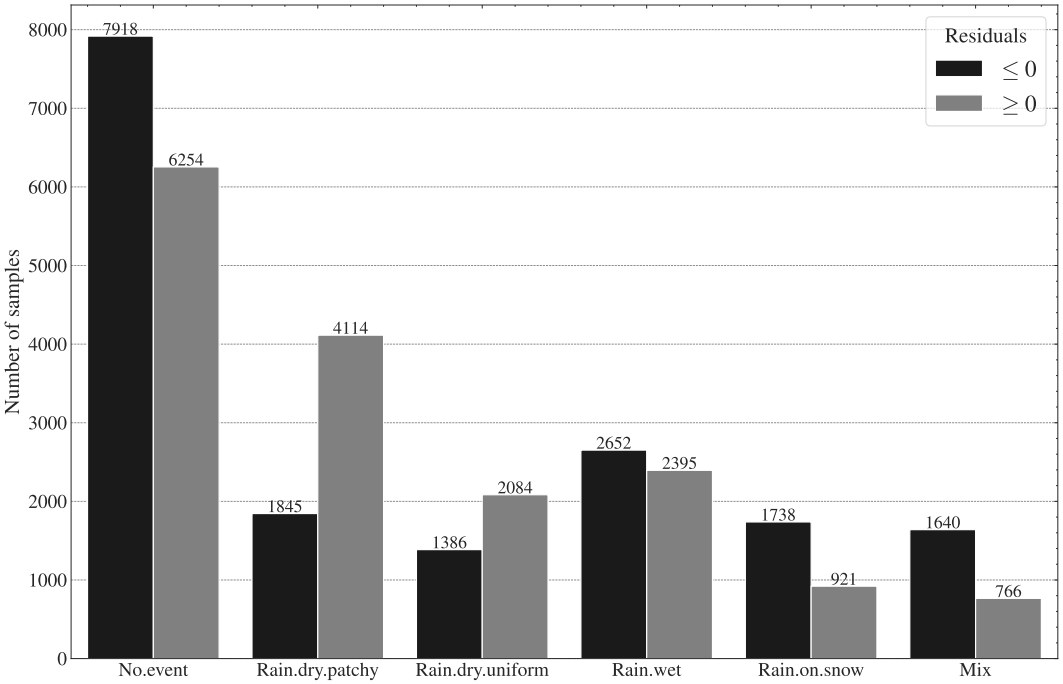

Figure 3.10: Number of nitrate samples from all catchments with positive and negative residuals for each event type.

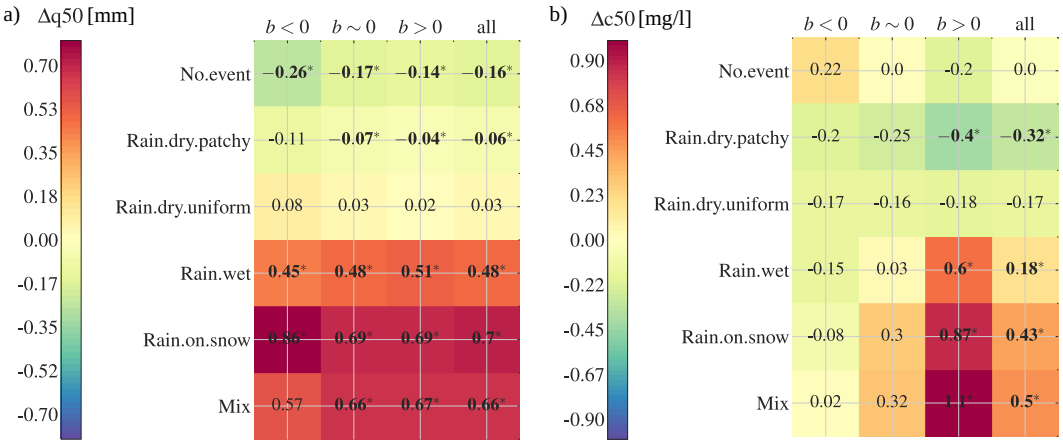

Figure 3.11: Heatmaps of differences between samples taken during different event types or No.event and all samples (analogous to Figure 3.5) for (a) discharge and (b) concentration of nitrate, averaged across different groups of catchments, considering all nitrate data for each event type and No.event. The three first columns of the heatmap correspond to one of the long-term export patterns (i.e., dilution (slope $b < 0$), neutral (slope $b \sim 0$), and enrichment (slope $b > 0$)) and the fourth column corresponds to all study catchments. Bold font and * indicates significant differences (Kruskal–Wallis test, $p < 0.05$).

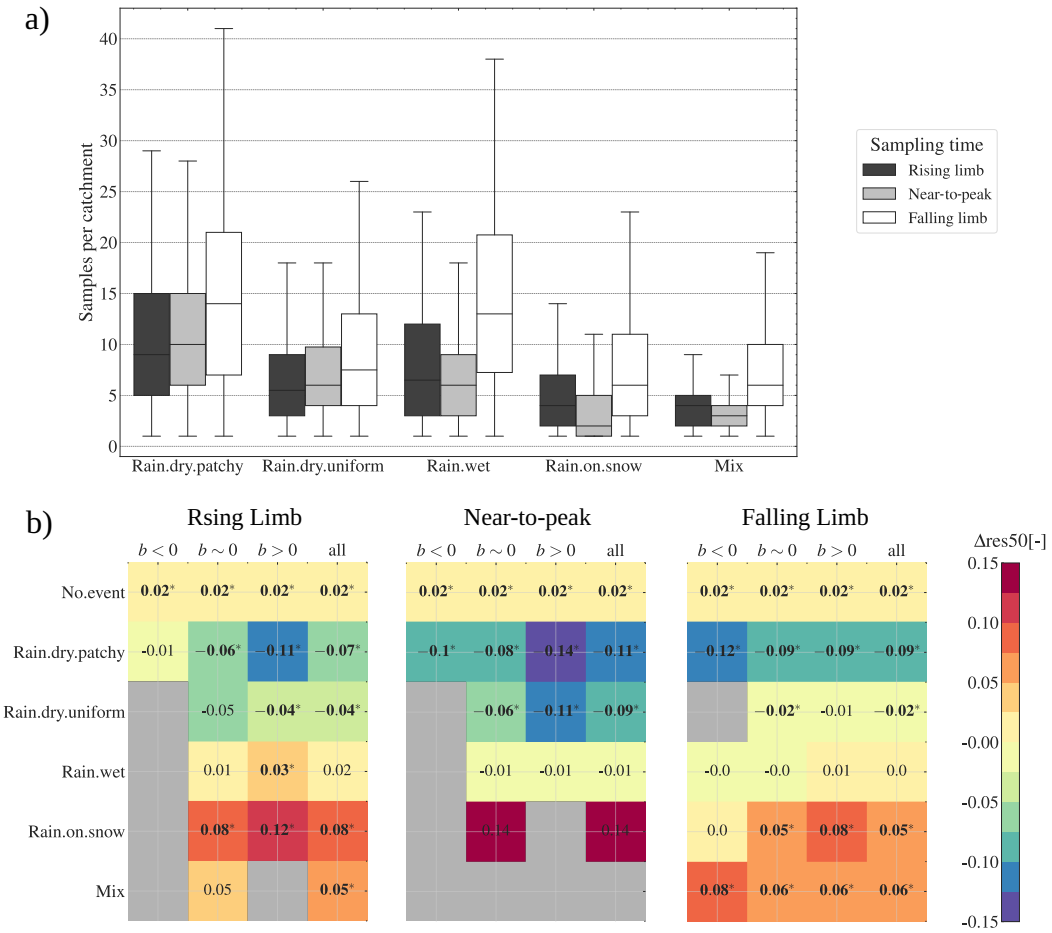

Figure 3.12: (a) Number of samples per catchment per event type corresponding to the samples taken during the rising limb, falling limb, or near to the peak (i.e., samples taken from one day before to one day after the peak of the hydrograph). (b) Median deviations of nitrate concentrations from the long-term C–Q relationships (Δres_{50}) for samples taken during the rising limb, falling limb, and near to the peak. Deviations are computed analogously as for Fig. 3.5 in the main manuscript. The three first columns of the heatmap correspond to one of the long-term export patterns (i.e., dilution (slope $b < 0$), neutral (slope $b \sim 0$), and enrichment (slope $b > 0$)), and the fourth column corresponds to all study catchments. Bold font and * indicate significant differences (Kruskal–Wallis test, $p < 0.05$) between median deviations across catchments for each event type and median deviation across catchments of all nitrate samples. At least 5 catchments with sufficient data (more than 10 samples per event type) are required to evaluate the significance of the deviations. Gray squares indicate cases where this requirement is not met.

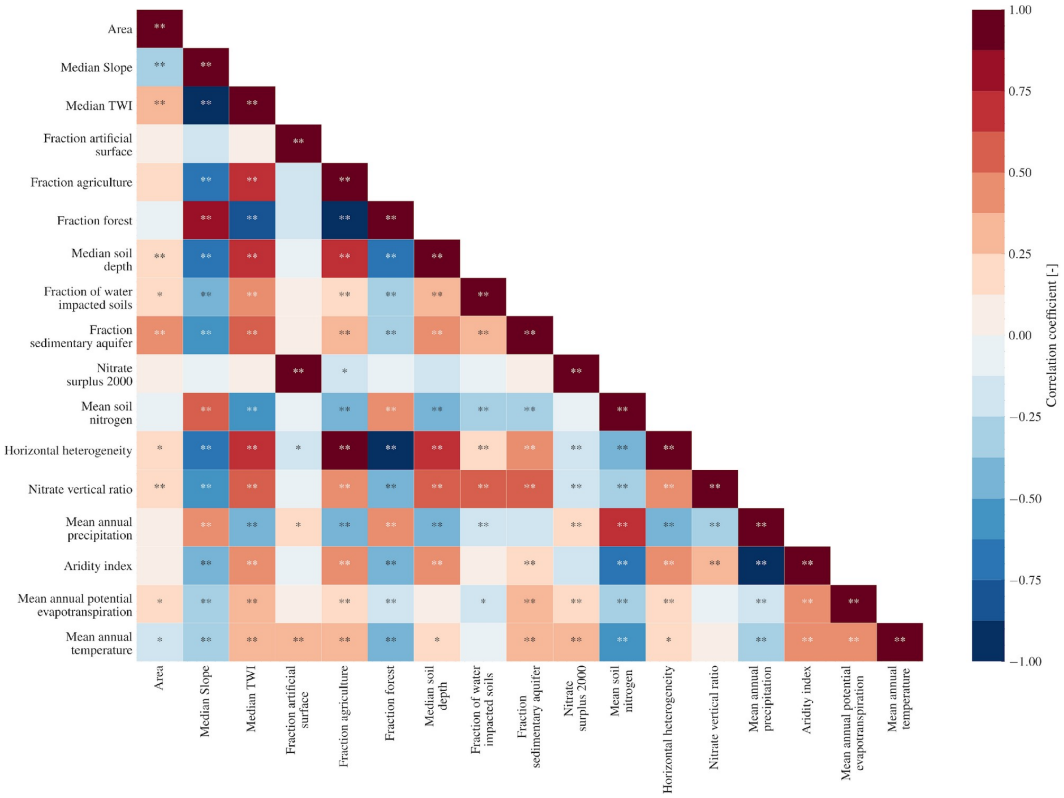

Figure 3.13: Spearman rank correlation coefficient between catchment descriptors. Significant correlations are indicated as * for $p < 0.05$ and ** for $p < 0.01$.

Table 3.1: Thresholds and variables used for classification of runoff events (modified from Tarasova et al. [1].

Layer	Selected indicator	Expression	Thresholds	Performed Split
a) Inducing event	Ratio of event rainfall volume and total event precipitation volume	$\frac{R_{x,y,t}}{P_{x,y,t}}$	0.95	Rainfall vs. Mix or Rain.on.snow
	Normalized spatial covariance of event-averaged snow cover and rainfall	$\frac{\mathrm{cov}_{x,y}(SWE_t, R_t)}{SWE_{x,y,t} \times R_{x,y,t}}$	0	Rain.on.snow vs. Mix
b) Wetness state	Catchment-averaged antecedent soil moisture	$SM_{x,y}(t_0)$	$max(\kappa)$	Wet vs Dry
c) Spatial distribution of mositure	Spatial coefficient of variation of antecedent soil moisture	$\frac{\sqrt{\mathrm{var}_{x,y}(SM_{t_0})}}{SM_{x,y,t}}$	Q_2	Uniform vs Patchy

Note: Input data is grid-based, for each cell (x, y) and time step t during an event the following variables are provided: event rainfall rate $R(x, y, t)$ [mm]; total event precipitation rate $P(x, y, t)$ [mm/day] and snow water equivalent $SWE(x, y, t)$ [mm]. At the beginning of each event (t_0) antecedent soil moisture $SM(x, y, t_0)$ [-] is provided. Q_2 correspond to median value and κ is the curvature of a nonlinear function that describes the relation between event runoff coefficients and simulated soil moisture (Tarasova et al., 2018). Rainfall data was obtained from REGNIE data set (Rauthe et al., 2013). Snow water equivalent and soil moisture were simulated by the mHM model (Samaniego et al 2010; Kumar et al 2013) and provided in Zink et al. (2017).

Table 3.2: Catchment descriptors used for correlation analysis. (according to Ebeling et al. [2]).

Category	Variable	Unit	Description
Topography	Area	km^2	Catchment area
	Median Slope	°	Mean topographic slope of catchment
	Median TWI	-	Mean topographic wetness index
Land Cover	Fraction of agriculture	-	Fraction of agricultural land cover
	Fraction of forest	-	Fraction of forested land cover
Soil & Aquifer	Median soil depth	cm	Median depth to bedrock in the catchment
	Fraction of sedimentary aquifer	-	Fraction of sedimentary aquifer
Nutrient source	Nitrate surplus 2000	$kgN\ ha^{-1}y^{-1}$	Mean nitrogen surplus per catchment during sampling period (2000–2015) including N surplus on agricultural land and atmospheric deposition on non-agricultural areas
	Horizontal heterogeneity	-	Slope of relative frequency of source areas in classes of flow distances to stream as a proxy for horizontal source heterogeneity
	Nitrate vertical ratio	-	Mean ratio between potential seepage and groundwater NO3-N concentrations as proxy for vertical concentration heterogeneity
Hydrometeorology	Mean annual precipitation	$mm\ y^{-1}$	Mean annual precipitation for the period 1986–2015
	Mean annual potential evapotranspiration	$mm\ y^{-1}$	Mean annual potential evapotranspiration for the period 1986–2015
	Aridity index	-	Fraction of mean annual potential evapotranspiration and mean annual precipitation
	Mean annual temperature	° C	Mean annual air temperature for the period 1986–2015

4

Mapping Hydrological Connectivity from Soil Moisture Patterns: An Explainable AI Perspective on Nitrate Modeling

In the United States, agricultural fertilizers and wastewater effluents are primary sources of nitrate pollution [173, 174]. Although regulations have partially reduced these inputs by limiting fertilizer application and improving wastewater treatment techniques, nitrate contamination persists in many catchments due to nitrogen input excess and long-lasting legacy effects of nitrate in the soil [122, 175].

Point sources, such as wastewater plants, directly discharge nutrients into streams, elevating nitrate concentration during low flows [70, 176]. In contrast, diffuse sources of nitrogen, such as agricultural lands, release nitrate from fertilizer inputs accumulated in the soil organic matter over several years [23, 109]. Organic nitrogen in the soil is converted into exportable nitrate by soil microorganisms through the process of mineralization [36] and can be transported to streams through diverse hydrological pathways, collectively referred to as hydrological connectivity [177, 147].

Hydrological connectivity, defined as the passage of water from one part of the landscape to another [49], depends on rainfall, evapotranspiration, and static landscape characteristis, such as land cover, topography, and soil properties [49, 50]. During dry conditions, low soil moisture and deeper groundwater tables disconnect shallow flow pathways, decreasing the discharge rates [54, 71]. In these conditions, hillslopes are hydrologically disconnected, and in-stream nitrate originates from older groundwater, near-stream areas, or sewage discharge in urbanized catchments [69, 26, 70].

Longer transit times of groundwater favor denitrification processes that can remove a large portion of the nitrogen from the water, given a sufficient supply of electron donors [178]. Additionally, riparian areas near the stream, where dissolved organic carbon serves as an

electron donor, can be a hotspot of denitrification [158, 179]. Conversely, during wet conditions, soil moisture is high and the shallow subsurface storages are full; therefore, transit times along connected subsurface flow paths become shorter, and a larger portion of the catchment becomes hydrologically connected [180, 181, 96].

This shift in transit times toward younger water decreases the biogeochemical reaction times of denitrification in the catchment [182, 183, 43]. Moreover, during wet conditions, the river network expands, connecting hillslopes to streams and increasing the hydrological transport of water and nitrate [184, 185]. Despite ongoing research on the interplay of hydrological connectivity and riverine nitrate concentrations, the spatial and temporal complexity of these processes remains an unsolved problem in hydrology [186].

Direct measurements of hydrological connectivity at larger scales are mostly not feasible, due to the difficulty of continuously measuring it at different locations within a catchment (e.g., installing and monitoring numerous in-situ soil moisture sensors and wells). Such extensive measurements are generally possible only in experimental catchments [e.g., 147, 53]. An alternative way to represent hydrological connectivity is through accessible proxies [31]. Discharge rates, a catchment-average proxy for hydrological connectivity, have been directly used to infer solute dynamics at the outlet of a catchment using concentration-discharge (C–Q) relationships [125]. The shape of the nitrate C–Q relationship informs us about the availability and spatial distribution of solute sources, their connectivity to streams, and biogeochemical processes that can remove or retain nitrate within the catchment [126, 128, 45]. Based on the slope of the C–Q relationship in logarithmic space, three different export patterns are typically defined: dilution (negative slope), enrichment (positive slope), and neutral (slope close to 0). For example, a catchment with diffuse sources far from the stream network might increase the transport of nitrate concentration during wet conditions when sources are connected to the stream, producing a positive C–Q relationship. Conversely, catchments with point sources or contaminated aquifers exhibit increased nitrate concentration during low flows, producing a negative C–Q relationship. Nevertheless, C–Q relationships often exhibit considerable scatter as a result of the interaction between sources and variable runoff generation processes, which can be linked to different levels of hydrological connectivity [187, 188, 47]. Other proxies of hydrological connectivity include accessible parameters such as the event runoff coefficient [e.g., 51, 52], average groundwater levels [e.g., 53, 54], or average soil moisture [e.g., 55]. While these aggregated proxies can infer the general hydrological states of the catchment, they fail to capture the spatial heterogeneity of hydrological pathways [56], which is crucial for defining targeted nutrient management strategies.

The spatial patterns of soil moisture provide valuable proxies for hydrological connectivity (Figure 4.1). With the increase of hydrological connectivity levels, the spatial heterogeneity of soil moisture also increases [Figure 4.9, 57, 58, 59], and lateral flow processes shape the spatial variability by following topographic convergence zones [60, 61]. The spatial patterns of soil moisture reveal active areas of redistribution and storage of water that serve as pathways of nutrient transport and transformation [189]. Conversely, during dry conditions (Figure 4.1, left panel), soil moisture patterns are controlled by soil properties and changes in vegetation, as vertical water fluxes (e.g., evapotranspiration) dominate soil moisture dynamics [190, 62]. The rapid transition between wet and dry states is reflected in soil moisture patterns, revealing

temporal shifts in water dynamics [61, 189, 62]. The advent of more satellite soil moisture data [e.g., SMAP; 191] provides the opportunity to explore spatial components of hydrological connectivity and stream nitrate concentrations. However, its application for understanding and predicting nitrate remains challenging due to the nonlinearity of nitrate transport and transformation processes.

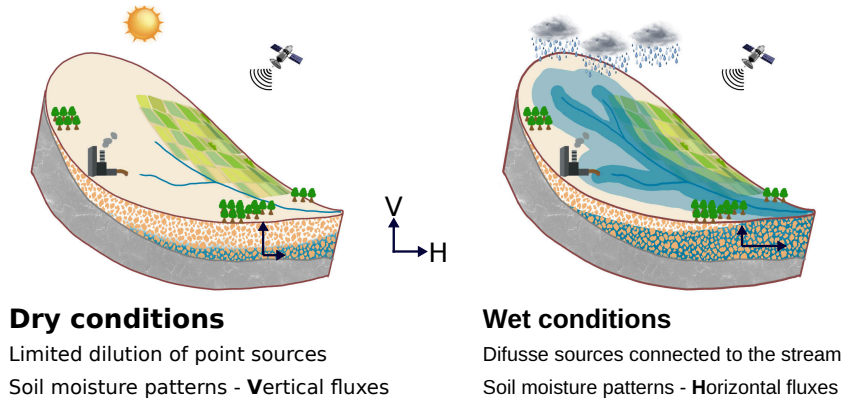

Figure 4.1: Relationship of spatial soil moisture observations and the nutrient dynamics in a catchment from dry to wet conditions of hydrological connectivity. Point sources (e.g., urban or industrial areas) and diffuse sources (e.g., agricultural fields) are illustrated within this framework. The dominance of soil moisture patterns is shown with the relative sizes of two connected arrows: the vertical fluxes (V, e.g., evapotranspiration, infiltration) and the horizontal fluxes (H, e.g., subsurface lateral flow or surface runoff). The catchment is conceptualized with the soil compartment divided in a permeable sandy brown layer and a deeper more impermeable gray layer.

Artificial intelligence (AI) is revolutionizing how we analyze data and develop hypotheses by identifying non-linear patterns within complex datasets [192, 193]. The advancement of AI, explainable AI (XAI), and novel environmental datasets offer new ways of harnessing critical information and interpreting their relationships [194]. Although different studies have used machine learning and XAI to identify the main drivers of mean nitrate concentration across diverse catchments [195, 196] or to simulate daily nitrate concentration in neighboring agricultural catchments [197, 198], it is not yet fully understood how the spatial components of hydrological connectivity affect temporal nitrate dynamics at the catchment scale.

In this study, we hypothesize that, beyond discharge, spatial patterns of soil moisture provide additional information for representing hydrological connectivity over time and predicting nitrate concentration, as they capture key spatial features of connectivity. Moving beyond studies based on localized field observations [e.g., 199, 55], we test this hypothesis by training a multi-branch deep learning model to predict daily nitrate concentrations and verifying that model decisions align with known physical processes using explainable AI (XAI). We trained the model across nine catchments in the United States, integrating discharge time series, catchment characteristics, and soil moisture maps obtained from SMAP-HydroBlocks, the first 30 m satellite-based surface soil moisture dataset for the United States [200]. By combining hyper-resolution land surface modeling, satellite observations from NASA's SMAP mission, and in-situ measurements, SMAP-HydroBlocks, in conjunction with XAI, provides a unique opportunity to map hydrological connectivity hotspots where soil-water interactions play a major role. Leveraging advanced analytical techniques and high-resolution data, our study

contributes to the development of tools for more effective mitigation of nitrate pollution in water bodies.

4.1 Methods

4.1.1 Datasets

4.1.1.1 Site of Study

We selected nine mesoscale catchments in the northeastern United States based on data availability and diversity of land uses (Table 4.1, Figure 4.8). The area of the selected study catchments ranges from 137 km^2 to 8870 km^2 and is primarily covered by agriculture (6 % to 89 %, with a median portion of agricultural land cover of 72 %), forest (0 % to 20 %, with a median portion of 8 %), and urban areas (6 % to 71 %, with a median portion of 10 %). The study catchments are similar in terms of climatic conditions: mean annual precipitation ranges from 835 mm/year to 1104 mm/year, and mean annual temperature ranges from 7.6 °C to 12.3 °C.

4.1.1.2 Discharge and nitrate concentration gauge observations

We obtained quality-checked daily discharge and nitrate concentrations for each catchment outlet from the National Water Information System of the United States Geological Survey for the period 2015–2019, when soil moisture data was available (Figure 4.9). Both discharge and nitrate concentrations are measured through continuous probes and aggregated by the water authorities to a daily scale. In contrast to discharge, high-resolution nitrate observations are relatively scarce and only available for recent years [201]. We only considered timesteps with nitrate measurements and filled rare missing values of discharge by linear interpolation. Across the study catchments, mean nitrate concentration ranges from 0.9 mg/L NO_3-N to 8 mg/L NO_3-N, and mean daily discharge ranges from 0.37 mm/d to 1.45 mm/d during the study period. The coefficient of variation of daily discharge (cvQ) was larger than the coefficient of variation of nitrate concentration (cvC) in every catchment, with the ratio of the coefficient of variation of concentration and discharge (cvC/cvQ) ranging from 0.19 to 0.94. The slopes of the C–Q relationship (linear regression in the logarithmic space) ranged from -0.66 to 0.76, with two catchments exhibiting dilution patterns (slope < -0.1), one catchment a neutral pattern (slope ≈ 0), and six catchments exhibiting enrichment patterns (slope > 0.1).

We extracted 30 m resolution soil moisture time series maps from SMAP-HydroBlocks [200], which is available for the period from 2015 to 2019 in the United States. SMAP-HydroBlocks estimates top 5 cm soil moisture with a 2-3 days revisit time by integrating hyper-resolution land surface modeling, radiative transfer modeling, and satellite observations from NASA's Soil Moisture Active Passive Mission. SMAP-HydroBlocks includes a machine learning-based bayesian merging scheme trained on soil moisture ground in-situ observations to assimilate model and satellite brightness temperature observations [202]. SMAP-HydroBlocks outperforms other SMAP products across 1,192 observational sites, offering higher spatial detail and an improved representation of spatial variability [200].

To obtain daily soil moisture maps, we linearly interpolated time gaps shorter than 5 days. We converted the original soil moisture data from volumetric water content to percentage using temporal pixel-wise min-max normalization for each catchment to account for the heterogeneity of soil porosity. As reported in Vergopolan et al. [200], SMAP-HydroBlocks is expected to have high uncertainties in urban areas, given limitations in characterizing hydrological processes in urban areas, as well as limited land surface model capability in representing urban drainage networks. Consequently, urban regions produced strong spatial discontinuities that might negatively impact the performance of the explainable AI [203]. Therefore, we masked urban areas from the soil moisture maps and imputed the missing values by linearly interpolating the values from the neighboring pixels. In addition, we removed pixels outside the catchment boundaries to ensure that the model learns only from data within the catchment. However, because the deep learning model does not allow missing values and setting them to 0 would create strong discontinuities, we interpolated these values from neighboring pixels to maintain data consistency [204, 205]. To address computational limitations, we reduced the spatial resolution of the soil moisture maps to $1\,\mathrm{km}^2$. Subsequently, to develop a multi-catchment model (a single model applied to all the catchments), we standardized the gridded input size by rescaling them to a 69×69 pixel bounding box using nearest-neighborhood interpolation. For small catchments, this process involved upscaling the data to fit the bounding box, whereas for larger catchments, we downscaled the data, resulting in a coarser final spatial resolution. Following this process, the final spatial resolutions of soil moisture maps across catchments range from $1\,\mathrm{km}^2$ to $4\,\mathrm{km}^2$ (see Table 4.1).

To inform the model about potential hydrological pathways, we added the height above the nearest drainage for each catchment as a static map (HAND, Figure 4.9) [206, 207]. HAND is a commonly used proxy for hydrological flow paths because it directly represents differences in potential energy in the landscape that generate runoff [208]. We computed HAND maps at 30 m $\times$ 30 m resolution and aggregated them to 1 km to match soil moisture resolution using the RichDEM library [209].

4.1.1.3 Static proxies for nitrate inputs

For our model, we derived static proxies for nitrate inputs (one value per catchment) by using the fraction of urban areas as a point source indicator and the diffuse nitrogen surplus as a diffuse source indicator. We obtained the fraction of urban areas and catchment boundaries from the GAGES-II dataset [210] and calculated the catchment-specific mean nitrogen surplus (excluding human waste) for the period 2000–2017 using data from [173]. The fraction of urban areas ranges from 6 % to 71 % across the study catchments, and the mean nitrogen surplus ranges from $3345\,\mathrm{kg/km}^2$ to $9299\,\mathrm{kg/km}^2$ across the study catchments (Table 4.1).

4.1.2 Deep learning model

We configured a deep learning model structure to predict daily stream nitrate concentration in multiple catchments using daily discharge, spatial patterns of soil moisture, static HAND maps, and static proxies of diffuse and point sources as potential predictors (Figure 4.2).

Table 4.1: Characteristics of study catchments: location, area, climate variables (mean annual precipitation and temperature), the mean annual nitrogen surplus (N surp.), land cover percentages (urban, forest and agriculture), and final spatial resolution of soil moisutre maps for the model (SM res.).

Site Name	**State**	**Area [km²]**	**Ppt [mm/y]**	**Temp. [ºC]**	**Urb. [%]**	**For. [%]**	**Agr. [%]**	**N surp. [kg/km²]**	**SM res. [km]**
Iroquois River Near Foresman	Indiana	1168	96.8	9.7	6.1	8.4	83.9	7992	1.0
Kankakee River At Shelby	Indiana	4587	99.9	9.6	8.7	11.4	72.0	6479	1.0
Kankakee River At Davis	Indiana	1371	101.2	9.5	9.8	11.6	67.1	6467	1.8
Yahara River At Windsor	Wisconsin	191	84.4	7.6	10.9	3.2	83.1	6845	1.0
Kankakee River At Dunns Bridge	Indiana	3467	100.1	9.6	8.9	12.3	70.8	6473	1.0
Rock Creek At Joyce Rd Washington	Dist. Of Columbia	137	110.4	12.3	71.0	20.3	6.0	3345	1.0
Yahara River Near Fulton	Wisconsin	1259	86.0	7.6	22.3	6.1	59.0	5893	4.0
Spoon River Near St. Joseph	Illinois	339	98.6	10.7	10.5	0.2	89.1	8738	1.3
Raccoon River At Van Meter	Iowa	8870	83.5	8.7	6.7	3.2	86.4	9299	1.0

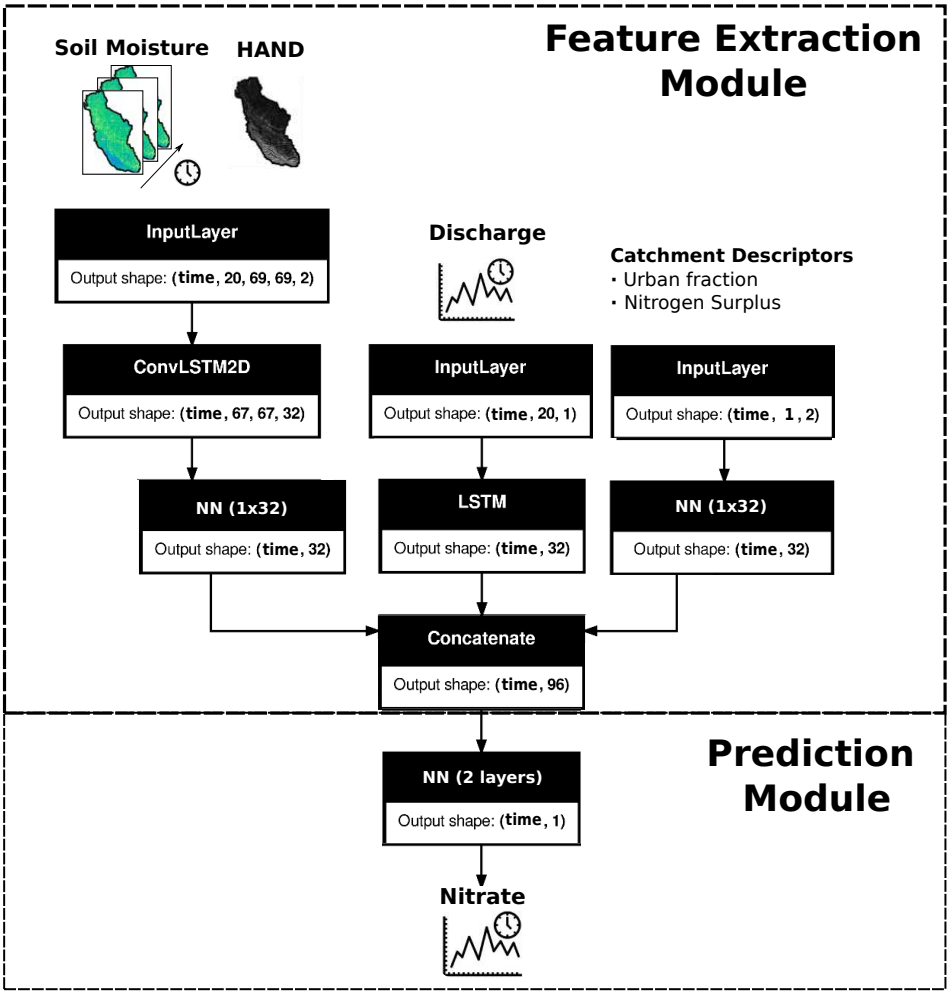

Figure 4.2: Simplified multi-branch deep learning model structure (for the detailed version refer to Figure S3). The model consists of two main parts: the feature extraction module and prediction module. The feature extraction module contains 3 branches in parallel. The first branch (left) consists of a ConvLSTM model that incorporates daily soil moisture maps and a static map of the Height Above the Nearest Drainage (HAND) for each of the study catchments. A single neural network reduces the dimension of the ConvLSTM outputs to fit the size of the other two branches. The second branch (middle) consists of a LSTM model that incorporates daily discharge time series and the third branch consists of a single dense layer that processes the static proxies of nitrogen inputs (i.e., mean annual nitrogen surplus and the fraction of urban areas). The outputs of the feature extraction module feed a prediction module that uses a dense neural network of 2 layers of 9 neural networks each to predict daily nitrate time series for each catchment. All catchment information is organized sequentially for the model training. The dimensions of each layer output is shown as output shape, where time is the first dimension of every element of the model.

4.1.2.1 Deep learning model structure

The model setup consists of two sequential modules: a feature extraction module and a prediction module. The feature extraction module processes data in three parallel branches: discharge time series, spatial patterns of soil moisture together with HAND maps, and static catchment characteristics. The first branch utilizes a Convolutional LSTM network [ConvLSTM; 211] that incorporates daily spatial soil moisture patterns and HAND maps. ConvLSTM combines LSTM with Convolutional Neural Networks in order to extract spatial patterns of two-dimensional data and their temporal dependencies. The second branch incorporates a Long Short-Term Memory (LSTM) model using daily discharge time series as input data [212]. The LSTM model is the current state-of-the-art for time-series data modeling in hydrology, as it considers the temporal dependencies observed in hydroclimatic time series, and it has been successfully used to simulate discharge and nitrate concentrations [213, 214, 197]. The LSTM and ConvLSTM branches process sequences of data with a length of 20 days to capture antecedent catchment wetness conditions. The third branch consists of a single-layer neural network that processes the static catchment descriptors: mean nitrogen surplus and fraction of urban areas. The three branch outputs (i.e., the feature extraction module outputs) must have the same dimension to perform fair comparisons using XAI methods [215]; therefore, a single-layer neural network reduces the dimension of the ConvLSTM branch. The prediction module processes the feature extraction module outputs with a sequence of three-layer neural networks, accounting for possible complex interactions between soil moisture patterns, discharge, and static proxies for nitrogen input to predict the time series of nitrate concentration at the catchment outlets. Each branch of the model employs dropout and L1 regularization based on the Least Absolute Shrinkage and Selection Operator (LASSO) to tackle overfitting [216]. We tested different sequence lengths, neural network structures, alternative structures to reduce the ConvLSTM, and L1 regularization parameters to optimize the model performance (Table 4.4).

We trained the model for all the study catchments simultaneously, transferring knowledge from one catchment to another. We split the time series of each catchment into training and testing sets (75% and 25%, respectively). We normalized the discharge and nitrate concentration time series across catchments using the Box-Cox transformation to stabilize the variance and to obtain data distributions closer to normal, improving the training process [217, 218]. We only used training data to fit Box-Cox parameters to avoid data leakage (i.e., preventing test data from being used during training) [219]. We used the Adam optimizer with an objective function that maximized the Nash-Sutcliffe efficiency (NSE), equally weighted for each catchment. We also computed Kling-Gupta Efficiency [KGE; 220] and root mean squared error (RMSE) to assess model performance. We incorporated early stopping methods to maximize the NSE [221]. Early stopping was based on the test performance to obtain a better fit for applying XAI, enhancing explainability. Additionally, we implemented early stopping on a random selection of 15% of the training data, referred to as validation data, to assess the model's generalization ability. This approach resulted in a median/mean decrease in performance of -4%/-15% in NSE across catchments (Table 4.3). We tested different configurations of the hyperparameters (Table 4.4) based on the validation subset. With the final hyperparameter set, we trained 20 versions of the model, each using a different random

seed to account for stochastic effects during training (e.g., initial weights, dropout selection) [194, 222], and we reported the results for the best 5 model realizations based on NSE efficiency in the test period. We trained the model using TensorFlow 2.16 and CUDA 12.3 in a GPU cluster, with a single model training taking one hour.

4.1.3 Explainable machine learning (XAI)

We use the Explainable AI (XAI) technique SHAP (SHapley Additive exPlanations) to disentangle the importance of discharge and spatial soil moisture patterns in predicting nitrate concentrations and to understand whether our model follows our prior physical knowledge about nitrate dynamics [223, 224]. SHAP values are based on the Shapley value concept from cooperative game theory [225], which estimates the marginal contribution of each input feature to any model prediction.

SHAP values are model-agnostic and adhere to the additivity principle, where the sum of SHAP values $\mathrm{SHAP}_{i,t,\mathbf{x}_i}$ for all input features i across its dimensions $\mathbf{x}_i$ and a reference NO_3-N_0 equals the predicted value NO_3-N_t at timestep t [Equation 4.1, 226]. Hence, SHAP values quantify the positive or negative contribution of each input feature to the predicted target.

$$NO_3\text{-}N_t = \sum_i \mathrm{SHAP}_{i,t,\mathbf{x}_i} + NO_3\text{-}N_0 \tag{4.1}$$

Reference conditions are represented with a background dataset that must be selected according to the objectives of the explainable method [227]. For instance, if the aim is to explain the overall model behavior, the entire training period or a representative subset should be selected as a reference. In our case, we aim to understand how the model simulates nitrate dynamics for different catchments individually, to contrast with our prior knowledge across catchments with different C–Q patterns. Therefore, for each catchment separately, we selected a background set consisting of 100 random time steps from its training period, and we used the testing period timesteps to compute the SHAP values of the input variables. Correspondingly, we obtained non-zero values for the variables that vary over time, i.e., discharge and soil moisture patterns.

We computed SHAP values using the prediction module of our model, as the three inputs of this module have the same size for feature importance comparison. We then computed the feature importance (SHAP importance) of discharge and soil moisture patterns by summing the absolute SHAP values in their second dimension (Equation 4.2, Figure 4.2) for each time step, obtaining a time series of SHAP importance values for the testing period for each of the two features. In addition, to estimate the importance of variables on model performance, we compare SHAP importance with the permutation feature importance method for discharge and soil moisture patterns and report the model performance when excluding these variables (Table 4.3).

$$\text{SHAP Importance}_{i,t}(\%) = \frac{\sum_{\vec{\mathbf{x}}_i} |\mathrm{SHAP}_{i,t,\vec{\mathbf{x}}_i}|}{\sum_i \sum_{\vec{\mathbf{x}}_i} |\mathrm{SHAP}_{i,t,\vec{\mathbf{x}}_i}|} \times 100\% \tag{4.2}$$

Furthermore, we computed the the contribution of each feature accounting the direction (i.e., sign) during different levels of nitrate concentration, discharge and mean normalized soil

moisture series (SM_{mean}), which we use as an aggregated proxy of hydrologic connectivity for visualization purposes. We defined the ranges of discharge and nitrate concentration in four quartiles from low to high and hydrological connectivity based on mean normalized soil moisture as extremely dry ($SM_{mean} < 0.2$), transition from dry to average ($0.2 < SM_{mean} < 0.5$), transition from average to wet ($0.5 < SM_{mean} < 0.8$), and extremely wet ($SM_{mean} > 0.8$) conditions. We defined SHAP contribution of a feature i dividing by the sum of the SHAP values across its dimensions $\mathbf{x}_i$ at a given timestep t by the sum of the absolute values of the sums of SHAP values across the dimensions $\mathbf{x}_i$ at timestep t, and then multiplying by 100 (Equation 4.3). as the sum of SHAP values of discharge and soil moisture patterns in each timestep (i.e., maintaining the sign, 4.3)

$$\text{SHAPcontribution}_{i,t}(\%) = \frac{\sum_{\vec{\mathbf{x}}_i} \text{SHAP}_{i,\vec{\mathbf{x}}_i}}{\sum_i \sum_{\vec{\mathbf{x}}_i} |\text{SHAP}_{i,t,\vec{\mathbf{x}}_i}|} \times 100\% \tag{4.3}$$

Additionally, we examined where in the catchment the model utilized spatially distributed information of soil moisture by computing attention maps. Attention maps are a post-training approach to highlight the input pixels that influence predictions most [228]. To maintain the spatial dependencies, we computed SHAP values again, this time using the entire model (i.e., the feature extraction module and the prediction module). As SHAP values have the same dimensions as the input data, we used the gridded SHAP values of soil moisture to obtain attention maps by summing the absolute values of each pixel for each prediction of the testing period [226]. In these maps, each pixel value represents its contribution to making a given prediction and therefore helps to understand where in the catchment the model focuses its attention while making a prediction under different conditions.

AI-assisted tools, were used for proofreading to improve clarity and readability.

4.2 Results

The configured deep learning model could reproduce daily nitrate concentration with a median NSE of 0.67, a median KGE of 0.73, and a median RMSE of 0.49 mg/L for the test period across all study catchments (median of the 5 best out of 20 realizations, Figure 4.3b), which is substantially higher than the performance of C–Q relationships for the test period (log-log linear regression, median NSE of 0.27, median KGE of 0.37, median RMSE of 0.64, Table 4.2). Only for the largest catchment of our dataset, the Raccoon River at Van Meter (the last catchment in Figure 4.3b), the model fails to reproduce daily dynamics of nitrate during the test period (NSE of 0.08, KGE of 0.66, RMSE of 2.09) likely due to the spatial aggregation of soil moisture data over such a large area. However, for 6 out of the 9 catchments, NSE is above 0.5, KGE is above 0.65, and RMSE is below 0.85 (Figure 4.3b, Table 4.2), with a similar performance compared to other studies despite using shorter time series [e.g., 197]. Model performance in the testing period varies between different realizations, with a standard deviation of $\sigma_{NSE} < 0.13$ ($\sigma_{KGE} < 0.11$, $\sigma_{RMSE} < 0.15$) for every catchment, except for the failed catchment Raccoon River ($\sigma_{NSE} = 0.19$, $\sigma_{KGE} = 0.04$, $\sigma_{RMSE} = 0.21$).

We selected two distinct examples in terms of performance and long-term nitrate export pattern (Figure 4.3c-f): the River Kankakee catchment at Davis, Indiana, (median performance

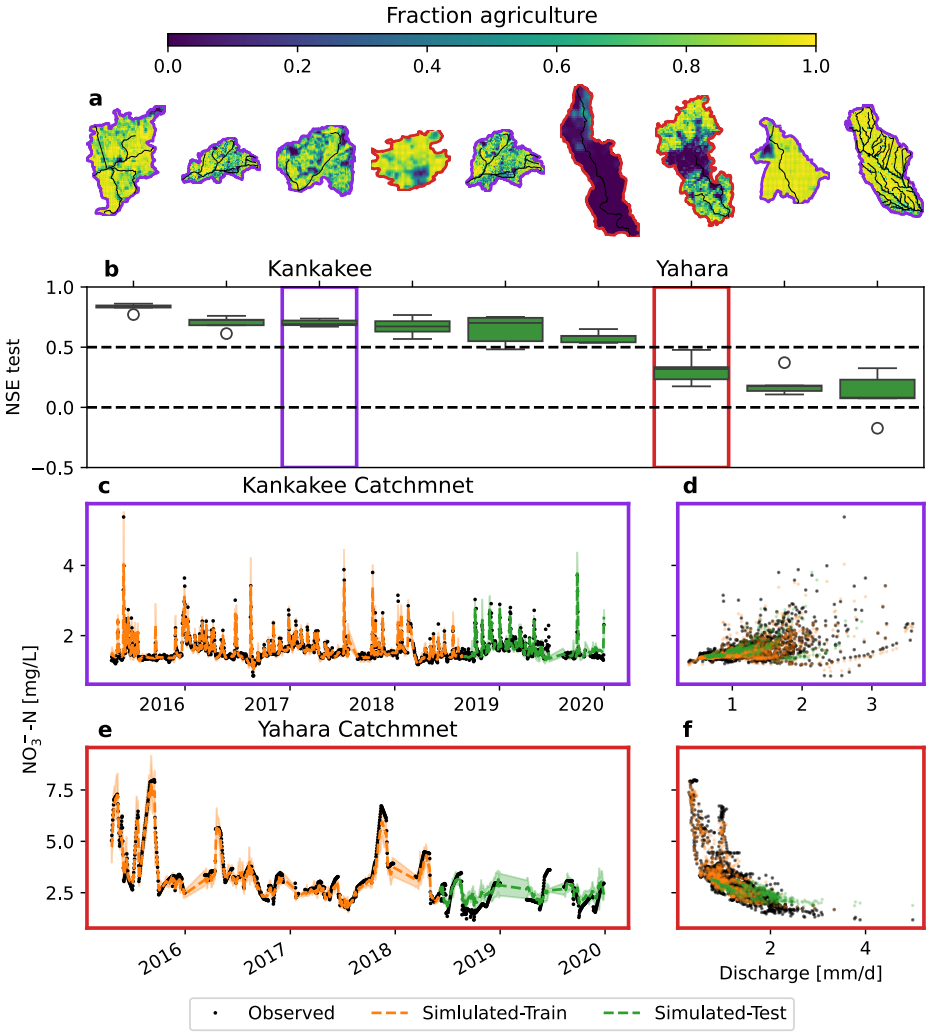

Figure 4.3: Model performance for nine study catchments: a) distribution of agricultural areas in the study catchments organized from left to right based on median model performance during test period. All enrichment catchments (positive C–Q relationship) are marked by a purple outline. Two dilution catchments (negative C–Q relationship) and the one chemostatic catchment (C–Q slope close to zero) are indicated by a red outline. b) NSE values for the test period of the 5 out of 20 best model realizations, the purple and red rectangles show the two representative catchments that we exemplify in this study: the Kankakee catchment and the Yahara catchment, respectively. c-d) Observed nitrate time series and mean simulated values across the 5 realizations during the training period and test period for the Kankakee catchment, characterized by a positive C–Q relationship (i.e., enrichment pattern), and e-f) same for the Yahara catchment, characterized by the negative C–Q relationship (i.e., dilution pattern). The colored bands in panels c and e represent the range of daily simulated nitrate values for the 5 realizations. The simulated time series of all study catchments are shown in Figure 4.11.

NSE of 0.69, KGE of 0.85, RMSE of 0.19) with a positive C–Q relationship (i.e., enrichment), and the River Yahara catchment near Futton (median performance NSE of 0.32, KGE of 0.47, RMSE 0.49) with a negative C–Q relationship (i.e., dilution). The C–Q pattern in both cases is well represented (Figures 4.3d and 4.3f), showing the capabilities of the model to capture these two contrasting behaviors, which also apply to the other catchments (Figure 4.11). The performance of the model remains consistent over time across different realizations, as indicated by the low variability in the simulated nitrate concentration time series. Specifically, the spread of realizations is minimal, as shown by the narrow colored bands in the two exemplary catchments (Figures 4.3c and 4.3e), as well as across the other catchments (Figure 4.11).

4.2.1 Exploring model behavior using XAI

We applied the XAI method SHAP to uncover model decisions, assess the importance of the input features in each prediction, and evaluate whether the model aligns with the prior hydrological knowledge on nitrate export dynamics at catchment scale.

4.2.1.1 Overall input variable importance using SHAP values

Results show a median SHAP feature importance value of 69.5% for discharge and 30.5% for spatial patterns of soil moisture across all catchments (Figure 4.4a), with the median SHAP feature importance of spatial patterns of soil moisture ranging from 18% to 43% across catchments. Median SHAP feature importance across catchments is similar for different model realizations (ranging from 26% to 39% for spatial patterns of soil moisture and 60% to 73% for discharge), indicating a consistency of solutions selected by the model in the different realizations (Figure 4.4b). The importance of spatial patterns of soil moisture is additionally confirmed by its high permutation feature importance (32%) and a 11% to 14% drop in the model performance when the soil moisture data is excluded (NSE, Table 4.3). In addition, model performance drops by 5%-11% when excluding HAND maps and by 6% to 12% when including maps of fraction of agriculture.

We explored SHAP values under different conditions for the two exemplary catchments (Figure 4.4c, d). The Kankakee River in Davis (which exhibits an enrichment C–Q pattern) shows a relatively higher SHAP importance (absolute feature importance) of soil moisture compared to all other catchments (Figure 4.4b). Accounting for the sign of SHAP values, we observed that SHAP contribution of both discharge and soil moisture changes from negative to positive as nitrate concentrations increase (Figure 4.4c), with soil moisture being relatively more important for predicting nitrate values below the average (average NO_3-N of 1.63 mg/L for the test period), compared to high nitrate concentrations. In this catchment, when mean soil moisture of the catchment transitions from dry to wet states on average (i.e., hydrological connectivity expands), the importance of discharge and soil moisture shifts. During dry periods (i.e., $SM_{mean} < 0.2$, Figure 4.4d) in this catchment, SHAP contribution of soil moisture are closer to zero (i.e., to the background level) compared to discharge, indicating that the prediction of low nitrate concentrations is largely based on discharge alone. During transitional periods from dry and intermediate wetness states (i.e., $0.2 < SM_{mean} < 0.5$, Figure 4.4d), spatial patterns of soil moisture dominate nitrate predictions (SHAP contribution close to -100%), indicating reduced nitrate transport during drier conditions. During transitional periods

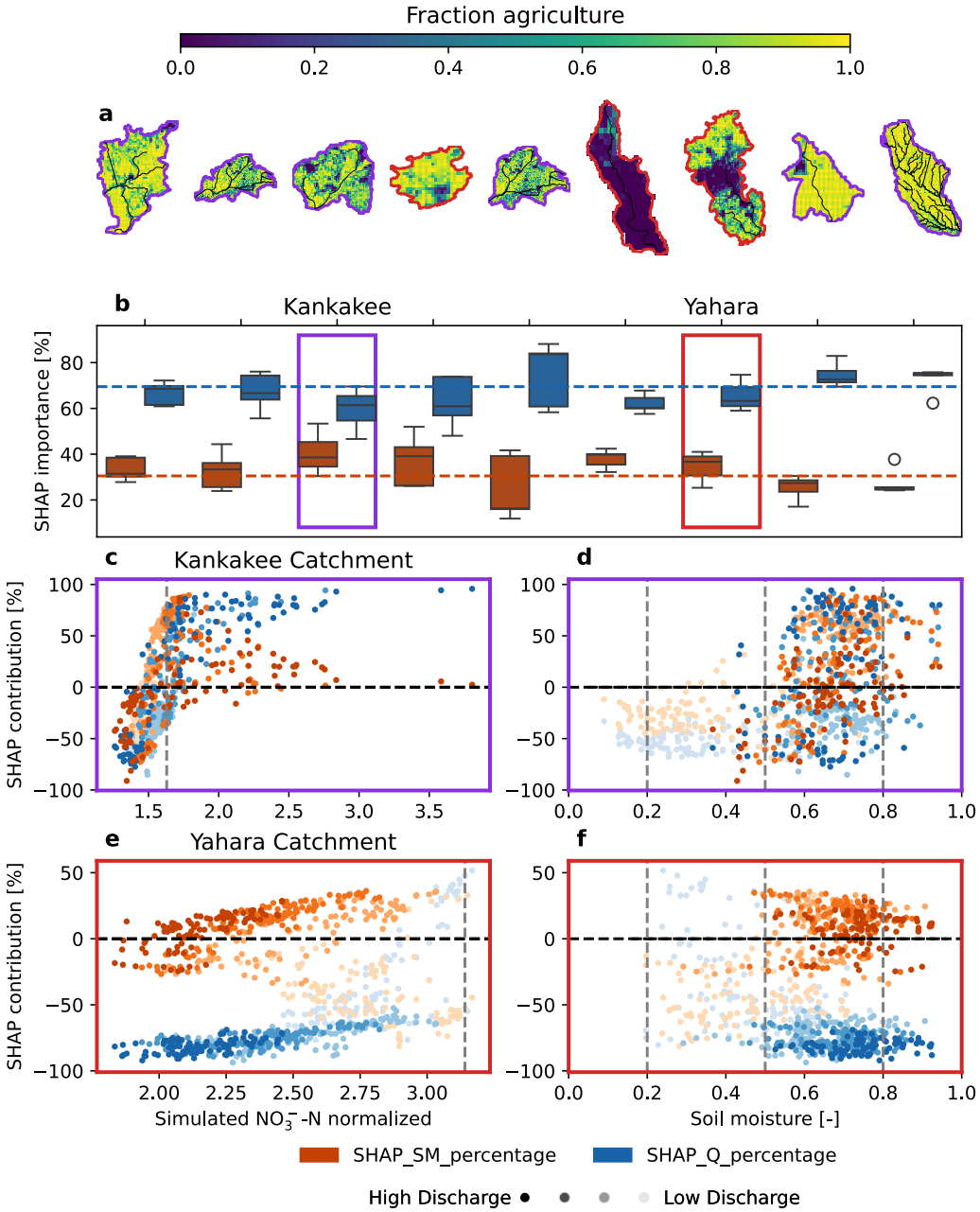

Figure 4.4: SHAP Feature importance during the test period for the nine study catchments: a) Distribution of agricultural areas in the study catchments, organized from left to right, based on median model performance. All enrichment catchments (positive C–Q relationship) are marked by a purple outline. Two dilution catchments (negative C–Q relationship) and the one chemostatic catchment (C–Q slope close to zero) are indicated by a red outline. b) Median SHAP importance of soil moisture and discharge across the 5 best model realizations out of 20. The purple and red rectangles show the selected two example catchments: the Kankakee catchment and Yahara catchment, respectively. c) Mean SHAP contribution across model realizations as a function of nitrate concentration for the Kankakee catchment (enrichment pattern). d) Mean SHAP contribution across model realizations as a function of catchment-averaged soil moisture for the Kankakee catchment. e) Mean SHAP contribution across model realizations as a function of nitrate concentration for the Yahara catchment (dilution pattern). f) Mean SHAP contribution across model realizations as a function of catchment-averaged soil moisture for the Yahara catchment. Discharge levels from low to high are defined based on observed discharge quartiles during the testing period for each catchment in panels c-f. Vertical dashed lines in gray in c) and e) show the mean simulated NO_3-N in the test period, and in d) and f) the wetness states (i.e., hydrological connectivity) from dry periods ($SM_{mean} < 0.2$), transitional periods from dry and intermediate state ($0.2 < SM_{mean} < 0.5$), transitional periods from intermediate to wet conditions ($0.5 < SM_{mean} < 0.8$), and wet conditions ($SM_{mean} > 0.8$).

from intermediate to wet conditions (i.e., $0.5 < \mathrm{SM}_{\mathrm{mean}} < 0.8$, Figure 4.4d), the contribution of soil moisture patterns is mostly positive and its importance increases with connectivity level, indicating an increase in nitrate transport. During wet conditions ($\mathrm{SM}_{\mathrm{mean}} > 0.8$, Figure 4.4d), the contribution of soil moisture remains stable, while discharge contribution depends on the discharge level itself, in line with the expected enrichment C–Q behavior (Figure 4.9). Similarly, most enrichment catchments exhibited a shift in soil moisture SHAP contribution from negative to positive as mean soil moisture transitions from dry to wet conditions (Figure 4.12). The shift in the dominance of discharge and soil moisture patterns highlights the importance of hydrological connectivity in predicting nitrate transport. In extremely dry periods with disconnected flow paths and in wet periods where most flow paths are activated, the predictive power of soil moisture patterns decreases but unfolds its full potential during the transition period.

For the Yahara catchment, the importance of spatial patterns of soil moisture in predicting nitrate increases under lower discharge levels and higher nitrate concentrations (Figure 4.4e). From dry to average wetness conditions, SHAP contribution of soil moisture shifts nitrate concentration to lower values, while during average to wet conditions, soil moisture SHAP contribution is rather positive. However, under these conditions, the overall contribution is always lower than 40%. Discharge SHAP contribution is especially high (i.e., almost -100%) during wet soil moisture conditions and when discharge levels are high (dark blue dots in Figure 4.4f), suggesting a dominance of a diluting effect by discharge surplus.

4.2.1.2 Attention maps of soil moisture patterns

The selected XAI method enables not only examination of the average feature importance under varying conditions, but also identification of the specific locations where the model concentrates its attention during prediction. We explored the attention maps for different conditions in our two example catchments: the Kankake catchment at Davis (enrichment) and the Yahara River catchment near Futton (dilution). For the enrichment catchment, the median attention maps during the test period exhibit that the most relevant pixels are concentrated in the near-stream zones (i.e., areas with small height above the nearest drainage, HAND), where land cover is mainly agriculture (Figure 4.5a, Figure 4.6a). Indeed, half of the model attention is concentrated in the near-stream areas with HAND values (height above nearest drainage) below 38 m (vertical dashed line in Figure 4.5a). Locations closer to the stream (i.e., low HAND) exhibit a higher variability of SHAP values, while in zones located further away from the streams, absolute SHAP values tend to zero. When we compare the attention of each pixel during periods with high nitrate concentrations and average conditions (i.e., difference in attention between timesteps at the highest quartile of nitrate concentration and median attention across timesteps for each pixel), we observe an overall increase in the attention during the high nitrate concentration periods for the enrichment catchment within near-stream zones (Figure 4.5b). Between high connectivity and median conditions (i.e., the difference in attention between timesteps at the highest quartile of catchment-averaged soil moisture and the median attention across all timesteps), the model shows increased attention in near-stream zones. During high hydrological connectivity, the total feature importance of spatial patterns of soil moisture rises to 50% (Figure 4.5c, boxplot), which, in combination with positive SHAP

values shown in Figure 4.4d during wet periods, indicates that soil moisture patterns in these areas particularly contribute to the predictions when the model attempts to simulate high nitrate concentrations.

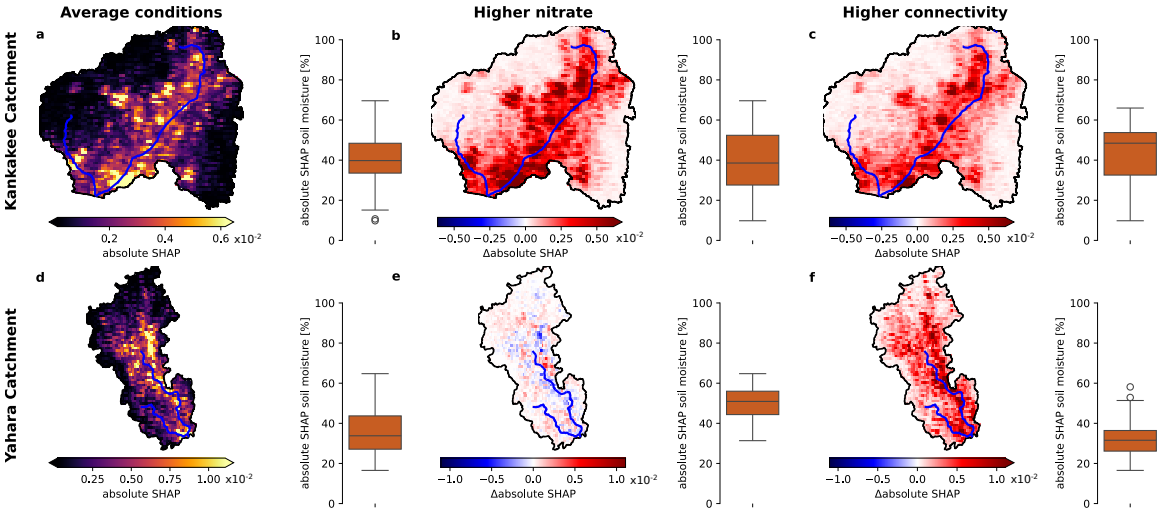

Figure 4.5: Attention maps of the Kankakee (top panel) and Yahara catchments (bottom panel) computed as absolute SHAP values (the values are in Box-Cox transformed units of nitrate during the test period). a) and d) show median attention maps across the test period; b) and e) show the difference between attention maps during periods with high nitrate concentrations (i.e., the highest quartile of observed nitrate concentration during the test period) and median attention maps; c) and f) show the difference between attention maps during the periods associated with high levels of hydrological connectivity (i.e., the highest quartile of catchment-averaged observed soil moisture during the test period) and median attention maps, for the Kankakee (enrichment) and Yahara (dilution) catchments, respectively. The river network is shown in blue for each attention map. Boxplots at the right of each attention map show the relative feature importance of spatial patterns of soil moisture during average conditions (see Figure 4.4b), during high nitrate concentrations and during high levels of hydrological connectivity, respectively.

4.3 Discussion

We present, to our knowledge, the first successful attempt to model nitrate concentration time series across catchments using a multi-branch deep learning model that incorporates spatially distributed soil moisture data and discharge time series. Despite the short time series (less than 4 years), the model can satisfactorily capture nitrate dynamics in 8 out of 9 catchments that exhibit diverse landscape, agriculture distribution, nitrogen surplus, and concentration-discharge patterns. In the following sections, we discuss the insights gained from our modeling framework, the application of explainable AI (XAI) techniques, and the limitations and future opportunities that this work presents.

4.3.1 Soil moisture patterns as a proxy of hydrological connectivity

We demonstrated that antecedent and concurrent spatial patterns of soil moisture, together with discharge information, can more accurately represent nitrate concentration dynamics at the catchment scale, which can be indicative of hydrological connectivity as it shapes

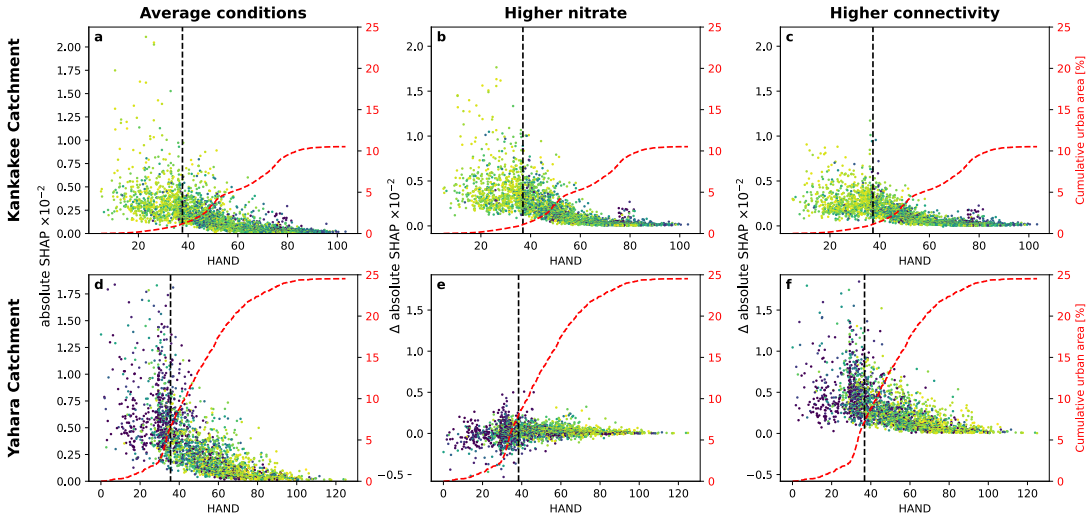

Figure 4.6: Scatterplots of pixel-wise model's attention computed as absolute SHAP values and the corresponding height above the nearest drainage (HAND) for the Kankakee (a, b, c) and Yahara (d, e, f) catchments computed as the absolute SHAP values in the Box-Cox transformed units of nitrate during the test period. The cumulative urban areas of the catchment are plotted in the right y-axis. a) and d) show median attention across the test period; b) and e) show the difference between attention during periods with high nitrate concentrations (i.e., the highest quartile of observed nitrate concentrations during the test period) and median attention; c) and f) show the difference between attention during periods with high level of hydrological connectivity (i.e., the highest quartile of mean observed soil moisture during the test period) and median attention, for the Kankakee (enrichment) and Yahara (dilution) catchments, respectively. HAND is plotted in the x-axis and the colorbar shows the fraction of agriculture of each pixel. The vertical dashed line shows the HAND value at which 50% of the attention is reached.

nitrate transport and transformation [72, 183, 31]. While high levels of discharge dilute nitrate released from point sources, nitrate from agricultural sources travels across the landscape to streams through a variety of flow paths progressively activated with the increase of hydrological connectivity [229, 230]. Since discharge provides only a catchment average signature of overall wetness and connectivity conditions in temperate climates, the spatial patterns of soil moisture in addition to HAND maps provide crucial information about the potential spatial variability of hydrological pathways [231, 230]. Indeed, incorporating soil moisture patterns considerably improves the performance of the model (Table 4.3) and accounts for 30.5% of the predicted values according to SHAP feature importance computation.

Results are consistent with our hypothesis across all study catchments characterized by different C–Q relationships. On the one hand, in the catchments with a positive C–Q relationship, the spatial patterns of soil moisture and discharge control the nitrate transport from diffuse agricultural sources (Figure 4.13). During extremely low levels of hydrological connectivity, soil moisture patterns have a relatively lower explanatory power on nitrate concentration compared to discharge (Figure 4.7b). During extremely dry conditions in enrichment catchments, spatial patterns of soil moisture rather represent the vertical fluxes of water in the catchment (e.g., evapotranspiration or infiltration) than hydrological connectivity that can produce lateral flow, transporting nitrate to streams [190]. In the transition from dry to wet conditions, namely the expansion phase, both discharge and soil moisture contribute to an increase in the predicted nitrate concentrations as hydrological connectivity increases. We observe that under these expanding conditions, the model is able to infer the activation of hydrological pathways that increase nitrate transport from spatial patterns of soil moisture and discharge. During extremely wet conditions, the importance of soil moisture spatial patterns remained at a similar value ($\sim$ 40–50%, Figure 4.7b, Figure 4.12), while nitrate concentration increased in enrichment catchments. As the spatial variability of soil moisture increases with higher levels of hydrological connectivity in most of the study catchments (7 out of 9 catchments, Figure 4.9), similarly to other studies [57, 58, 59], we did not find strong signs of homogenization of moisture under extremely wet conditions that could decrease the attention of the model during these conditions (Figure 4.9).

On the other hand, catchments with a negative C–Q relationship have a high fraction of urban areas near the stream network, suggesting that point sources of nitrate shape the dilution C–Q pattern [232]. XAI analyses show two contrasting behaviors in these catchments between discharge and spatial patterns of soil moisture (Figure 4.7d). Similarly to enrichment catchments, spatial patterns of soil moisture increase the predicted nitrate concentration during wet periods and reduce nitrate concentration during dry periods, as they reproduce the diffuse sources dynamics in the catchment. However, the model learns the dilution effect of discharge in these catchments, decreasing nitrate concentration with increased levels of hydrological connectivity. The increase in nitrate concentration during dry conditions caused by discharge is supported by extensive literature on the effect of point sources acting as constant effluents increasing nitrate concentration in rivers during low flows due to a lack of dilution [70, 176, 233].

As we observed in our XAI-based modeling study, considering not only discharge but also spatial patterns of soil moisture enhances the ability to predict nitrate dynamics at the

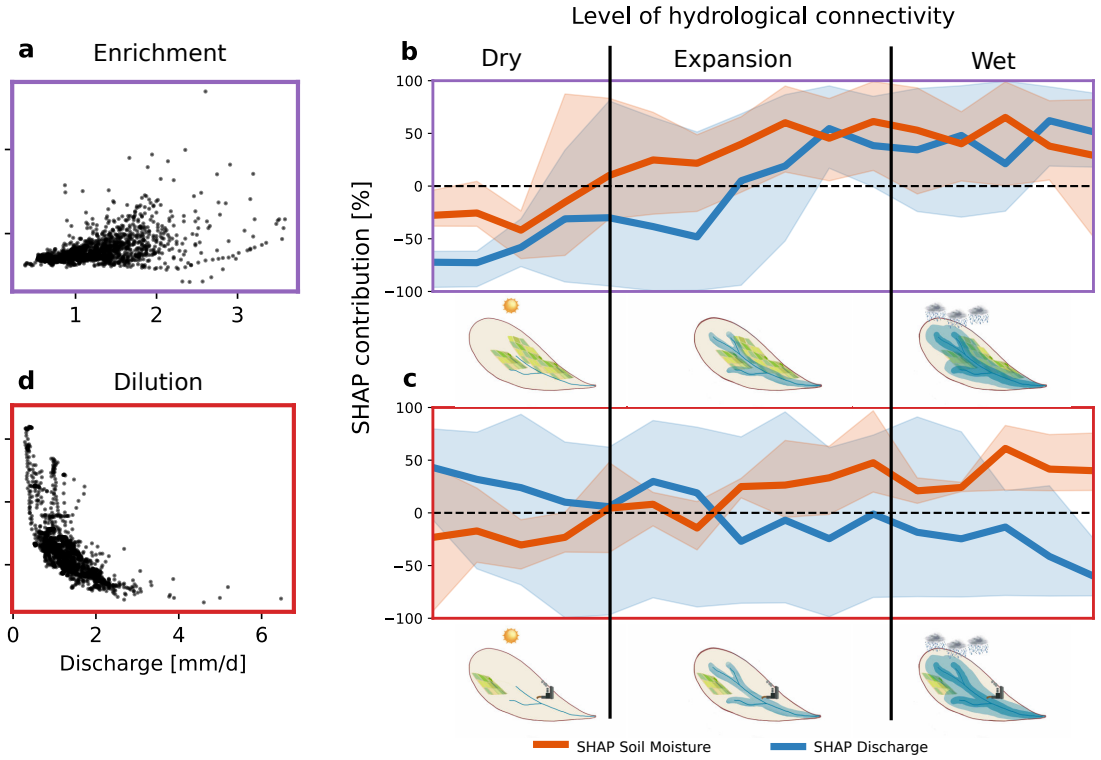

Figure 4.7: Synthesis of all catchments. a) and c) show the concentration-discharge relationship for the examplary Kankakee (enrichment) and Yahara (dilution) catchments as example diagrams, respectively; b) summarizes the feature importance computed as SHAP contribution for the five enrichment catchments (excluding the failed Raccoon catchment) across different hydrological connectivity levels, defined as deciles of catchment-averaged soil moisture for each catchment; d) presents the same for the two dilution catchments and the one chemostatic catchment. Colored bands show the range of values across catchments, and the colored lines the mean values across catchments.

catchment scale. Discharge alone, as an indicator of catchment average wetness state, overlooks spatially heterogeneous runoff generation processes and solute transport pathways, particularly when catchments are not very dry or nearly saturated. For instance, the contraction or expansion of the river network has a strong impact on nutrient delivery by directly influencing riparian area retention and removal of nitrate [184, 185, 158]. Additionally, spatial information on soil moisture provides insights into ephemeral stream dynamics, which has a direct impact on the transport of nutrients in hillslopes and in drier climates [72, 31]. These factors suggest that the combined use of discharge and spatial patterns of soil moisture serves as a more effective indicator of the catchment hydrological connectivity state to predict nitrate dynamics.

4.3.2 XAI based approach test mechanistic drivers of nitrate dynamics

With the advent of explainable AI (XAI) techniques, we can now address the "black box" nature of machine learning models, allowing us to judge the explainability and reject models if they are not in line with mechanistic understanding. While XAI can not establish causal relationships, it can reveal informative statistical relationships between variables, helping to test challenging geoscientific hypotheses [194].

In this study, we grounded our hypothesis based on the evidence from well-studied field sites reported in the literature: spatial patterns of soil moisture are indicative of hydrological connectivity and hence can be useful for predicting nitrate dynamics at catchment outlets. We adopted this hypothesis-driven approach in our explainable machine learning framework and used SHAP, to quantify the contribution of spatial patterns of soil moisture and to understand the model reasoning behind predictions. The results are not sensitive to the choice of XAI method as soil moisture importance is consistent between SHAP method and permutation feature importance. Moreover, it is in line with a drop of model performance when spatial patterns of soil moisture are excluded from training, corroborating that soil moisture spatial patterns in addition to discharge can capture temporal nitrate dynamics at the catchment scale.

As several studies use XAI to find dominant drivers for different processes [e.g., 196], by using the presented framework we can explore XAI attention maps to understand the daily nitrate dynamics and spatial dependence of soil moisture in multiple catchments. These diagnostic maps can be used to check whether or not the model focuses its attention on parts of the catchment of notable physical relevance. We observed that in this study the model primarily focuses on near-stream areas of the catchments, where hydrological connectivity alters more frequently throughout the year compared to hillslopes. Moreover, spatial patterns of soil moisture in these areas suggest a decrease in nitrate concentration during dry periods. The near-stream zones, and in particular, the riparian areas, are connected for longer periods during the year, including dry periods, and they are the hotspots for biogeochemical processes such as denitrification that can decrease nitrate concentrations [184, 158, 156].

We observed that the model behavior changes in catchments with different land cover in near-stream areas, suggesting a potential link between near-stream sources and nitrate dynamics (Figure 4.6). Pinpointing sources of nitrate in the landscape during different hydrological conditions is complex. Different studies inferred the link between locations of nitrate sources and nitrate dynamics based on catchment-aggregated spatial indexes [e.g.,

landscape configuration indexes; 234, 33], by using physically based or conceptual models [e.g., 148, 43], by exploring different runoff event responses [e.g., 75, 41], or by directly measuring hillslope connectivity in experimental catchments [e.g., 147]. However, little research has explicitly utilized spatially distributed data to pinpoint heterogeneous nitrate sources in the landscape under varying conditions. Although the proposed modeling framework does not directly consider the location of sources, results suggest a potential link between near-stream sources and nitrate concentration. These promising results encourage future studies to use similar approaches to directly link hotspots of nitrate under different hydrological conditions. In addition, presented findings suggest that in such critical areas, it might be worth analyzing soil moisture patterns at even higher spatial resolution.

The incorporation of hybrid satellite-based soil moisture information in our XAI framework demonstrates that novel hyperresolution products can be used to explore hydrological connectivity in greater detail. This approach is particularly valuable given the challenges of measuring hydrological connectivity at larger scales and for extended time periods. Manual observations of catchment saturation at multiple locations are not feasible in most of the catchments and are typically applicable only for relatively small areas [e.g., 147]. Even with advancements such as unmanned aerial vehicles (UAVs), gamma ray sensors, and cosmic ray neutron probes for monitoring hydrological processes, it remains impractical to monitor large catchments over extended durations due to operational costs and infrastructure limitations [235, 236, 237]. Therefore, currently only hyper-resolution hybrid satellite products, such as SMAP-HydroBlocks, offer a realistic and effective option for developing scalable nitrate modeling capabilities that incorporate spatially heterogeneous processes in environmental science.

4.3.3 Limitations and future work

Although the model captured nitrate dynamics in most of the catchments, its performance was lowest in the Raccoon River, the largest catchment in the dataset. The spatial aggregation of soil moisture data over such a large area likely resulted in a loss of fine-scale hydrological connectivity signals, which are better preserved in smaller catchments. Indeed, the SHAP importance of soil moisture in this catchment was minimal compared to discharge, indicating that the model could not effectively learn from spatial soil moisture patterns. To address this issue, future model applications in large catchments could benefit from pre-selecting hydrologically connected areas rather than aggregating soil moisture data over the entire catchment, ensuring that fine-scale connectivity signals remain well represented.

Large datasets are critical for training accurate and generalizable Deep Learning models [238, 239]. Nevertheless, the availability of daily nitrate data is limited to short time spans and a few developed countries as measuring nitrate at this frequency is labor-intensive [201]. With the growth in open-access initiatives (e.g., National Ecological Observatory Network in the U.S., Edmonds et al. [240]; Erlenbach catchments in Switzerland, Knapp et al. [48]), research across countries using high-frequency data is becoming more feasible. However, most of the initiatives are still concentrated in the U.S. and Europe. Additionally, the availability of soil moisture data for four years in the United States constrains the broader applicability of the presented approach. Future versions of hyperresolution soil moisture products, such

as SMAP-HydroBlocks, may expand datasets temporally and geographically, enabling the development of more generalized models [241].

An important limitation of the proposed modeling framework is that strong spatial discontinuities distort attention maps, as noted by [203]. This limitation reduces the model ability to capture the spatial distribution of sources such as agriculture or urban areas. We found that removing urban areas and imputing values helped maintain data consistency. However, when using land cover maps (i.e., fraction of agriculture) strong gradients at land-use transitions still impact model training by disproportionately focusing attention on these areas and decreasing model performance (Table 4.2). One possible solution could be training separate modules for different land use categories after smoothing (e.g., urban vs. agricultural land cover) to reduce the confounding effects of mixed land uses on attention maps.

The contrasting results in terms of model behavior in catchments with different nitrate sources in near-stream areas suggest the potential to directly identify nitrate hotspots. However, with the presented approach, it is not possible to establish relationships that could pinpoint these areas. Future research could expand our approach beyond hydrological connectivity by incorporating the spatial distribution of nitrate sources and explicitly identifying potential hotspots under different hydrological conditions. However, current nitrogen surplus or fertilization application maps have spatial resolutions that might still be too coarse for these objectives [e.g., 173, 242, 243].

Lastly, the issues associated with the uncertainty and limited causality of machine learning approaches are worth noting here. Complex machine learning models can converge on multiple optima. By using multiple model realizations, we address the uncertainty of interpretations, which is a common pitfall [194], and we obtained a strong consistency across the model realizations in each individual catchment (Figure 4.3b). We mitigate the equifinality problem by selecting the best five performing model realizations and ensuring that explanations are consistent for different model realizations. However, it may still yield varying interpretations by XAI methods. Consequently, the relationships uncovered using XAI provide a sense of correctness regarding their alignment with prior knowledge but should not be directly interpreted as causal relationships [194]. Despite the need for further research to generalize the model and to incorporate more input information to identify nutrient hotspots, we have laid the groundwork for future efforts to provide XAI assessments that could improve water quality management at the catchment scale.

4.4 Chapter conclusions

In this study, we tested the hypothesis that spatial patterns of soil moisture are indicative of hydrological connectivity and can enhance capabilities for modeling stream nitrate concentrations using multi-branch deep learning models and explainable AI (XAI). To address this hypothesis, we developed a deep learning model that explicitly considers spatial patterns of soil moisture and discharge time series, which respectively serves as spatially distributed and catchment-aggregated proxies of hydrological connectivity. According to the XAI method SHAP, spatial patterns of soil moisture account for 30% of the feature importance, with discharge accounting for 70%. The role of soil moisture in nitrate predictability is also

evidenced by a decrease of 14% in the performance (NSE) when soil moisture spatial patterns are excluded from model training. Our results show that the spatial patterns of soil moisture are particularly helpful in predicting nitrate export patterns, especially when the catchment is in transitional periods from dry to wet or when the catchment is nearly saturated, when most lateral flow paths are activated.

We showed how XAI helped us to verify that the deep learning model decisions align with the known physical processes. The model supports our hypothesis, demonstrating distinct explanations across catchments with contrasting C–Q patterns. In catchments with positive C–Q patterns, nitrate dynamics are controlled by interactions between diffuse sources and hydrological connectivity, as evidenced by an increase in nitrate concentrations during wet periods. In contrast, catchments with negative C–Q relationships, dominated by point sources near stream networks, discharge and soil moisture patterns are opposed. When catchments are wetter, spatial patterns of soil moisture result in higher simulated nitrate levels, reflecting the expected interactions between diffuse sources and hydrological connectivity. Conversely, higher discharge values decrease nitrate concentrations due to a dominating dilution effect in these catchments.

XAI attention maps enabled us to identify where in the landscape the deep learning model focuses its attention, pointing to near-stream zones as the most important areas of catchments for accurate nitrate predictions. This is in line with our hydrological understanding of the system, as near-stream zones are more frequently connected to the river and they include riparian areas that are known to play a key role in nitrate transport and transformation. However, our approach can further provide source- and process-related information that enable understanding of nitrate dynamics at the catchment scale.

Acknowledging the limitations of our framework (e.g., data availability, uncertainties, and limited causality), our work provides the first successful attempt to enhance nitrate concentration predictions by taking advantage of spatial patterns of soil moisture. Our study highlights the great potential of deep learning and XAI to identify important areas for hydrological connectivity, paving the way for future research that may explicitly identify hot spots of nitrate contamination. The main findings of this study can be summarized as follows:

1. Developed a multi-branch deep learning model to predict daily nitrate concentrations in 9 catchments using streamflow data and high-resolution satellite soil moisture maps (SMAP-Hydroblocks). The model achieved a median Nash-Sutcliffe Efficiency of 0.64 in 8 out of 9 catchments.

2. Spatial soil moisture patterns contributed approximately 30% to the model's feature importance for nitrate prediction. Removing these patterns reduced model performance by about 14%.

3. Explainable AI (XAI) techniques identified near-stream hydrological connectivity hotspots as key regions for predicting nitrate export.

4. This study demonstrates the potential of combining XAI with remote sensing data to improve nitrate predictions and to map informative areas for nitrate export.

Data availability statement: All data, software, and research objects used in this study are openly available to ensure transparency and reproducibility. Daily discharge and nitrate concentration data for each catchment outlet were obtained from the U.S. Geological Survey (USGS) National Water Information System (NWIS) and can be accessed at: `https://waterservices.usgs.gov`. We show each site number as ID USGS in Table S1 in Supporting Information, the paratemerCD as "0060" (flow), "99133," and "00631" (nitrate plus nitrite concentration). Soil moisture time series were extracted from the open-access SMAP-HydroBlocks dataset [244], available on Zenodo: `https://doi.org/10.5281/zenodo.4558783`. Catchment characteristics were derived from: The GAGES-II dataset /citeFalcone2011, available at: `https://water.usgs.gov/GIS/metadata/usgswrd/XML/gagesII_Sept2011.xml`. The National Land Cover Database (NLCD) [245], available at: `https://www.mrlc.gov/data/nlcd-2016-land-cover-conus`. Nitrogen surplus data were sourced from [173]. Elevation data were obtained from the Shuttle Radar Topography Mission (SRTM) Digital Elevation Model (DEM) dataset, which is freely available at: `https://doi.org/10.5066/F7PR7TFT`.

4.5 Supporting Information

Table 4.2: Summary of model performance metrics. The median and standard deviation of model performance in the test period is shown using the median Nash-Sutcliffe efficiency (NSE), Kling-Gupta efficiency (KGE) and the root mean squared error (RMSE). We also fit a linear model in the log space (C–Q) to predict nitrate concentration (C) from discharge observations (Q) using the training data and show the performance metrics in the testing period.

Site Name	Iroquois River Near Foresman	Kankakee River At Shelby	Kankakee River At Davis	Yahara River At Windsor	Kankakee River At Dunns Bridge	Rock Creek At Joyce Rd Washington	Yahara River Near Fulton	Spoon River Near St. Joseph	Raccoon River At Van Meter
Site ID	5524500	5518000	5515500	5427718	5517500	1648000	5430175	3336900	5484500
Median NSE	0.84	0.73	0.69	0.67	0.7	0.59	0.32	0.18	0.08
Std NSE	0.03	0.06	0.03	0.08	0.12	0.05	0.12	0.1	0.19
Median KGE	0.82	0.74	0.85	0.73	0.76	0.63	0.47	0.48	0.66
Std KGE	0.06	0.05	0.05	0.05	0.08	0.06	0.11	0.06	0.04
Median RMSE	1.12	0.35	0.19	0.82	0.41	0.19	0.49	2.16	2.09
Std RMSE	0.11	0.03	0.01	0.1	0.08	0.01	0.04	0.14	0.22
C-Q NSE	0.56	0.41	0.21	0.41	0.27	-0.44	0.62	-0.02	-2.3
C-Q KGE	0.53	0.45	0.22	0.36	0.37	-0.35	0.76	0.49	0.14
C-Q RMSE	1.83	0.52	0.3	1.11	0.64	0.36	0.37	2.4	3.95

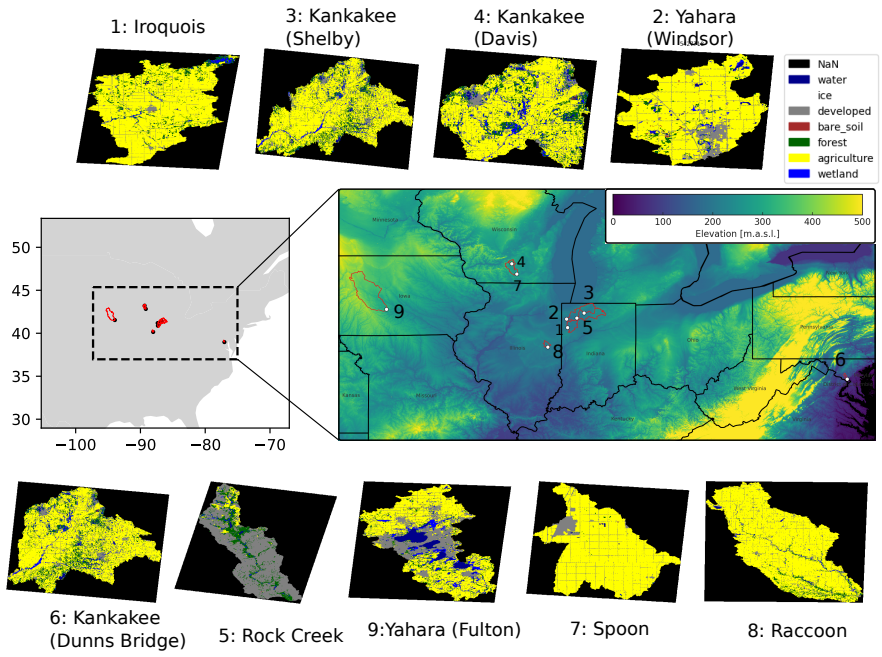

Figure 4.8: Location and land cover of the nine study catchments. The central left panel shows the geographical location of the catchments, with the dashed box indicating the zoomed-in region. The central right panel provides a closer view of this region and topography (Mapzen, Global Terrain Tiles), with each catchment labeled from 1 to 9. Surrounding panels display the detailed land cover types for each catchment, including water, ice, developed areas, bare soil, forest, agriculture, and wetlands.

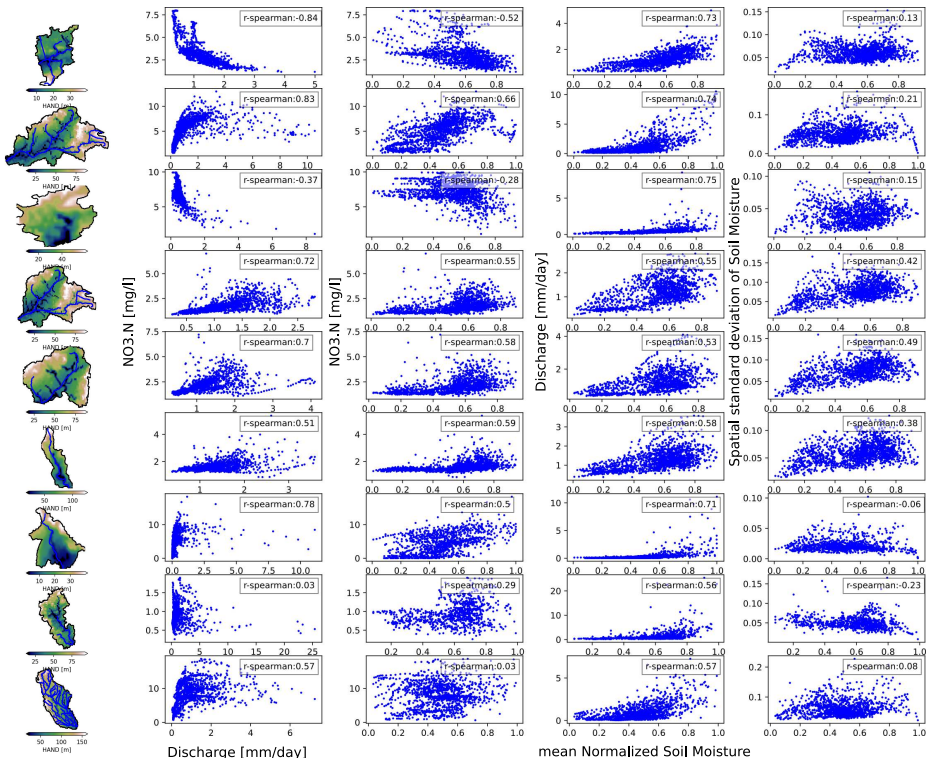

Figure 4.9: Height above the nearest drainage (HAND, first column) and the relationships between nitrate concentration, discharge, standard deviation of normalized soil moisture and mean normalized soil moisture for each catchment. The spearman coefficient between each pair of time series is shown in each panel.

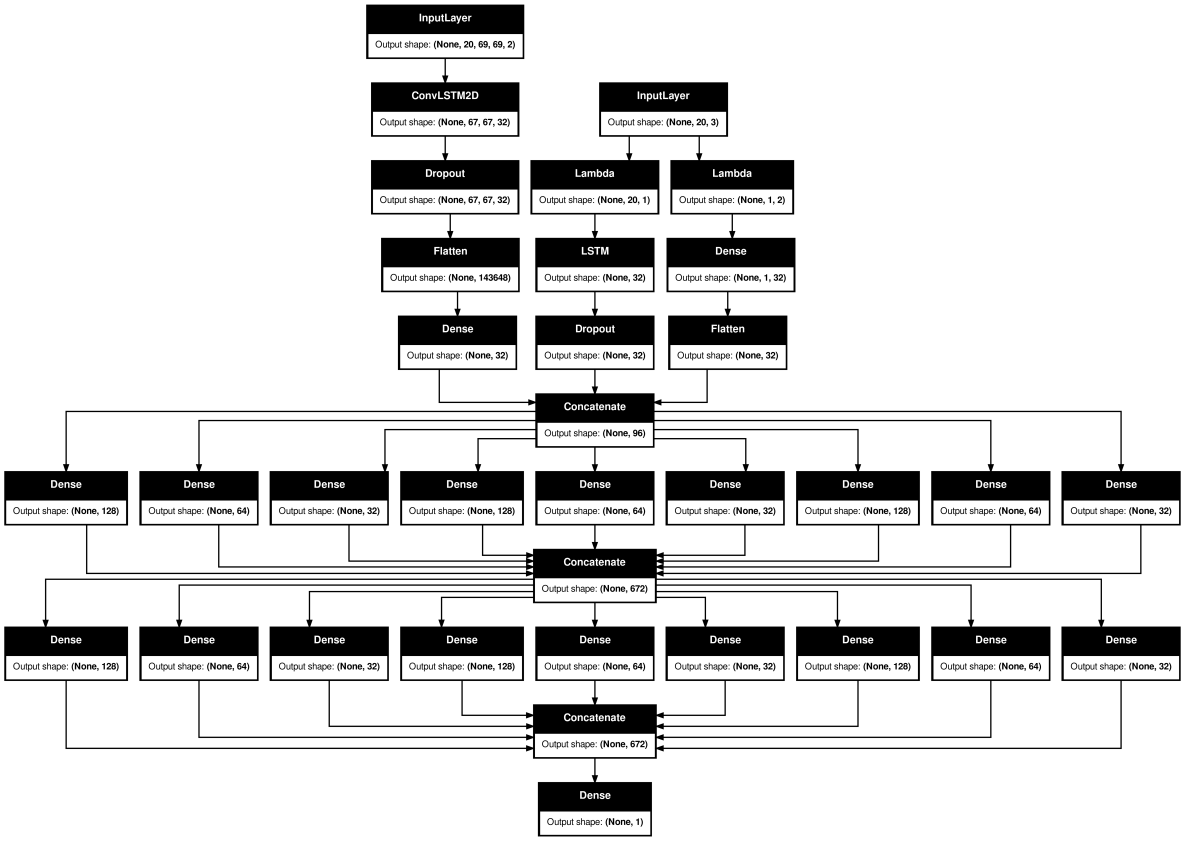

Figure 4.10: Detailed model structure shown in Figure 2 in the main manuscript. The dimensions of each layer output is shown as output shape, where None represents any time dimension. The Lambda layer splits the data between time series of discharge and static parameters (i.e., mean nitrogen surplus and fraction of urban areas) as both input data are treated as a single input by the model.

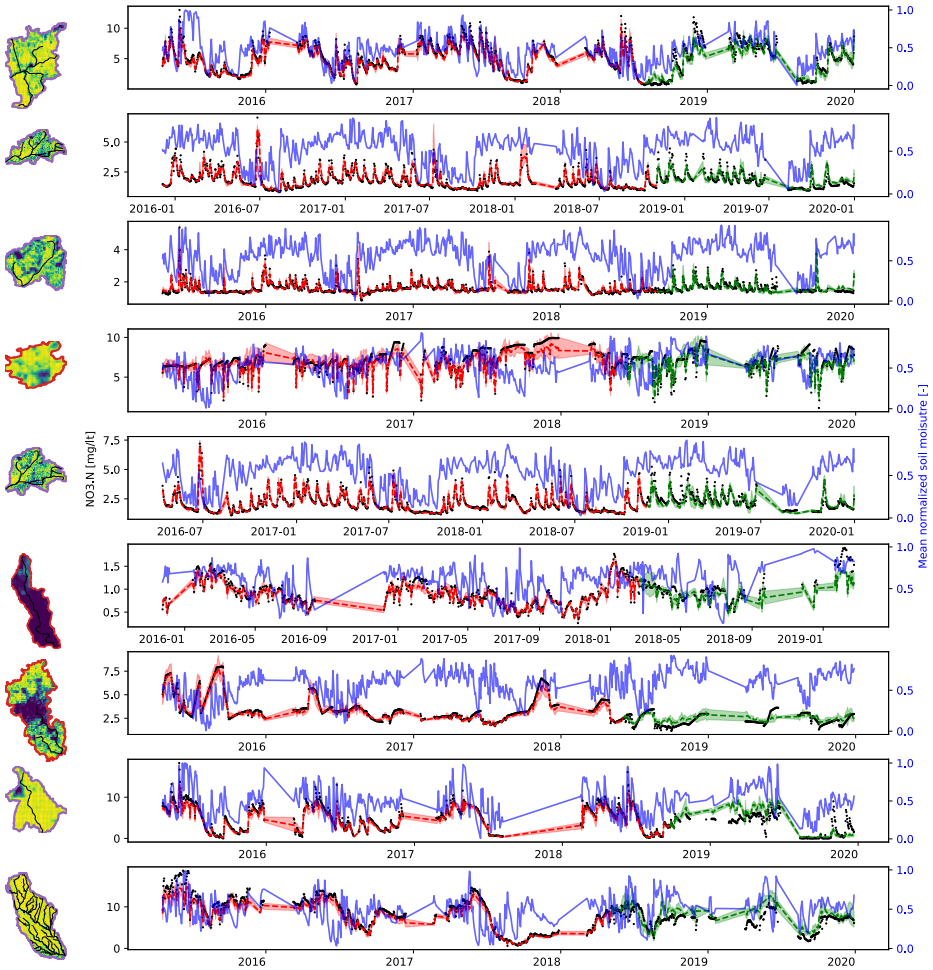

Figure 4.11: Time series of observed and simulated nitrate for all the study catchments. The normalized soil moisture is plotted in the second y-axis. The training and testing period are shown in red and green respectively, with a color band according to minimum and maximum predicted values across different model realizations.

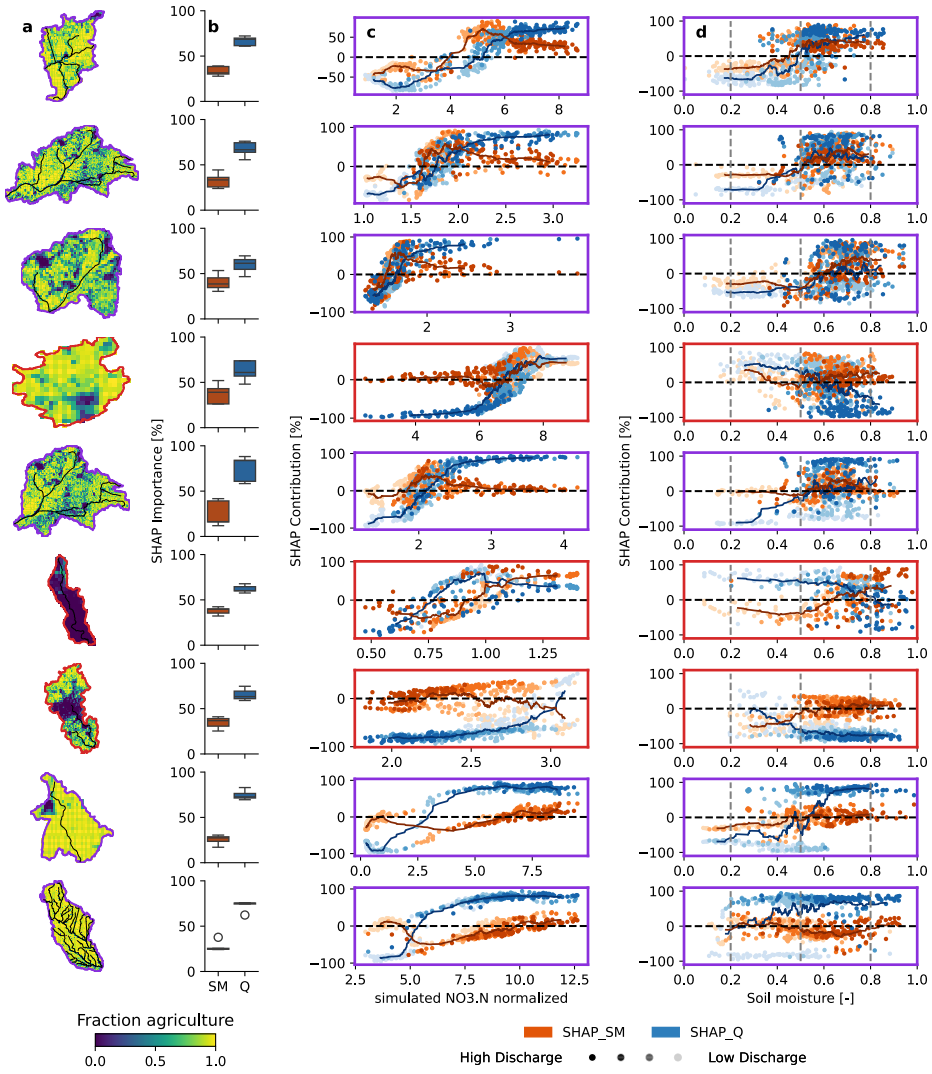

Figure 4.12: a) Catchment fraction of agriculture maps, b) SHAP importance of discharge and soil moisture across model realizations,c) and d) SHAP contribution of soil moisture and discharge for the study catchments durind different values of predicted nitrate and catchment-average soil moisture. The color of the axes represent the dominant C–Q pattern, with purple outlines representing enrichment catchments and the red outlines representing the two dilution and one chemostatic catchments.

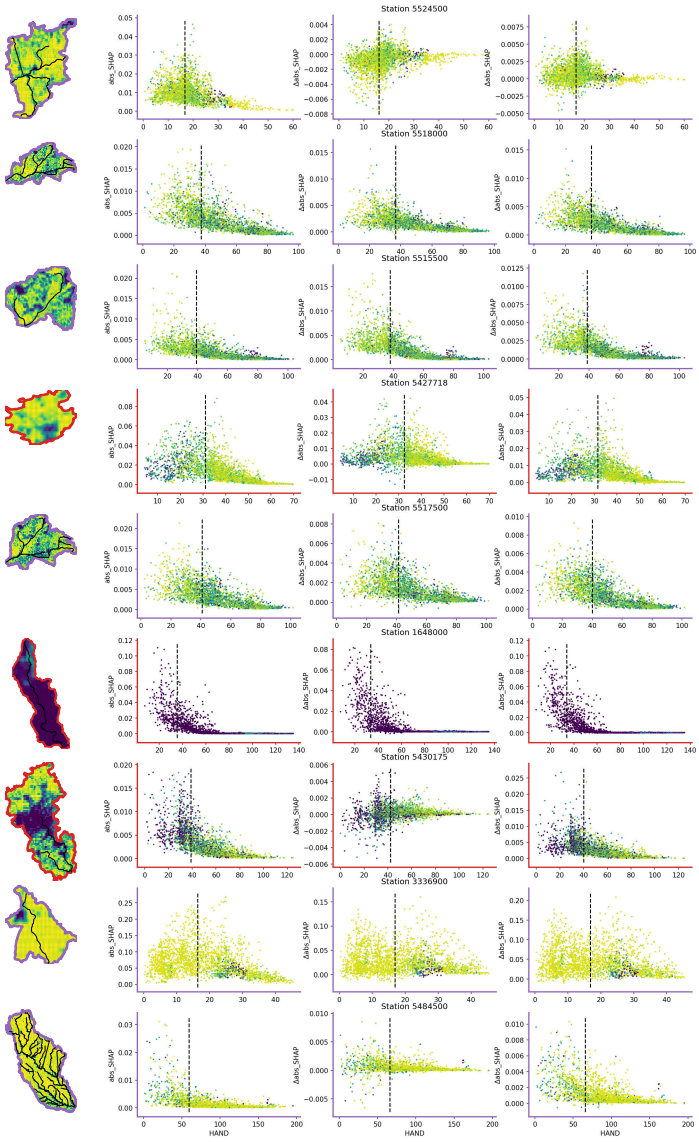

Figure 4.13: Scatterplots of pixel-wise model's attention and the corresponding height above the nearest drainage (HAND) for all catchments computed as the absolute SHAP values in the model Box-Cox transformed units of nitrate during the test period. First column show median attention across the test period; second column show the difference between attention during periods with high nitrate concentrations (i.e., the highest quartile of observed nitrate concentrations during the test period) and median attention; the third column show the difference between attention during periods with high level of hydrological connectivity (i.e., the highest quartile of mean observed soil moisture during the test period) and median attention, for the Kankakee (enrichment) and Yahara (dilution) catchments, respectively. HAND is plotted in the x-axis and the colorbar shows the fraction of agriculture of each pixel. The vertical dashed line shows the HAND value where 50% of the importance is reached. The color of the axes represent the dominant C–Q pattern, with purple outlines representing enrichment catchments and the red outlines representing the two dilution and one chemostatic catchments. the x-axis and the colorbar shows the fraction of agriculture of each pixel. The vertical dashed line shows the HAND value where 50% of the importance is reached. The color of the axes represent the dominant C–Q pattern, with purple outlines representing enrichment catchments and the red outlines representing the two dilution and one chemostatic catchments.

Table 4.3: Model performance for the base model reported in the main text and models excluding discharge (no Q), excluding soil moisture patterns (no SM), excluding HAND (no HAND), incorporating land cover static map as the fraction of agriculture (with LC), and using early stopping on a validation set selected as random 10% of the training data (train-val.-test) . Median and mean NSE performance across catchments is shown for the 20 model realizations and for the best 5 realizations in terms of mean NSE. Last column shows the difference in NSE performance between the different cases and the base model reported in results.

Experiment	**Runs**	**Median NSE**			**Mean NSE**			**Δ NSE**	
		train	**val.**	**test**	**train**	**validation**	**test**	**median**	**mean**
Base	20	0.86	-	0.55	0.84	-	0.46	0%	0%
	5 best	0.90	-	0.63	0.88	-	0.53	0%	0%
no SM	20	0.59	-	0.49	0.60	-	0.40	-10%	-14%
	5 best	0.62	-	0.56	0.60	-	0.46	-11%	-14%
no Q	20	0.79	-	0.12	0.72	-	0.04	-77%	-92%
	5 best	0.76	-	0.20	0.70	-	0.17	-68%	-68%
no HAND	20	0.77	-	0.51	0.85	-	0.39	-6%	-16%
	5 best	0.93	-	0.60	0.88	-	0.47	-5%	-11%
with LC	20	0.84	-	0.58	0.82	-	0.40	5%	-14%
	5 best	0.83	-	0.60	0.86	-	0.46	-6%	-12%
train-val.-test	20	0.95	0.92	0.58	0.95	0.91	0.32	6%	-31%
	5 best	0.94	0.91	0.61	0.94	0.91	0.45	-4%	-15%

Table 4.4: Sensitivity analyses around selected hyperparameters, evaluated as the model performance in the validation period (15% of the training data). The selected parameters are learning rate (Lr) 0.0009, 32 Filters for LSTM and ConvLSTM, batch size of 32, sequence length (seq_len) of 20 days, regularization L1 (Lasso) parameter of E-8, and structure 3 of the predicting module, which consist on 2 layers of 9 neural networks each. We tried other structures of the predictive module; one layer of three neural networks (Structure 1), 2 layers of 5 neural networks (Structure 2) and three layers of 5 neural networks (Structure 4). We tried different structures to reduce the ConvLSTM dimension as GlobalMaxPooling, GlobalAveragePooling and Conv2D modules.

Parameter	**Median NSE Validation**	**Mean NSE Validation**
Lr: 0.0008	0.916	0.913
Lr: 0.0009	0.916	0.917
Lr: 0.001	0.910	0.901
Filters: 16	0.682	0.697
Filters: 64	0.777	0.743
batch_size: 16	0.715	0.780
batch_size: 64	0.799	0.746
seq_len: 10	0.468	0.440
seq_len: 30	0.839	0.773
reg_coef: E-6	0.706	0.727
reg_coef: E-7	0.730	0.733
Structure 1	0.852	0.816
Structure 2	0.758	0.744
Structure 4	0.722	0.744
GlobalMaxPooling	0.912	0.904
GlobalAveragePooling	0.908	0.882
Conv2D	0.912	0.904

5

Conclusions and Future Avenues

This chapter summarizes and discusses the key findings and open questions regarding the research objectives of this dissertation, highlighting the progress achieved in understanding nitrate dynamics during hydrological events using data driven methods and large sample datasets. Moreover, building on the results shown before, this chapter discusses the future opportunities and challenges in the research field.

5.1 Conclusions

This dissertation explored the impact of hydrological events on nitrate dynamics at the catchment scale and their drivers using data driven methods and large sample water quality datasets. While nitrate concentration in streams depends on hydrological conditions, the nonlinearities, multiple drivers and distinct sources of nitrate transport and transformation pose a challenge to disentangle the main processes by studying single locations separately. This work takes advantage of newly available water quality datasets and hydrological event characterization to understand the main controls of nitrate responses during hydrological events (chapters 2 and 3), as well as available spatially distributed soil moisture datasets and machine learning models (chapter 4).

The main goal of this thesis is to understand the responses of nitrate concentration during hydrological events across different catchments. Chapter 2 reported a general reduction in nitrate concentrations in German streams during drought and post-drought periods. Specifically, 40% of the catchments showed a significant reduction during droughts, while 20% exhibited a significant decrease during post-drought, compared to no-drought conditions. These findings indicate that the persistent disconnection of hydrological pathways generally reduces nitrate transport and that drought effects often persist into the post-drought period. Nevertheless, results differ when studying the winter periods, with wetter catchments with less nitrogen retention showing a significant increase of nitrate during winter droughts. These results highlight the importance of retention processes and wetness of the catchments during winter droughts, revealing the interplay between hydrological connectivity and removal processes across catchments.

Moreover, wetter catchments with more nitrogen surplus exhibit a significant increase of nitrate during post-drought periods in winter, posing a threat of episodes of extremely high nitrate concentration and load during this period. These results evidence the accumulation of nitrogen and post-drought flush of nitrate in catchments with sufficient diffuse inputs and transport capacity.

Chapter 4 highlights that diffrences in runoff generation processes, expressed by diffrent runoff event types, can also alter nitrate dynamics. Snow-impacted events increased nitrate mobilization in streams, whereas runoff events triggered by rainfall following dry antecedent conditions led to decreased nitrate concentrations in the majority of catchments. The main difference between these event types lies in hydrological connectivity, which is quantified using event runoff coefficients. Snow-impacted events often occur during wet periods, exporting laterally nutrients from agricultural fields. Nevertheless, during dry antecedent conditions the reduction of transport as a result of hydrological pathways disconnection decrease nitrate concentration but also hints the potential reduction of nitrogen in the stream by biogeochemical processes, highlighting the interplay between transport and transformation during these types of events.

By analyzing hydrological events from droughts to runoff events the main controls of nitrate dynamics across catchments were identified. During droughts, hydrological connectivity decreases the nitrate concentration in streams. Moreover, during winter droughts catchments hydrological connectivity in combination with biogeochemical retention processes affect nitrate responses. Hydrological connectivity is also important for nitrate post-drought flush, with wetter catchments transporting nitrate excess during winter after a drought. During runoff events hydrological connectivity modulates the nitrate excess transport during snow-impacted events and an interplay between biogeochemical processes and lack of connectivity was found during runoff events with dry antecedent conditions. Particularly significant decrease in nitrate concentration was found in events with dry antecedent conditions and spatially heterogeneous distribution of soil moisture, indicating that the spatial component of hydrological connectivity plays a role in nitrate dynamics.

Building on the importance of spatial distribution of soil moisture shown in Chapter 3, Chapter 4 explores the relationship between spatial patterns of hydrological connectivity and nitrate concentration. Using soil moisture maps from satellite based products and daily measured nitrate concentration in 9 catchments in the United States, a deep learning model was developed to extract spatial features of soil moisture maps to successfully predict daily nitrate concentrations. Using explainable artificial intelligence (XAI) methods the importance of spatial patterns of soil moisture was quantified to be 30% in comparison to discharge, the catchment-aggregated proxy of hydrological connectivity. It was found that during transitional periods from dry to wet or when the catchments are nearly saturated, spatial patterns of soil moisture were more informative. This highlights the potential link between spatial distribution of soil moisture and the activation of shallow flow paths that transport nitrate from the land to the streams. The XAI method identified that near-stream areas in catchments are more informative about nitrate dynamics, suggesting the use of this information for better understanding nitrate dynamics.

5.2 Future Avenues

5.2.1 Implications for water quality management

These findings show in which cases hydrological events can lead to unexpected nutrient transport and which catchment characteristics modulate these responses. During snow-impacted runoff events, flat agricultural catchments in Germany are prone to export higher nitrate concentrations. During winter post-drought periods, wet catchments with excess fertilizer are prone to nutrient flushing. Such information can be used to target water quality measures in order to prevent episodes of high nutrient transport to water bodies, reducing environmental risks for rivers, lakes, and marine systems.

We observed that retention processes significantly decrease nitrate concentration during droughts across all four seasons (Figures 2.3, 2.14, 2.15 and 2.16). During runoff events triggered by rainfall on dry soils, the decrease in nitrate concentration might also be related to runoff generation in retention areas such as riparian zones. Future work might investigate across a large number of catchments how wetlands and preserved riparian areas can reduce the occurrence of high-nitrate episodes during runoff events.

Incorporating the learnings from this work into modeling frameworks could help improve the prediction of contaminant responses during hydrological events. For example, we observed the importance of the runoff coefficient during runoff events, hence, incorporating hydrological events characteristics in statistical models that predict nitrate may improve our predictive capacity. Moreover, the set of analyses and tools provided here can be extended to other compounds. For example, organic carbon might also be affected by runoff effects, and phosphate can increase during droughts according to the C–Q analyses in Germany [2].

Based on these findings, several practical considerations emerge for future water quality management. Management strategies should place greater emphasis on spatially targeted interventions, particularly in riparian zones and wetlands, which act as key control points for nitrate retention and export. Enhancing or restoring these landscape features could help mitigate nitrate pulses during hydrological events. Given the strong role of event-based mobilization in driving nitrate concentrations, the timing of nitrogen application should be reconsidered. By leveraging climatic information, fertilizer use could be adjusted to avoid periods of high mobilization potential—such as immediately before snowmelt or following extended droughts, when nitrate flushing is more likely. These adjustments would align agricultural practices more closely with catchment-scale water quality goals under changing climate conditions.

5.2.2 Anthropogenic impact and Climate change impact

Anthropogenic nitrogen inputs have long been recognized as the most important cause of nitrate contamination [42]. However, this thesis demostrates how the interplay between human-induced landscape modifications and hydrological events influence nitrate dynamics, especially when excess nitrogen input results in unexpected nitrate concentrations after droughts or during snow-impacted runoff events. Although changes in fertilizer regulation and improvements in wastewater treatment technologies have reduced average concentrations, legacy nitrogen stored in the soil persists, and runoff events can mobilize nitrogen accumulated during past periods

[23]. Landscape modification is one of the main drivers of increased nitrate concentrations during hydrological events (e.g., agricultural land fraction and nitrogen surplus controls snow-impacted runoff events responses and winter post-drought nitrate flushes). Nevertheless, further work is needed to explicitly evaluate how changes in the location of agricultural sources, as well as in crop types, affect nitrate concentration responses during hydrological events across catchments.

Moreover, projected changes in the frequency and type of hydrological events due to climate change underscore the need to assess their environmental impacts [222]. Climate models suggest increasing drought frequency in several regions (e.g., Central and Eastern Europe), raising the risk of winter post-drought periods with elevated nitrate concentrations [82, 83]. Conversely, shifts in runoff generation processes may lead to fewer snow-impacted events in Germany and more rainfall-driven events with dry antecedent conditions, potentially decreasing the risk of high-nitrate episodes [222]. These contrasting trends highlight the importance of understanding how changes in hydrological event occurrence affect nitrate mobilization and export. Future research should integrate climate projections with landscape and hydrological data to better predict nitrate dynamics under evolving conditions. In this context, data-driven approaches offer promising tools for incorporating knowledge of hydrological change into water quality management, enabling the evaluation of combined effects from runoff generation processes, drought variability, and nitrate responses at the catchment scale.

5.2.3 The interplay between transport and transformation of nitrate

The analyses demonstrate that both transport and transformation processes are important during hydrological events. During hydrological droughts and runoff events preceded by dry antecedent conditions, the interplay between limited hydrological connectivity from diffuse sources to streams and in-stream retention is often indistinguishable. Biogeochemical processes that remove nitrate become increasingly significant during low-flow periods when catchments are hydrologically more disconnected [109]. For example, catchment characteristics that promote nitrate removal explain some variations in nitrate response across catchments during winter droughts, when there is less hydrological connectivity compared to normal winters. Nevertheless, the effect of low winter temperatures on in-stream nitrate uptake is not clear as the interplay between less transport from diffuse sources and biogeochemical retention is not fully understood, showing that disentangling transport from transformation processes at the catchment scale is challenging without direct measurements of biogeochemical processes.

Techniques to quantify denitrification, such as isotopic analyses or high-frequency measurements [35, 5] are limited to a few study sites. Modeling approaches also typically require calibrated denitrification rates or the need to estimate separately transport and reaction, which can suffer from equifinality [246]. The growing number of study sites with high-frequency monitoring of nitrogen and water isotopes offers an opportunity to conduct multi-site studies to extend knowledge of denitrification to ungauged catchments. In addition, the use of source-related tracers [e.g., Cl^- from fertilizers, 130] or geogenic tracers to partition groundwater and subsurface flow contributions can also improve our understanding of nitrate transformation and help target water quality strategies more effectively.

5.2.4 Deep learning and the opportunities to analyze spatial data

Chapter 4 shows the potential of spatially distributed data and deep learning to explore hypotheses about catchment functioning. The results demonstrate that soil moisture maps derived from satellite data contain useful information to simulate nitrate concentration. These findings highlight the potential of improving the identification of hot spots and hot moments using novel deep learning approaches and new remote sensing datasets.

The application of machine learning offers opportunities to test scientific hypotheses about system functioning [194]. This work tested the hypothesis that spatial patterns of soil moisture can inform diffuse nitrogen transport to streams. By leveraging advanced machine learning models, it is now possible to explore statistical relationships across data types (e.g., time series, satellite data, static maps). For instance, one can identify runoff generation zones during runoff events by analyzing soil moisture maps while predicting discharge at the outlet of the catchments. Incorporating well-level data could help identify recharge zones, and by predicting geogenic compounds, one could better partition groundwater versus surface/subsurface flow contributions.

Moreover, deep learning offers potential for completing missing data and interpolating low-frequency samples to estimate long-term trends or improve flux estimates. The increasing availability of water quality data, both as input and target variables, provides new opportunities to improve predictions in ungauged catchments using AI models. This has already been applied successfully for parameters such as dissolved oxygen and water temperature [247]. However, more work is needed to predict nutrient concentrations in ungauged catchments due to data constraints and more complex dynamics [248].

Taken together, these future research directions and methodological advancements should ultimately feed back into improved water quality management, highlighting the need for integrated, event-informed, and spatially explicit strategies to reduce nitrate export under changing environmental conditions.

A

List of Publications and Author Contributions

This section outlines the chapters in this dissertation, which are based on published papers and have been modified. The author contributions, aligned with the Contributor Roles Taxonomy suggested by Allen et al. (2019)germanb1 , are detailed below.

Chapter 2

This chapter presents a formatted version of the original paper by Saavedra, F., Musolff A., Von Freyberg J., Merz R., Knöller K., Müller C., Brunner M., and Tarasova L. (2024). *Winter post-droughts amplify extreme nitrate concentrations in German rivers.*, published in Environmental Research Letters, 19(2)024007, `https://doi.org/10.1088/1748-9326/ad19ed`. Reproduced under the terms of the Creative Commons Attribution 4.0 License (CC BY 4.0).

Author contributions

- FS Conceptualization, Methodology, Validation, Formal analysis, Investigation, Data curation, Writing - original draft, Writing - review and editing, Visualization.
- AM Conceptualization, Writing - review and editing, Supervision.
- JF Conceptualization, Writing - review and editing, Supervision.
- RM Conceptualization, Writing - review and editing, Supervision.
- KK Conceptualization, Writing - review and editing, Supervision.
- CM Conceptualization, Writing - review and editing, Supervision.
- MB Conceptualization, Writing - review and editing, Supervision.
- LT Conceptualization, Writing - review and editing, Supervision, Project administration.

Chapter 3

This chapter presents a formatted version of the original paper by Saavedra, F., Musolff, A., von Freyberg, J., Merz, R., Basso, S., and Tarasova, L. (2022). *Disentangling scatter in long-term concentration–discharge relationships: The role of event types.* Hydrology and Earth System Sciences, 26(23), 6227–6245 `https://doi.org/10.5194/hess-26-6227-2022`.

Author contributions

- FS Conceptualization, Methodology, Validation, Formal analysis, Investigation, Data curation, Writing - original draft, Writing - review and editing, Visualization.
- AM Conceptualization, Writing - review and editing, Supervision.
- JF Conceptualization, Writing - review and editing, Supervision.
- RM Conceptualization, Writing - review and editing, Supervision.
- SB Conceptualization, Writing - review and editing, Supervision.
- LT Conceptualization, Writing - review and editing, Supervision, Project administration.

---

[0]Allen, L., O'Connell, A., and Kiermer, V. (2019). How can we ensure visibility and diversity in research contributions? How the Contributor Role Taxonomy (CRediT) is helping the shift from authorship to contributorship. *Learned Publishing*, *32*(1), 71–74. https://doi.org/10.1002/leap.1210

B

Declaration under Oaths

Ich erkläre an Eides statt, dass ich die Arbeit selbstständig und ohne fremde Hilfe verfasst, keine anderen als die von mir angegebenen Quellen und Hilfsmittel benutzt und die den benutzten Werken wörtlich oder inhaltlich entnommenen Stellen als solche kenntlich gemacht habe.

I declare under penalty of perjury that this thesis is my own work entirely and has been written without any help from other people. I used only the sources mentioned and included all the citations correctly both in word or content.

Unterschrift des Antragstellers	**Datum**
Signature of the applicant	*Date*

C

Curriculum Vitae

PERSONAL INFORMATION

Name	Felipe Saavedra Meléndez
Sex	Male
Nationality	Chilean

WORK EXPERIENCE

05.2016 – 01.2020 **Advanced Mining Technology Center, *University of Chile***
Associate Researcher
Santiago, Chile

03.2016 – 01.2017 **Fundación Somos Agua**
Co-founder and Researcher
Santiago, Chile

08.2014 – 05.2016 **KAS, Consulting**
External Consultant
Santiago, Chile

08.2015 – 01.2016 **Civil Engeneering Department, *University of Chile***
Research Assistant
Santiago, Chile

EDUCATION

2017 – 2019	**Universidad de Chile**, Santiago, Chile *Master of Science in Engineering, specialization in Water Resources and Environmental Hydraulics* Grade: 1.7 (converted to German grading system)
2007 – 2014	**Universidad de Chile**, Santiago, Chile *Civil Engineer, specialization in Sanitary and Environmental Hydraulics* Grade: 2.0 (converted to German grading system)
2003 – 2006	**Colegio Alemán de San Felipe**, Chile *High School Diploma*

SKILLS

Languages	English *(proficient)*, Spanish *(native)* German *(B1 level)*
Programming	Python *(proficient)*, Matlab *(proficient)* Bash *(proficient)*, R *(proficient)* C++ *(proficient)*, Fortran *(basic)* Javascript *(proficient)*, Visual Basic *(basic)*
Software	QGIS, LaTeX, Git, GRASS, SAGA Google Earth Engine Hydrological models (WEAP, DHSVM, HBV, FUSE)
Laboratory and Field work	Water Quality Analysis, Water quality and snow sampling
Driving Licences	Chile

SCIENTIFIC PUBLICATIONS

Peer-Reviewed Journal Papers

2024 **Saavedra, F.**, Musolff, A., von Freyberg, J., Merz, R., Knöller, K., Müller, C., Brunner, M., Tarasova, L. (2024). Winter post-droughts amplify extreme nitrate concentrations in German rivers. *Environ. Res. Lett.* **19**(2), 024007. https://doi.org/10.1088/1748-9326/ad19ed

2023 Bieroza, M., Acharya, S., Benisch, J., ter Borg, R.N., Hallberg, L., Negri, C., Pruitt, A., Pucher, M., **Saavedra, F.**, Staniszewska, K., van't Veen, S.G.M., Vincent, A., Winter, C., Basu, N.B., Jarvie, H.P., Kirchner, J.W. (2023). Advances in catchment science, hydrochemistry, and aquatic ecology enabled by high-frequency water quality measurements. *Environ. Sci. Technol.* **57**(12), 4701–4719. https://doi.org/10.1021/acs.est.2c07798

Wachholz, A., Dehaspe, J., Ebeling, P., Kumar, R., Musolff, A., **Saavedra, F.**, Winter, C., Yang, S., Graeber, D. (2023). Stoichiometry on the edge – humans induce strong imbalances of reactive C:N:P ratios in streams. *Environ. Res. Lett.* **18**(4), 044016. https://doi.org/10.1088/1748-9326/acc3b1

2022 **Saavedra, F.A.**, Musolff, A., von Freyberg, J., Merz, R., Basso, S., Tarasova, L. (2022). Disentangling scatter in long-term concentration–discharge relationships: the role of event types. *Hydrol. Earth Syst. Sci.* **26**(23), 6227–6245. https://doi.org/10.5194/hess-26-6227-2022

2020 **Saavedra, F.**, Cortés, G., Viale, M., Margulis, S., McPhee, J. (2020). Atmospheric Rivers Contribution to the Snow Accumulation Over the Southern Andes (26.5° S–37.5° S). *Frontiers in Earth Science* **8**. https://doi.org/10.3389/feart.2020.00261

CONFERENCE PRESENTATIONS

2024 N. Vergopolan, **F. Saavedra**, L. Tarasova, V.U. Krishnan, K. Lanka, J. Blekking, et al. Advancing water and food security with AI and hyper-resolution soil moisture data. *AGU Fall Meeting Abstracts*, GC54B-01. DOI (AGU abstract link)

F. Saavedra, N. Vergopolan, A. Musolff, R. Merz, C. Winter, L. Tarasova. Uncovering the impact of hydrological connectivity on nitrate transport at the catchment scale using explainable AI. *EGU General Assembly*, Abstract 11159. https://doi.org/10.5194/egusphere-egu24-11159

2022 **F. Saavedra**, A. Musolff, J. von Freyberg, R. Merz, S. Basso, L. Tarasova. Can runoff event types explain some scatter in nitrate C–Q relationships? *EGU General Assembly*, Abstract EGU22-11933. https://doi.org/10.5194/egusphere-egu22-11933

2021 **F. Saavedra**, A. Musolff, J. von Freyberg, R. Merz, S. Basso, L. Tarasova. Disentangling scatter in long-term C–Q relationships: the role of runoff events. *AGU Fall Meeting Abstracts*, H25X-1300. DOI (AGU abstract link)

2019 S. Montserrat, G. Zegers, A. Navarrete, **F. Saavedra**, D. Dionizis, M. Lagos, et al. Characterising mineral and metal transport in acidic rivers under current and future climatic conditions. *EGU General Assembly 2019*. Link to abstract

F. Saavedra, G. Cortés, M. Viale, S. Margulis, J. McPhee. Atmospheric rivers contribution to Andean snow accumulation. *EGU General Assembly 2019*. Link to abstract

2018 **F. Saavedra**, G. Cortés, S. Margulis, M. Viale, J. McPhee. Atmospheric Rivers contribution to the snow accumulation over the Southern Andes (26.5°S–37.5°S). *2nd International Atmospheric Rivers Conference*.

2017 X. Vargas, J. McPhee, T. Gómez, **F. Saavedra**. Hydrological analysis of the April 2016 flood in the Mapocho River. *XXIII Congreso Chileno de Ingeniería Hidráulica*.

A. Parra, **F. Saavedra**, N. Morales, J. McPhee. Mine scheduling considering hydrologic scenarios. *Geomin Mineplanning 2017*.

2015 **F. Saavedra**, J. McPhee, A. Lara. Application of the DHSVM model to forested microcatchments in the Corral region, Los Ríos. *XXII Congreso Chileno de Ingeniería Hidráulica*.

THESES

2014 Saavedra Meléndez, F.A. (2014). "Application of the DHSVM Model on Forested Micro-Catchments in the Corral Region, Los Ríos." *Undergraduate Thesis*, University of Chile. https://repositorio.uchile.cl/handle/2250/131082

2019 Saavedra, F.A. (2019). "Magíster en Ciencias de la Ingeniería, mención Recursos y Medio Ambiente Hídrico." *Master's Thesis*, University of Chile. https://repositorio.uchile.cl/handle/2250/173407

Invited Talks

2023 **Felipe Saavedra**. Nitrate, droughts and runoff events: The effect of extreme hydrological events on nitrate transport in German catchments. *Seminario Internacional de Ciencias Forestales: Bosques, Agua y Biodiversidad*. Invited speaker. Virtual, February 15, 2023.

2022 **Felipe Saavedra**. Effects of hydrological events on nitrate mobilization and delivery in German river catchments. *Water Resources and Environment – Webinars 2022*. DIC, Universidad de Chile. Virtual, November 24, 2022.

2023 **Felipe Saavedra**, A. Musolff, J. von Freyberg, R. Merz, K. Knöller, C. Müller, et al. Post-drought nitrate mobilization in German catchments. *Solicited talk at the EGU General Assembly 2023*. https://doi.org/10.5194/egusphere-egu23-7069

AWARDS

2017 Research internship scholarship awarded by the University of Chile for Master's students. Host institution: University of California, Los Angeles (UCLA), USA (Feb – Jun 2017).

JOURNAL REVIEWERS

- WIREs Water
- Hydrological Processes
- Science of the Total Environment

References

[1] L. Tarasova et al. “A Process-Based Framework to Characterize and Classify Runoff Events: The Event Typology of Germany”. In: *Water Resources Research* 56.5 (May 2020), e2019WR026951. ISSN: 0043-1397, 1944-7973. DOI: 10.1029/2019WR026951. (Visited on 05/06/2025).

[2] Pia Ebeling et al. “Archetypes and Controls of Riverine Nutrient Export Across German Catchments”. In: *Water Resources Research* 57.4 (Apr. 2021), e2020WR028134. ISSN: 0043-1397, 1944-7973. DOI: 10.1029/2020WR028134. (Visited on 05/06/2025).

[3] Xiaolin Zhang et al. “Analyzing Impacts of Seasonality and Landscape Gradient on Event-Scale Nitrate-Discharge Dynamics Based on Nested High-Frequency Monitoring”. In: *Journal of Hydrology* 591 (Dec. 2020), p. 125585. ISSN: 00221694. DOI: 10.1016/j.jhydrol.2020.125585. (Visited on 05/06/2025).

[4] Ken Takai. “The Nitrogen Cycle: A Large, Fast, and Mystifying Cycle”. In: *Microbes and Environments* 34.3 (Sept. 2019), pp. 223–225. ISSN: 1342-6311. DOI: 10.1264/jsme2.ME3403rh. (Visited on 06/02/2025).

[5] Astrid Johannsen, Kirstin Dähnke, and Kay Emeis. “Isotopic Composition of Nitrate in Five German Rivers Discharging into the North Sea”. In: *Organic Geochemistry* 39.12 (Dec. 2008), pp. 1678–1689. ISSN: 01466380. DOI: 10.1016/j.orggeochem.2008.03.004. (Visited on 05/06/2025).

[6] Erik Jeppesen et al. “Climate Change Effects on Nitrogen Loading from Cultivated Catchments in Europe: Implications for Nitrogen Retention, Ecological State of Lakes and Adaptation”. In: *Hydrobiologia* 663.1 (Mar. 2011), pp. 1–21. ISSN: 0018-8158, 1573-5117. DOI: 10.1007/s10750-010-0547-6. (Visited on 05/06/2025).

[7] Morgane Le Moal et al. “Eutrophication: A New Wine in an Old Bottle?” In: *Science of The Total Environment* 651 (Feb. 2019), pp. 1–11. ISSN: 00489697. DOI: 10.1016/j.scitotenv.2018.09.139. (Visited on 05/06/2025).

[8] J. Mateo-Sagasta, S. Marjani Zadeh, and H. Turral. *More People, More Food... Worse Water? - Water Pollution from Agriculture: A Global Review*. Rome, Italy: FAO, 2018. ISBN: 978-92-5-130729-8. (Visited on 11/04/2022).

[9] Thomas C. Malone and Alice Newton. “The Globalization of Cultural Eutrophication in the Coastal Ocean: Causes and Consequences”. In: *Frontiers in Marine Science* 7 (Aug. 2020), p. 670. ISSN: 2296-7745. DOI: 10.3389/fmars.2020.00670. (Visited on 05/06/2025).

[10] Markus Weitere et al. “Disentangling Multiple Chemical and Non-Chemical Stressors in a Lotic Ecosystem Using a Longitudinal Approach”. In: *Science of The Total Environment* 769 (May 2021), p. 144324. ISSN: 00489697. DOI: 10.1016/j.scitotenv.2020.144324. (Visited on 05/06/2025).

[11] Hans W. Paerl. “Coastal Eutrophication and Harmful Algal Blooms: Importance of Atmospheric Deposition and Groundwater as “New” Nitrogen and Other Nutrient Sources”. In: *Limnology and Oceanography* 42.5part2 (July 1997), pp. 1154–1165. ISSN: 0024-3590, 1939-5590. DOI: 10.4319/lo.1997.42.5_part_2.1154. (Visited on 05/06/2025).

[12] Arthur H. W. Beusen et al. “Global Riverine N and P Transport to Ocean Increased during the 20th Century despite Increased Retention along the Aquatic Continuum”. In: *Biogeosciences* 13.8 (Apr. 2016), pp. 2441–2451. ISSN: 1726-4189. DOI: 10.5194/bg-13-2441-2016. (Visited on 05/06/2025).

[13] Pamela A. Green et al. “Pre-Industrial and Contemporary Fluxes of Nitrogen through Rivers: A Global Assessment Based on Typology”. In: *Biogeochemistry* 68.1 (Mar. 2004), pp. 71–105. ISSN: 0168-2563. DOI: 10.1023/B:BIOG.0000025742.82155.92. (Visited on 05/06/2025).

[14] Luis Lassaletta et al. “50 Year Trends in Nitrogen Use Efficiency of World Cropping Systems: The Relationship between Yield and Nitrogen Input to Cropland”. In: *Environmental Research Letters* 9.10 (Oct. 2014), p. 105011. ISSN: 1748-9326. DOI: 10.1088/1748-9326/9/10/105011. (Visited on 05/06/2025).

[15] Rolf Nieder, Dinesh K. Benbi, and Heinrich W. Scherer. “Fixation and Defixation of Ammonium in Soils: A Review”. In: *Biology and Fertility of Soils* 47.1 (Jan. 2011), pp. 1–14. ISSN: 1432-0789. DOI: 10.1007/s00374-010-0506-4. (Visited on 06/03/2025).

[16] Yanyan Liu et al. “Distinct Roles of Bacteria and Fungi in Mediating Soil Extracellular Enzymes under Long-Term Nitrogen Deposition in Temperate Plantations”. In: *Forest Ecology and Management* 529 (Feb. 2023), p. 120658. ISSN: 0378-1127. DOI: 10.1016/j.foreco.2022.120658. (Visited on 06/03/2025).

[17] M.E. Guntiñas et al. “Effects of Moisture and Temperature on Net Soil Nitrogen Mineralization: A Laboratory Study”. In: *European Journal of Soil Biology* 48 (Jan. 2012), pp. 73–80. ISSN: 11645563. DOI: 10.1016/j.ejsobi.2011.07.015. (Visited on 05/06/2025).

[18] M Lee et al. “Globally Prevalent Land Nitrogen Memory Amplifies Water Pollution Following Drought Years”. In: *Environmental Research Letters* 16.1 (Jan. 2021), p. 014049. ISSN: 1748-9326. DOI: 10.1088/1748-9326/abd1a0. (Visited on 05/06/2025).

[19] W.A House, D.V Leach, and P.D Armitage. “Study of Dissolved Silicon, and Nitrate Dynamics in a Fresh Water Stream”. In: *Water Research* 35.11 (Aug. 2001), pp. 2749–2757. ISSN: 00431354. DOI: 10.1016/S0043-1354(00)00548-0. (Visited on 05/06/2025).

[20] Bijay-Singh and Eric Craswell. "Fertilizers and Nitrate Pollution of Surface and Ground Water: An Increasingly Pervasive Global Problem". In: *SN Applied Sciences* 3.4 (Mar. 2021), p. 518. ISSN: 2523-3971. DOI: 10.1007/s42452-021-04521-8. (Visited on 11/04/2022).

[21] Nandita B. Basu, Sally E. Thompson, and P. Suresh C. Rao. "Hydrologic and Biogeochemical Functioning of Intensively Managed Catchments: A Synthesis of Top-down Analyses". In: *Water Resources Research* 47.10 (Oct. 2011), 2011WR010800. ISSN: 0043-1397, 1944-7973. DOI: 10.1029/2011WR010800. (Visited on 05/06/2025).

[22] K J Van Meter et al. "The Nitrogen Legacy: Emerging Evidence of Nitrogen Accumulation in Anthropogenic Landscapes". In: *Environmental Research Letters* 11.3 (Mar. 2016), p. 035014. ISSN: 1748-9326. DOI: 10.1088/1748-9326/11/3/035014. (Visited on 05/06/2025).

[23] S Y Chang et al. "Chesapeake Legacies: The Importance of Legacy Nitrogen to Improving Chesapeake Bay Water Quality". In: *Environmental Research Letters* 16.8 (Aug. 2021), p. 085002. ISSN: 1748-9326. DOI: 10.1088/1748-9326/ac0d7b. (Visited on 05/06/2025).

[24] J.W. Jawitz et al. "Disaggregating Landscape-Scale Nitrogen Attenuation Along Hydrological Flow Paths". In: *Journal of Geophysical Research: Biogeosciences* 125.2 (Feb. 2020), e2019JG005229. ISSN: 2169-8953, 2169-8961. DOI: 10.1029/2019JG005229. (Visited on 05/06/2025).

[25] K J Van Meter and N B Basu. "Time Lags in Watershed-Scale Nutrient Transport: An Exploration of Dominant Controls". In: *Environmental Research Letters* 12.8 (Aug. 2017), p. 084017. ISSN: 1748-9326. DOI: 10.1088/1748-9326/aa7bf4. (Visited on 05/06/2025).

[26] Sema Karakurt et al. "Dynamics of Wastewater Effluent Contributions in Streams and Impacts on Drinking Water Supply via Riverbank Filtration in Germany—A National Reconnaissance". In: *Environmental Science & Technology* 53.11 (June 2019), pp. 6154–6161. ISSN: 0013-936X. DOI: 10.1021/acs.est.8b07216. (Visited on 10/08/2024).

[27] C. Brannon Andersen, Gregory P. Lewis, and Kenneth A. Sargent. "Influence of Wastewater-Treatment Effluent on Concentrations and Fluxes of Solutes in the Bush River, South Carolina, during Extreme Drought Conditions". In: *Environmental Geosciences* 11.1 (Mar. 2004), pp. 28–41. ISSN: 1075-9565. DOI: 10.1306/eg.10200303017. (Visited on 05/06/2025).

[28] Uwe Häußermann et al. "Nitrogen Soil Surface Budgets for Districts in Germany 1995 to 2017". In: *Environmental Sciences Europe* 32.1 (Dec. 2020), p. 109. ISSN: 2190-4707, 2190-4715. DOI: 10.1186/s12302-020-00382-x. (Visited on 05/06/2025).

[29] Larry J. Puckett, Anthony J. Tesoriero, and Neil M. Dubrovsky. "Nitrogen Contamination of Surficial Aquifers—A Growing Legacy". In: *Environmental Science & Technology* 45.3 (Feb. 2011), pp. 839–844. ISSN: 0013-936X, 1520-5851. DOI: 10.1021/es1038358. (Visited on 05/06/2025).

[30] Tim Covino. “Hydrologic Connectivity as a Framework for Understanding Biogeochemical Flux through Watersheds and along Fluvial Networks”. In: *Geomorphology* 277 (Jan. 2017), pp. 133–144. ISSN: 0169555X. DOI: 10.1016/j.geomorph.2016.09.030. (Visited on 05/06/2025).

[31] Theresa Blume and H.J. (Ilja) Van Meerveld. “From Hillslope to Stream: Methods to Investigate Subsurface Connectivity”. In: *WIREs Water* 2.3 (May 2015), pp. 177–198. ISSN: 2049-1948, 2049-1948. DOI: 10.1002/wat2.1071. (Visited on 05/06/2025).

[32] L.J. Bracken et al. “Concepts of Hydrological Connectivity: Research Approaches, Pathways and Future Agendas”. In: *Earth-Science Reviews* 119 (Apr. 2013), pp. 17–34. ISSN: 00128252. DOI: 10.1016/j.earscirev.2013.02.001. (Visited on 05/06/2025).

[33] Antoine Casquin et al. “The Influence of Landscape Spatial Configuration on Nitrogen and Phosphorus Exports in Agricultural Catchments”. In: *Landscape Ecology* 36.12 (Dec. 2021), pp. 3383–3399. ISSN: 0921-2973, 1572-9761. DOI: 10.1007/s10980-021-01308-5. (Visited on 05/06/2025).

[34] Andreas Musolff et al. “Catchment Controls on Solute Export”. In: *Advances in Water Resources* 86 (Dec. 2015), pp. 133–146. ISSN: 0309-1708. DOI: 10.1016/j.advwatres.2015.09.026. (Visited on 09/02/2021).

[35] Michael Rode et al. “Continuous In-Stream Assimilatory Nitrate Uptake from High-Frequency Sensor Measurements”. In: *Environmental Science & Technology* 50.11 (June 2016), pp. 5685–5694. ISSN: 0013-936X, 1520-5851. DOI: 10.1021/acs.est.6b00943. (Visited on 05/06/2025).

[36] Jia Xin et al. “The Missing Nitrogen Pieces: A Critical Review on the Distribution, Transformation, and Budget of Nitrogen in the Vadose Zone-Groundwater System”. In: *Water Research* 165 (Nov. 2019), p. 114977. ISSN: 00431354. DOI: 10.1016/j.watres.2019.114977. (Visited on 06/15/2021).

[37] Lukas Knoll, Lutz Breuer, and Martin Bach. “Nation-Wide Estimation of Groundwater Redox Conditions and Nitrate Concentrations through Machine Learning”. In: *Environmental Research Letters* 15.6 (June 2020), p. 064004. ISSN: 1748-9326. DOI: 10.1088/1748-9326/ab7d5c. (Visited on 05/06/2025).

[38] Joni Dehaspe et al. “Bending of the Concentration Discharge Relationship Can Inform about In-Stream Nitrate Removal”. In: *Hydrology and Earth System Sciences* 25.12 (Dec. 2021), pp. 6437–6463. ISSN: 1607-7938. DOI: 10.5194/hess-25-6437-2021. (Visited on 05/06/2025).

[39] R. Kumar et al. “Strong Hydroclimatic Controls on Vulnerability to Subsurface Nitrate Contamination across Europe”. In: *Nature Communications* 11.1 (Dec. 2020), p. 6302. ISSN: 2041-1723. DOI: 10.1038/s41467-020-19955-8. (Visited on 05/06/2025).

[40] Michel Meybeck and Florentina Moatar. “Daily Variability of River Concentrations and Fluxes: Indicators Based on the Segmentation of the Rating Curve”. In: *Hydrological Processes* 26.8 (Apr. 2012), pp. 1188–1207. ISSN: 0885-6087, 1099-1085. DOI: 10.1002/hyp.8211. (Visited on 05/06/2025).

[41] Lucy A. Rose, Diana L. Karwan, and Sarah E. Godsey. "Concentration–Discharge Relationships Describe Solute and Sediment Mobilization, Reaction, and Transport at Event and Longer Timescales". In: *Hydrological Processes* 32.18 (Aug. 2018), pp. 2829–2844. ISSN: 0885-6087, 1099-1085. DOI: 10.1002/hyp.13235. (Visited on 05/06/2025).

[42] Nandita B. Basu et al. "Nutrient Loads Exported from Managed Catchments Reveal Emergent Biogeochemical Stationarity". In: *Geophysical Research Letters* 37.23 (2010). ISSN: 1944-8007. DOI: 10.1029/2010GL045168. (Visited on 05/06/2022).

[43] A. Musolff et al. "Emergent Archetype Patterns of Coupled Hydrologic and Biogeochemical Responses in Catchments". In: *Geophysical Research Letters* 44.9 (May 2017), pp. 4143–4151. ISSN: 0094-8276, 1944-8007. DOI: 10.1002/2017GL072630. (Visited on 05/06/2025).

[44] Pia Ebeling et al. "Long-Term Nitrate Trajectories Vary by Season in Western European Catchments". In: *Global Biogeochemical Cycles* 35.9 (Sept. 2021), e2021GB007050. ISSN: 0886-6236, 1944-9224. DOI: 10.1029/2021GB007050. (Visited on 05/06/2025).

[45] F. Moatar et al. "Elemental Properties, Hydrology, and Biology Interact to Shape Concentration-discharge Curves for Carbon, Nutrients, Sediment, and Major Ions". In: *Water Resources Research* 53.2 (Feb. 2017), pp. 1270–1287. ISSN: 0043-1397, 1944-7973. DOI: 10.1002/2016WR019635. (Visited on 05/06/2025).

[46] Ann Louise Heathwaite and Magdalena Bieroza. "Fingerprinting Hydrological and Biogeochemical Drivers of Freshwater Quality". In: *Hydrological Processes* 35.1 (Jan. 2021), e13973. ISSN: 0885-6087, 1099-1085. DOI: 10.1002/hyp.13973. (Visited on 05/06/2025).

[47] Camille Minaudo et al. "Seasonal and Event-Based Concentration-Discharge Relationships to Identify Catchment Controls on Nutrient Export Regimes". In: *Advances in Water Resources* 131 (Sept. 2019), p. 103379. ISSN: 03091708. DOI: 10.1016/j.advwatres.2019.103379. (Visited on 05/06/2025).

[48] Julia L. A. Knapp et al. "Concentration–Discharge Relationships Vary among Hydrological Events, Reflecting Differences in Event Characteristics". In: *Hydrology and Earth System Sciences* 24.5 (May 2020), pp. 2561–2576. ISSN: 1607-7938. DOI: 10.5194/hess-24-2561-2020. (Visited on 05/06/2025).

[49] Louise J. Bracken and Jacky Croke. "The Concept of Hydrological Connectivity and Its Contribution to Understanding Runoff-Dominated Geomorphic Systems". In: *Hydrological Processes* 21.13 (2007), pp. 1749–1763. ISSN: 1099-1085. DOI: 10.1002/hyp.6313. (Visited on 10/07/2024).

[50] Irantzu Lexartza-Artza and John Wainwright. "Hydrological Connectivity: Linking Concepts with Practical Implications". In: *CATENA* 79.2 (Nov. 2009), pp. 146–152. ISSN: 0341-8162. DOI: 10.1016/j.catena.2009.07.001. (Visited on 10/10/2024).

[51] L. Tarasova et al. "Exploring Controls on Rainfall-Runoff Events: 1. Time Series-Based Event Separation and Temporal Dynamics of Event Runoff Response in Germany". In: *Water Resources Research* 54.10 (Oct. 2018), pp. 7711–7732. ISSN: 0043-1397, 1944-7973. DOI: 10.1029/2018WR022587. (Visited on 05/06/2025).

[52] R. Merz, G. Blöschl, and J. Parajka. "Spatio-Temporal Variability of Event Runoff Coefficients". In: *Journal of Hydrology* 331.3 (Dec. 2006), pp. 591–604. ISSN: 0022-1694. DOI: 10.1016/j.jhydrol.2006.06.008. (Visited on 04/19/2022).

[53] Kelsey G. Jencso et al. "Hydrologic Connectivity between Landscapes and Streams: Transferring Reach- and Plot-scale Understanding to the Catchment Scale". In: *Water Resources Research* 45.4 (Apr. 2009), 2008WR007225. ISSN: 0043-1397, 1944-7973. DOI: 10.1029/2008WR007225. (Visited on 05/06/2025).

[54] M. Rinderer, H. J. van Meerveld, and B. L. McGlynn. "From Points to Patterns: Using Groundwater Time Series Clustering to Investigate Subsurface Hydrological Connectivity and Runoff Source Area Dynamics". In: *Water Resources Research* 55.7 (2019), pp. 5784–5806. ISSN: 1944-7973. DOI: 10.1029/2018WR023886. (Visited on 02/14/2025).

[55] D. Penna et al. "The Influence of Soil Moisture on Threshold Runoff Generation Processes in an Alpine Headwater Catchment". In: *Hydrology and Earth System Sciences* 15.3 (Mar. 2011), pp. 689–702. ISSN: 1607-7938. DOI: 10.5194/hess-15-689-2011. (Visited on 10/08/2024).

[56] Noemi Vergopolan et al. "High-Resolution Soil Moisture Data Reveal Complex Multi-Scale Spatial Variability Across the United States". In: *Geophysical Research Letters* 49.15 (2022), e2022GL098586. ISSN: 1944-8007. DOI: 10.1029/2022GL098586. (Visited on 11/17/2024).

[57] Kendra E. Kaiser and Brian L. McGlynn. "Nested Scales of Spatial and Temporal Variability of Soil Water Content Across a Semiarid Montane Catchment". In: *Water Resources Research* 54.10 (2018), pp. 7960–7980. ISSN: 1944-7973. DOI: 10.1029/2018WR022591. (Visited on 02/14/2025).

[58] U. Rosenbaum et al. "Seasonal and Event Dynamics of Spatial Soil Moisture Patterns at the Small Catchment Scale". In: *Water Resources Research* 48.10 (2012). ISSN: 1944-7973. DOI: 10.1029/2011WR011518. (Visited on 12/05/2024).

[59] James S. Famiglietti et al. "Field Observations of Soil Moisture Variability across Scales". In: *Water Resources Research* 44.1 (2008). ISSN: 1944-7973. DOI: 10.1029/2006WR005804. (Visited on 12/05/2024).

[60] Andrew W Western et al. "Spatial Correlation of Soil Moisture in Small Catchments and Its Relationship to Dominant Spatial Hydrological Processes". In: *Journal of Hydrology* 286.1 (Jan. 2004), pp. 113–134. ISSN: 0022-1694. DOI: 10.1016/j.jhydrol.2003.09.014. (Visited on 12/05/2024).

[61] Rodger B. Grayson et al. "Preferred States in Spatial Soil Moisture Patterns: Local and Nonlocal Controls". In: *Water Resources Research* 33.12 (Dec. 1997), pp. 2897–2908. ISSN: 0043-1397, 1944-7973. DOI: 10.1029/97WR02174. (Visited on 05/06/2025).

[62] Xiaole Han et al. "The Dominant Control of Relief on Soil Water Content Distribution During Wet-Dry Transitions in Headwaters". In: *Water Resources Research* 57.11 (2021), e2021WR029587. ISSN: 1944-7973. DOI: 10.1029/2021WR029587. (Visited on 12/05/2024).

[63] P. Reich and P. S. Lake. “Extreme Hydrological Events and the Ecological Restoration of Flowing Waters”. In: *Freshwater Biology* 60.12 (2014), pp. 2639–2652. ISSN: 1365-2427. DOI: 10.1111/fwb.12508. (Visited on 06/03/2025).

[64] Z. W. Kundzewicz and P. Matczak. “Extreme Hydrological Events and Security”. In: *Proceedings of IAHS*. Vol. 369. Copernicus GmbH, June 2015, pp. 181–187. DOI: 10.5194/piahs-369-181-2015. (Visited on 06/03/2025).

[65] Anne F. Van Loon. “Hydrological Drought Explained”. In: *WIREs Water* 2.4 (July 2015), pp. 359–392. ISSN: 2049-1948, 2049-1948. DOI: 10.1002/wat2.1085. (Visited on 05/06/2025).

[66] Marcus A. Hardie et al. “Effect of Antecedent Soil Moisture on Preferential Flow in a Texture-Contrast Soil”. In: *Journal of Hydrology* 398.3-4 (Feb. 2011), pp. 191–201. ISSN: 00221694. DOI: 10.1016/j.jhydrol.2010.12.008. (Visited on 05/06/2025).

[67] Adnan A. Basma et al. “Swelling-Shrinkage Behavior of Natural Expansive Clays”. In: *Applied Clay Science* 11.2 (Dec. 1996), pp. 211–227. ISSN: 0169-1317. DOI: 10.1016/S0169-1317(96)00009-9. (Visited on 06/03/2025).

[68] Jacob D. Petersen-Perlman, Ismael Aguilar-Barajas, and Sharon B. Megdal. “Drought and Groundwater Management: Interconnections, Challenges, and Policyresponses”. In: *Current Opinion in Environmental Science & Health* 28 (Aug. 2022), p. 100364. ISSN: 2468-5844. DOI: 10.1016/j.coesh.2022.100364. (Visited on 12/19/2022).

[69] Ashok Mishra, Ali Alnahit, and Barbara Campbell. “Impact of Land Uses, Drought, Flood, Wildfire, and Cascading Events on Water Quality and Microbial Communities: A Review and Analysis”. In: *Journal of Hydrology* 596 (May 2021), p. 125707. ISSN: 0022-1694. DOI: 10.1016/j.jhydrol.2020.125707. (Visited on 10/07/2024).

[70] Luke M. Mosley. “Drought Impacts on the Water Quality of Freshwater Systems; Review and Integration”. In: *Earth-Science Reviews* 140 (Jan. 2015), pp. 203–214. ISSN: 00128252. DOI: 10.1016/j.earscirev.2014.11.010. (Visited on 05/06/2025).

[71] D. Tetzlaff et al. “Storage Dynamics in Hydropedological Units Control Hillslope Connectivity, Runoff Generation, and the Evolution of Catchment Transit Time Distributions”. In: *Water Resources Research* 50.2 (2014), pp. 969–985. ISSN: 1944-7973. DOI: 10.1002/2013WR014147. (Visited on 02/14/2025).

[72] Faye N. Outram et al. “Antecedent Conditions, Hydrological Connectivity and Anthropogenic Inputs: Factors Affecting Nitrate and Phosphorus Transfers to Agricultural Headwater Streams”. In: *Science of The Total Environment* 545–546 (Mar. 2016), pp. 184–199. ISSN: 00489697. DOI: 10.1016/j.scitotenv.2015.12.025. (Visited on 05/06/2025).

[73] Molly R. Cain et al. “Antecedent Conditions Control Thresholds of Tile-Runoff Generation and Nitrogen Export in Intensively Managed Landscapes”. In: *Water Resources Research* 58.2 (Feb. 2022), e2021WR030507. ISSN: 0043-1397, 1944-7973. DOI: 10.1029/2021WR030507. (Visited on 05/06/2025).

[74] S. P. Inamdar et al. "The Impact of Storm Events on Solute Exports from a Glaciated Forested Watershed in Western New York, USA". In: *Hydrological Processes* 20.16 (Oct. 2006), pp. 3423–3439. ISSN: 0885-6087, 1099-1085. DOI: 10.1002/hyp.6141. (Visited on 05/06/2025).

[75] M. C. H. Vaughan et al. "High-frequency Dissolved Organic Carbon and Nitrate Measurements Reveal Differences in Storm Hysteresis and Loading in Relation to Land Cover and Seasonality". In: *Water Resources Research* 53.7 (July 2017), pp. 5345–5363. ISSN: 0043-1397, 1944-7973. DOI: 10.1002/2017WR020491. (Visited on 05/06/2025).

[76] M.J. Bowes et al. "Characterising Phosphorus and Nitrate Inputs to a Rural River Using High-Frequency Concentration–Flow Relationships". In: *Science of The Total Environment* 511 (Apr. 2015), pp. 608–620. ISSN: 00489697. DOI: 10.1016/j.scitotenv.2014.12.086. (Visited on 05/06/2025).

[77] Rémi Dupas et al. "Disentangling the Influence of Hydroclimatic Patterns and Agricultural Management on River Nitrate Dynamics from Sub-Hourly to Decadal Time Scales". In: *Science of The Total Environment* 571 (Nov. 2016), pp. 791–800. ISSN: 00489697. DOI: 10.1016/j.scitotenv.2016.07.053. (Visited on 05/06/2025).

[78] Andrea Butturini et al. "Cross-Site Comparison of Variability of DOC and Nitrate c–q Hysteresis during the Autumn–Winter Period in Three Mediterranean Headwater Streams: A Synthetic Approach". In: *Biogeochemistry* 77.3 (Feb. 2006), pp. 327–349. ISSN: 0168-2563, 1573-515X. DOI: 10.1007/s10533-005-0711-7. (Visited on 05/06/2025).

[79] Andreas Bauwe et al. "Classifying Hydrological Events to Quantify Their Impact on Nitrate Leaching across Three Spatial Scales". In: *Journal of Hydrology* 531 (Dec. 2015), pp. 589–601. ISSN: 00221694. DOI: 10.1016/j.jhydrol.2015.10.069. (Visited on 05/06/2025).

[80] Xiaofei Chen et al. "Impact of Climate and Geology on Event Runoff Characteristics at the Regional Scale". In: *Water* 12.12 (Dec. 2020), p. 3457. ISSN: 2073-4441. DOI: 10.3390/w12123457. (Visited on 05/06/2025).

[81] Margarita Saft et al. "The Influence of Multiyear Drought on the Annual Rainfall-runoff Relationship: An A Ustralian Perspective". In: *Water Resources Research* 51.4 (Apr. 2015), pp. 2444–2463. ISSN: 0043-1397, 1944-7973. DOI: 10.1002/2014WR015348. (Visited on 05/06/2025).

[82] Jonathan Spinoni et al. "Will Drought Events Become More Frequent and Severe in Europe?" In: *International Journal of Climatology* 38.4 (Mar. 2018), pp. 1718–1736. ISSN: 0899-8418, 1097-0088. DOI: 10.1002/joc.5291. (Visited on 05/06/2025).

[83] Andreas Wunsch, Tanja Liesch, and Stefan Broda. "Deep Learning Shows Declining Groundwater Levels in Germany until 2100 Due to Climate Change". In: *Nature Communications* 13.1 (Mar. 2022), p. 1221. ISSN: 2041-1723. DOI: 10.1038/s41467-022-28770-2. (Visited on 05/06/2025).

[84] Guillaume Vigouroux et al. “Trend Correlations for Coastal Eutrophication and Its Main Local and Whole-Sea Drivers – Application to the Baltic Sea”. In: *Science of The Total Environment* 779 (July 2021), p. 146367. ISSN: 00489697. DOI: 10.1016/j.scitotenv.2021.146367. (Visited on 05/06/2025).

[85] Michael J. Pennino, Jana E. Compton, and Scott G. Leibowitz. “Trends in Drinking Water Nitrate Violations Across the United States”. In: *Environmental Science & Technology* 51.22 (Nov. 2017), pp. 13450–13460. ISSN: 0013-936X, 1520-5851. DOI: 10.1021/acs.est.7b04269. (Visited on 05/06/2025).

[86] EEA. *The European Environment: State and Outlook 2020 : Knowledge for Transition to a Sustainable Europe.* LU: Publications Office, 2019. (Visited on 05/06/2025).

[87] Xiangqian Zhou et al. “Exploring the Relations between Sequential Droughts and Stream Nitrogen Dynamics in Central Germany through Catchment-Scale Mechanistic Modelling”. In: *Journal of Hydrology* 614 (Nov. 2022), p. 128615. ISSN: 00221694. DOI: 10.1016/j.jhydrol.2022.128615. (Visited on 05/06/2025).

[88] Susana Bernal et al. “Hydrological Extremes Modulate Nutrient Dynamics in Mediterranean Climate Streams across Different Spatial Scales”. In: *Hydrobiologia* 719.1 (Nov. 2013), pp. 31–42. ISSN: 0018-8158, 1573-5117. DOI: 10.1007/s10750-012-1246-2. (Visited on 05/06/2025).

[89] Jingshui Huang, Dietrich Borchardt, and Michael Rode. “How Do Inorganic Nitrogen Processing Pathways Change Quantitatively at Daily, Seasonal, and Multiannual Scales in a Large Agricultural Stream?” In: *Hydrology and Earth System Sciences* 26.22 (Nov. 2022), pp. 5817–5833. ISSN: 1607-7938. DOI: 10.5194/hess-26-5817-2022. (Visited on 05/06/2025).

[90] Stuart J. Khan et al. “Extreme Weather Events: Should Drinking Water Quality Management Systems Adapt to Changing Risk Profiles?” In: *Water Research* 85 (Nov. 2015), pp. 124–136. ISSN: 00431354. DOI: 10.1016/j.watres.2015.08.018. (Visited on 05/06/2025).

[91] E. Baurès et al. “Variation of Organic Carbon and Nitrate with River Flow within an Oceanic Regime in a Rural Area and Potential Impacts for Drinking Water Production”. In: *Journal of Hydrology* 477 (Jan. 2013), pp. 86–93. ISSN: 00221694. DOI: 10.1016/j.jhydrol.2012.11.006. (Visited on 05/06/2025).

[92] H. P. Jarvie et al. “Nutrient Water Quality of the Wye Catchment, UK: Exploring Patterns and Fluxes Using the Environment Agency Data Archives”. In: *Hydrology and Earth System Sciences* 7.5 (Oct. 2003), pp. 722–743. ISSN: 1607-7938. DOI: 10.5194/hess-7-722-2003. (Visited on 05/06/2025).

[93] M.T.H. Van Vliet and J.J.G. Zwolsman. “Impact of Summer Droughts on the Water Quality of the Meuse River”. In: *Journal of Hydrology* 353.1-2 (May 2008), pp. 1–17. ISSN: 00221694. DOI: 10.1016/j.jhydrol.2008.01.001. (Visited on 05/06/2025).

[94] Mei Han et al. “The Genetics of Nitrogen Use Efficiency in Crop Plants”. In: *Annual Review of Genetics* 49.1 (Nov. 2015), pp. 269–289. ISSN: 0066-4197, 1545-2948. DOI: 10.1146/annurev-genet-112414-055037. (Visited on 05/06/2025).

[95] Hayat Ullah et al. “Improving Water Use Efficiency, Nitrogen Use Efficiency, and Radiation Use Efficiency in Field Crops under Drought Stress: A Review”. In: *Advances in Agronomy*. Vol. 156. Elsevier, 2019, pp. 109–157. ISBN: 978-0-12-817598-9. DOI: 10.1016/bs.agron.2019.02.002. (Visited on 05/06/2025).

[96] Carolin Winter et al. *Droughts Can Reduce the Nitrogen Retention Capacity of Catchments*. May 2022. DOI: 10.1002/essoar.10511446.2. (Visited on 05/06/2025).

[97] Sonja Leitner et al. “Legacy Effects of Drought on Nitrate Leaching in a Temperate Mixed Forest on Karst”. In: *Journal of Environmental Management* 262 (May 2020), p. 110338. ISSN: 03014797. DOI: 10.1016/j.jenvman.2020.110338. (Visited on 05/06/2025).

[98] F. N. Outram et al. “High-Frequency Monitoring of Nitrogen and Phosphorus Response in Three Rural Catchments to the End of the 2011–2012 Drought in England”. In: *Hydrology and Earth System Sciences* 18.9 (Sept. 2014), pp. 3429–3448. ISSN: 1607-7938. DOI: 10.5194/hess-18-3429-2014. (Visited on 05/06/2025).

[99] M.D. Morecroft et al. “Effects of the 1995–1997 Drought on Nitrate Leaching in Lowland England”. In: *Soil Use and Management* 16.2 (June 2000), pp. 117–123. ISSN: 0266-0032, 1475-2743. DOI: 10.1111/j.1475-2743.2000.tb00186.x. (Visited on 05/06/2025).

[100] Tim P. Burt and Fred Worrall. “Stream Nitrate Levels in a Small Catchment in South West England over a Period of 35 Years (1970–2005)”. In: *Hydrological Processes* 23.14 (July 2009), pp. 2056–2068. ISSN: 0885-6087, 1099-1085. DOI: 10.1002/hyp.7314. (Visited on 05/06/2025).

[101] Karuna Jutglar et al. “Post-drought Increase in Regional-scale Groundwater Nitrate in Southwest Germany”. In: *Hydrological Processes* 35.8 (Aug. 2021), e14307. ISSN: 0885-6087, 1099-1085. DOI: 10.1002/hyp.14307. (Visited on 05/06/2025).

[102] Peter C. Van Metre et al. “High Nitrate Concentrations in Some Midwest United States Streams in 2013 after the 2012 Drought”. In: *Journal of Environmental Quality* 45.5 (Sept. 2016), pp. 1696–1704. ISSN: 0047-2425, 1537-2537. DOI: 10.2134/jeq2015.12.0591. (Visited on 05/06/2025).

[103] Pia Ebeling et al. *Water Quality, Discharge and Catchment Attributes for Large-Sample Studies in Germany – QUADICA*. Mar. 2022. DOI: 10.5194/essd-2022-6. (Visited on 05/06/2025).

[104] Manuela I Brunner et al. “Increasing Importance of Temperature as a Contributor to the Spatial Extent of Streamflow Drought”. In: *Environmental Research Letters* 16.2 (Feb. 2021), p. 024038. ISSN: 1748-9326. DOI: 10.1088/1748-9326/abd2f0. (Visited on 05/06/2025).

[105] Behzad Ahmadi, Ali Ahmadalipour, and Hamid Moradkhani. “Hydrological Drought Persistence and Recovery over the CONUS: A Multi-Stage Framework Considering Water Quantity and Quality”. In: *Water Research* 150 (Mar. 2019), pp. 97–110. ISSN: 00431354. DOI: 10.1016/j.watres.2018.11.052. (Visited on 05/06/2025).

[106] William H. Kruskal and W. Allen Wallis. "Use of Ranks in One-Criterion Variance Analysis". In: *Journal of the American Statistical Association* 47.260 (Dec. 1952), pp. 583–621. ISSN: 0162-1459, 1537-274X. DOI: 10.1080/01621459.1952.10483441. (Visited on 05/06/2025).

[107] Rémi Dupas et al. "Long-Term Nitrogen Retention and Transit Time Distribution in Agricultural Catchments in Western France". In: *Environmental Research Letters* 15.11 (Nov. 2020), p. 115011. ISSN: 1748-9326. DOI: 10.1088/1748-9326/abbe47. (Visited on 05/06/2025).

[108] A. Musolff et al. "Spatio-Temporal Controls of Dissolved Organic Carbon Stream Water Concentrations". In: *Journal of Hydrology* 566 (Nov. 2018), pp. 205–215. ISSN: 00221694. DOI: 10.1016/j.jhydrol.2018.09.011. (Visited on 05/06/2025).

[109] Sophie Ehrhardt et al. "Nitrate Transport and Retention in Western European Catchments Are Shaped by Hydroclimate and Subsurface Properties". In: *Water Resources Research* 57.10 (Oct. 2021), e2020WR029469. ISSN: 0043-1397, 1944-7973. DOI: 10.1029/2020WR029469. (Visited on 05/06/2025).

[110] Eva Sinha and Anna M. Michalak. "Precipitation Dominates Interannual Variability of Riverine Nitrogen Loading across the Continental United States". In: *Environmental Science & Technology* 50.23 (Dec. 2016), pp. 12874–12884. ISSN: 0013-936X, 1520-5851. DOI: 10.1021/acs.est.6b04455. (Visited on 05/06/2025).

[111] H. M. Johnson and E. G. Stets. "Nitrate in Streams During Winter Low-Flow Conditions as an Indicator of Legacy Nitrate". In: *Water Resources Research* 56.11 (Nov. 2020), e2019WR026996. ISSN: 0043-1397, 1944-7973. DOI: 10.1029/2019WR026996. (Visited on 05/06/2025).

[112] Andreas Hartmann et al. "Risk of Groundwater Contamination Widely Underestimated Because of Fast Flow into Aquifers". In: *Proceedings of the National Academy of Sciences* 118.20 (May 2021), e2024492118. ISSN: 0027-8424, 1091-6490. DOI: 10.1073/pnas.2024492118. (Visited on 05/06/2025).

[113] Masooma Batool et al. "Long-Term Annual Soil Nitrogen Surplus across Europe (1850–2019)". In: *Scientific Data* 9.1 (Oct. 2022), p. 612. ISSN: 2052-4463. DOI: 10.1038/s41597-022-01693-9. (Visited on 05/06/2025).

[114] K. D'Haene et al. "Spatial Distribution of the Relationship between Nitrate Residues in Soil and Surface Water Quality Revealed through Attenuation Factors". In: *Agriculture, Ecosystems & Environment* 330 (June 2022), p. 107889. ISSN: 01678809. DOI: 10.1016/j.agee.2022.107889. (Visited on 05/06/2025).

[115] L. E. Koenig et al. "Deconstructing the Effects of Flow on DOC, Nitrate, and Major Ion Interactions Using a High-Frequency Aquatic Sensor Network". In: *Water Resources Research* 53.12 (Dec. 2017), pp. 10655–10673. ISSN: 0043-1397, 1944-7973. DOI: 10.1002/2017WR020739. (Visited on 05/06/2025).

[116] Alban De Lavenne et al. “Quantifying Multi-Year Hydrological Memory with Catchment Forgetting Curves”. In: *Hydrology and Earth System Sciences* 26.10 (May 2022), pp. 2715–2732. ISSN: 1607-7938. DOI: 10.5194/hess-26-2715-2022. (Visited on 05/06/2025).

[117] P. G. Whitehead et al. “A Review of the Potential Impacts of Climate Change on Surface Water Quality”. In: *Hydrological Sciences Journal* 54.1 (Feb. 2009), pp. 101–123. ISSN: 0262-6667, 2150-3435. DOI: 10.1623/hysj.54.1.101. (Visited on 05/06/2025).

[118] Amy T. Hansen et al. “Contribution of Wetlands to Nitrate Removal at the Watershed Scale”. In: *Nature Geoscience* 11.2 (Feb. 2018), pp. 127–132. ISSN: 1752-0894, 1752-0908. DOI: 10.1038/s41561-017-0056-6. (Visited on 05/06/2025).

[119] Lorna J. Cole, Jenni Stockan, and Rachel Helliwell. “Managing Riparian Buffer Strips to Optimise Ecosystem Services: A Review”. In: *Agriculture, Ecosystems & Environment* 296 (July 2020), p. 106891. ISSN: 01678809. DOI: 10.1016/j.agee.2020.106891. (Visited on 05/06/2025).

[120] Brian E. Lapointe et al. “Nitrogen Enrichment, Altered Stoichiometry, and Coral Reef Decline at Looe Key, Florida Keys, USA: A 3-Decade Study”. In: *Marine Biology* 166.8 (Aug. 2019), p. 108. ISSN: 0025-3162, 1432-1793. DOI: 10.1007/s00227-019-3538-9. (Visited on 05/06/2025).

[121] H. J. M. Van Grinsven et al. “Management, Regulation and Environmental Impacts of Nitrogen Fertilization in Northwestern Europe under the Nitrates Directive; a Benchmark Study”. In: *Biogeosciences* 9.12 (Dec. 2012), pp. 5143–5160. ISSN: 1726-4189. DOI: 10.5194/bg-9-5143-2012. (Visited on 05/06/2025).

[122] Anthony J. Tesoriero et al. “Vulnerability of Streams to Legacy Nitrate Sources”. In: *Environmental Science & Technology* 47.8 (Apr. 2013), pp. 3623–3629. ISSN: 0013-936X, 1520-5851. DOI: 10.1021/es305026x. (Visited on 05/06/2025).

[123] M.Z. Bieroza et al. “The Concentration-Discharge Slope as a Tool for Water Quality Management”. In: *Science of The Total Environment* 630 (July 2018), pp. 738–749. ISSN: 00489697. DOI: 10.1016/j.scitotenv.2018.02.256. (Visited on 05/06/2025).

[124] Michael J. Bowes et al. “Identifying Priorities for Nutrient Mitigation Using River Concentration–Flow Relationships: The Thames Basin, UK”. In: *Journal of Hydrology* 517 (Sept. 2014), pp. 1–12. ISSN: 00221694. DOI: 10.1016/j.jhydrol.2014.03.063. (Visited on 05/06/2025).

[125] Sarah E. Godsey, James W. Kirchner, and David W. Clow. “Concentration–Discharge Relationships Reflect Chemostatic Characteristics of US Catchments”. In: *Hydrological Processes* 23.13 (June 2009), pp. 1844–1864. ISSN: 0885-6087, 1099-1085. DOI: 10.1002/hyp.7315. (Visited on 05/06/2025).

[126] Rémi Dupas et al. “Distribution of Landscape Units Within Catchments Influences Nutrient Export Dynamics”. In: *Frontiers in Environmental Science* 7 (Apr. 2019), p. 43. ISSN: 2296-665X. DOI: 10.3389/fenvs.2019.00043. (Visited on 05/06/2025).

[127] Wei Zhi et al. “Distinct Source Water Chemistry Shapes Contrasting Concentration-Discharge Patterns”. In: *Water Resources Research* 55.5 (May 2019), pp. 4233–4251. ISSN: 0043-1397, 1944-7973. DOI: 10.1029/2018WR024257. (Visited on 05/06/2025).

[128] J. Seibert et al. “Linking Soil- and Stream-Water Chemistry Based on a Riparian Flow-Concentration Integration Model”. In: *Hydrology and Earth System Sciences* 13.12 (Dec. 2009), pp. 2287–2297. ISSN: 1607-7938. DOI: 10.5194/hess-13-2287-2009. (Visited on 05/06/2025).

[129] Patrick J. Mulholland et al. “Stream Denitrification across Biomes and Its Response to Anthropogenic Nitrate Loading”. In: *Nature* 452.7184 (Mar. 2008), pp. 202–205. ISSN: 0028-0836, 1476-4687. DOI: 10.1038/nature06686. (Visited on 05/06/2025).

[130] Paolo Benettin, Ophélie Fovet, and Li Li. “Nitrate Removal and Young Stream Water Fractions at the Catchment Scale”. In: *Hydrological Processes* 34.12 (June 2020), pp. 2725–2738. ISSN: 0885-6087, 1099-1085. DOI: 10.1002/hyp.13781. (Visited on 05/06/2025).

[131] Scott F. Korom et al. “Aquifer Denitrification and in Situ Mesocosms: Modeling Electron Donor Contributions and Measuring Rates”. In: *Journal of Hydrology* 432–433 (Apr. 2012), pp. 112–126. ISSN: 00221694. DOI: 10.1016/j.jhydrol.2012.02.023. (Visited on 05/06/2025).

[132] F. Ortmeyer et al. “Comparison of Denitrification Induced by Various Organic Substances—Reaction Rates, Microbiology, and Temperature Effect”. In: *Water Resources Research* 57.11 (Nov. 2021), e2021WR029793. ISSN: 0043-1397, 1944-7973. DOI: 10.1029/2021WR029793. (Visited on 05/06/2025).

[133] Denis Curtin, Michael H. Beare, and Guillermo Hernandez-Ramirez. “Temperature and Moisture Effects on Microbial Biomass and Soil Organic Matter Mineralization”. In: *Soil Science Society of America Journal* 76.6 (Nov. 2012), pp. 2055–2067. ISSN: 0361-5995, 1435-0661. DOI: 10.2136/sssaj2012.0011. (Visited on 05/06/2025).

[134] Lidwien S.C. Vervloet et al. “Delay in Catchment Nitrogen Load to Streams Following Restrictions on Fertilizer Application”. In: *Science of The Total Environment* 627 (June 2018), pp. 1154–1166. ISSN: 00489697. DOI: 10.1016/j.scitotenv.2018.01.255. (Visited on 05/06/2025).

[135] S. E. Thompson et al. “Relative Dominance of Hydrologic versus Biogeochemical Factors on Solute Export across Impact Gradients”. In: *Water Resources Research* 47.10 (Oct. 2011), 2010WR009605. ISSN: 0043-1397, 1944-7973. DOI: 10.1029/2010WR009605. (Visited on 05/06/2025).

[136] A. Musolff et al. “Spatial and Temporal Variability in Concentration-Discharge Relationships at the Event Scale”. In: *Water Resources Research* 57.10 (Oct. 2021), e2020WR029442. ISSN: 0043-1397, 1944-7973. DOI: 10.1029/2020WR029442. (Visited on 05/06/2025).

[137] Ina Pohle et al. “A Framework for Assessing Concentration-Discharge Catchment Behavior From Low-Frequency Water Quality Data”. In: *Water Resources Research* 57.9 (Sept. 2021), e2021WR029692. ISSN: 0043-1397, 1944-7973. DOI: 10.1029/2021WR029692. (Visited on 05/06/2025).

[138] C.E.M. Lloyd et al. “Using Hysteresis Analysis of High-Resolution Water Quality Monitoring Data, Including Uncertainty, to Infer Controls on Nutrient and Sediment Transfer in Catchments”. In: *Science of The Total Environment* 543 (Feb. 2016), pp. 388–404. ISSN: 00489697. DOI: 10.1016/j.scitotenv.2015.11.028. (Visited on 05/06/2025).

[139] Galen Gorski and Margaret A. Zimmer. “Hydrologic Regimes Drive Nitrate Export Behavior in Human-Impacted Watersheds”. In: *Hydrology and Earth System Sciences* 25.3 (Mar. 2021), pp. 1333–1345. ISSN: 1607-7938. DOI: 10.5194/hess-25-1333-2021. (Visited on 05/06/2025).

[140] Ian Cartwright. “Concentration vs. Streamflow (C-Q) Relationships of Major Ions in South-Eastern Australian Rivers: Sources and Fluxes of Inorganic Ions and Nutrients”. In: *Applied Geochemistry* 120 (Sept. 2020), p. 104680. ISSN: 08832927. DOI: 10.1016/j.apgeochem.2020.104680. (Visited on 05/06/2025).

[141] Jacob S. Diamond and Matthew J. Cohen. “Complex Patterns of Catchment Solute–Discharge Relationships for Coastal Plain Rivers”. In: *Hydrological Processes* 32.3 (Jan. 2018), pp. 388–401. ISSN: 0885-6087, 1099-1085. DOI: 10.1002/hyp.11424. (Visited on 05/06/2025).

[142] N. J. Casson, M. C. Eimers, and S. A. Watmough. “Sources of Nitrate Export during Rain-on-Snow Events at Forested Catchments”. In: *Biogeochemistry* 120.1-3 (Aug. 2014), pp. 23–36. ISSN: 0168-2563, 1573-515X. DOI: 10.1007/s10533-013-9850-4. (Visited on 05/06/2025).

[143] C. Martin et al. “Seasonal and Interannual Variations of Nitrate and Chloride in Stream Waters Related to Spatial and Temporal Patterns of Groundwater Concentrations in Agricultural Catchments”. In: *Hydrological Processes* 18.7 (May 2004), pp. 1237–1254. ISSN: 0885-6087, 1099-1085. DOI: 10.1002/hyp.1395. (Visited on 05/06/2025).

[144] T.L. Veith, H.E. Preisendanz, and K.R. Elkin. “Characterizing Transport of Natural and Anthropogenic Constituents in a Long-Term Agricultural Watershed in the Northeastern United States”. In: *Journal of Soil and Water Conservation* 75.3 (May 2020), pp. 319–329. ISSN: 0022-4561, 1941-3300. DOI: 10.2489/jswc.75.3.319. (Visited on 05/06/2025).

[145] Stella Guillemot et al. “Spatio-Temporal Controls of C–N–P Dynamics across Headwater Catchments of a Temperate Agricultural Region from Public Data Analysis”. In: *Hydrology and Earth System Sciences* 25.5 (May 2021), pp. 2491–2511. ISSN: 1607-7938. DOI: 10.5194/hess-25-2491-2021. (Visited on 05/06/2025).

[146] Jana Von Freyberg et al. “Implications of Hydrologic Connectivity between Hillslopes and Riparian Zones on Streamflow Composition”. In: *Journal of Contaminant Hydrology*

169 (Nov. 2014), pp. 62–74. ISSN: 01697722. DOI: 10.1016/j.jconhyd.2014.07.005. (Visited on 05/06/2025).

[147] Carlos J. Ocampo, Murugesu Sivapalan, and Carolyn Oldham. "Hydrological Connectivity of Upland-Riparian Zones in Agricultural Catchments: Implications for Runoff Generation and Nitrate Transport". In: *Journal of Hydrology* 331.3-4 (Dec. 2006), pp. 643–658. ISSN: 00221694. DOI: 10.1016/j.jhydrol.2006.06.010. (Visited on 05/06/2025).

[148] Marc Stieglitz et al. "An Approach to Understanding Hydrologic Connectivity on the Hillslope and the Implications for Nutrient Transport". In: *Global Biogeochemical Cycles* 17.4 (Dec. 2003), 2003GB002041. ISSN: 0886-6236, 1944-9224. DOI: 10.1029/2003GB002041. (Visited on 05/06/2025).

[149] Theresa Blume, Erwin Zehe, and Axel Bronstert. "Rainfall—Runoff Response, Event-Based Runoff Coefficients and Hydrograph Separation". In: *Hydrological Sciences Journal* 52.5 (Oct. 2007), pp. 843–862. ISSN: 0262-6667, 2150-3435. DOI: 10.1623/hysj.52.5.843. (Visited on 05/06/2025).

[150] Andreas Musolff. *WQQDB - Water Quality and Quantity Data Base Germany: Metadata*. Feb. 2020. DOI: 10.4211/hs.a42addcbd59a466a9aa56472dfef8721. (Visited on 05/06/2025).

[151] Monika Rauthe et al. "A Central European Precipitation Climatology Part I: Generation and Validation of a High-Resolution Gridded Daily Data Set (HYRAS)". In: *Meteorologische Zeitschrift* 22.3 (July 2013), pp. 235–256. ISSN: 0941-2948. DOI: 10.1127/0941-2948/2013/0436. (Visited on 05/06/2025).

[152] Luis Samaniego, Rohini Kumar, and Sabine Attinger. "Multiscale Parameter Regionalization of a Grid-based Hydrologic Model at the Mesoscale". In: *Water Resources Research* 46.5 (May 2010), 2008WR007327. ISSN: 0043-1397, 1944-7973. DOI: 10.1029/2008WR007327. (Visited on 05/06/2025).

[153] R. Kumar, B. Livneh, and L. Samaniego. "Toward Computationally Efficient Large-Scale Hydrologic Predictions with a Multiscale Regionalization Scheme: LARGE-SCALE HYDROLOGIC PREDICTIONS". In: *Water Resources Research* 49.9 (Sept. 2013), pp. 5700–5714. ISSN: 00431397. DOI: 10.1002/wrcr.20431. (Visited on 05/06/2025).

[154] Matthias Zink et al. "A High-Resolution Dataset of Water Fluxes and States for Germany Accounting for Parametric Uncertainty". In: *Hydrology and Earth System Sciences* 21.3 (Mar. 2017), pp. 1769–1790. ISSN: 1607-7938. DOI: 10.5194/hess-21-1769-2017. (Visited on 05/06/2025).

[155] P. Branco, L. Torgo, and R. Ribeiro. *A Survey of Predictive Modelling under Imbalanced Distributions*. arXiv preprint arXiv:1505.01658. 2015.

[156] Jie Yang et al. "Exploring the Dynamics of Transit Times and Subsurface Mixing in a Small Agricultural Catchment". In: *Water Resources Research* 54.3 (Mar. 2018), pp. 2317–2335. ISSN: 0043-1397, 1944-7973. DOI: 10.1002/2017WR021896. (Visited on 05/06/2025).

[157] Zhufeng Fang et al. “Streamflow Partitioning and Transit Time Distribution in Snow-Dominated Basins as a Function of Climate”. In: *Journal of Hydrology* 570 (Mar. 2019), pp. 726–738. ISSN: 00221694. DOI: 10.1016/j.jhydrol.2019.01.029. (Visited on 05/06/2025).

[158] Stefanie R. Lutz et al. “How Important Is Denitrification in Riparian Zones? Combining End-Member Mixing and Isotope Modeling to Quantify Nitrate Removal from Riparian Groundwater”. In: *Water Resources Research* 56.1 (Jan. 2020), e2019WR025528. ISSN: 0043-1397, 1944-7973. DOI: 10.1029/2019WR025528. (Visited on 05/06/2025).

[159] Carolin Winter et al. *Explaining the Variability in High-Frequency Nitrate Export Patterns Using Long-Term Hydrological Event Classification*. Aug. 2021. DOI: 10.1002/essoar.10507676.1. (Visited on 05/06/2025).

[160] Brian L. McGlynn and Jan Seibert. “Distributed Assessment of Contributing Area and Riparian Buffering along Stream Networks”. In: *Water Resources Research* 39.4 (Apr. 2003), 2002WR001521. ISSN: 0043-1397, 1944-7973. DOI: 10.1029/2002WR001521. (Visited on 05/06/2025).

[161] Sergi Sabater et al. “Nitrogen Removal by Riparian Buffers along a European Climatic Gradient: Patterns and Factors of Variation”. In: *Ecosystems* 6.1 (Jan. 2003), pp. 0020–0030. ISSN: 1432-9840. DOI: 10.1007/s10021-002-0183-8. (Visited on 05/06/2025).

[162] Marc Schwientek, Karsten Osenbrück, and Matthias Fleischer. “Investigating Hydrological Drivers of Nitrate Export Dynamics in Two Agricultural Catchments in Germany Using High-Frequency Data Series”. In: *Environmental Earth Sciences* 69.2 (May 2013), pp. 381–393. ISSN: 1866-6280, 1866-6299. DOI: 10.1007/s12665-013-2322-2. (Visited on 05/06/2025).

[163] Judah Cohen, Hengchun Ye, and Justin Jones. “Trends and Variability in Rain-on-snow Events”. In: *Geophysical Research Letters* 42.17 (Sept. 2015), pp. 7115–7122. ISSN: 0094-8276, 1944-8007. DOI: 10.1002/2015GL065320. (Visited on 05/06/2025).

[164] R. Kunkel et al. “Groundwater-Borne Nitrate Intakes into Surface Waters in Germany”. In: *Water Science and Technology* 49.3 (Feb. 2004), pp. 11–19. ISSN: 0273-1223, 1996-9732. DOI: 10.2166/wst.2004.0152. (Visited on 05/06/2025).

[165] F. Wendland et al. “European Aquifer Typology: A Practical Framework for an Overview of Major Groundwater Composition at European Scale”. In: *Environmental Geology* 55.1 (July 2008), pp. 77–85. ISSN: 0943-0105, 1432-0495. DOI: 10.1007/s00254-007-0966-5. (Visited on 05/06/2025).

[166] O. Fovet et al. “Seasonal Variability of Stream Water Quality Response to Storm Events Captured Using High-Frequency and Multi-Parameter Data”. In: *Journal of Hydrology* 559 (Apr. 2018), pp. 282–293. ISSN: 00221694. DOI: 10.1016/j.jhydrol.2018.02.040. (Visited on 05/06/2025).

[167] P. Arias et al. *Climate Change 2021: The Physical Science Basis. Contribution of Working Group I to the Sixth Assessment Report of the Intergovernmental Panel on Climate Change, Technical Summary*. Tech. rep. Last accessed: 8 December 2022.

Intergovernmental Panel on Climate Change, 2021. URL: https://www.ipcc.ch/report/ar6/wg1/.

[168] A. Fontrodona Bach et al. "Widespread and Accelerated Decrease of Observed Mean and Extreme Snow Depth Over Europe". In: *Geophysical Research Letters* 45.22 (Nov. 2018). ISSN: 0094-8276, 1944-8007. DOI: 10.1029/2018GL079799. (Visited on 05/06/2025).

[169] Steven C. Chan et al. "Europe-Wide Precipitation Projections at Convection Permitting Scale with the Unified Model". In: *Climate Dynamics* 55.3-4 (Aug. 2020), pp. 409–428. ISSN: 0930-7575, 1432-0894. DOI: 10.1007/s00382-020-05192-8. (Visited on 05/06/2025).

[170] Mateusz Taszarek, Sebastian Kendzierski, and Natalia Pilguj. "Hazardous Weather Affecting European Airports: Climatological Estimates of Situations with Limited Visibility, Thunderstorm, Low-Level Wind Shear and Snowfall from ERA5". In: *Weather and Climate Extremes* 28 (June 2020), p. 100243. ISSN: 22120947. DOI: 10.1016/j.wace.2020.100243. (Visited on 05/06/2025).

[171] Aiguo Dai, Kevin E. Trenberth, and Taotao Qian. "A Global Dataset of Palmer Drought Severity Index for 1870–2002: Relationship with Soil Moisture and Effects of Surface Warming". In: *Journal of Hydrometeorology* 5.6 (Dec. 2004), pp. 1117–1130. ISSN: 1525-7541, 1525-755X. DOI: 10.1175/JHM-386.1. (Visited on 05/06/2025).

[172] Larisa Tarasova. *Classified Runoff Events*. Dec. 2019. DOI: 10.5281/ZENODO.3575024. (Visited on 05/06/2025).

[173] D. K. Byrnes, K. J. Van Meter, and N. B. Basu. "Long-Term Shifts in U.S. Nitrogen Sources and Sinks Revealed by the New TREND-Nitrogen Data Set (1930–2017)". In: *Global Biogeochemical Cycles* 34.9 (2020), e2020GB006626. ISSN: 1944-9224. DOI: 10.1029/2020GB006626. (Visited on 11/14/2024).

[174] William H. Schlesinger. "On the Fate of Anthropogenic Nitrogen". In: *Proceedings of the National Academy of Sciences* 106.1 (Jan. 2009), pp. 203–208. DOI: 10.1073/pnas.0810193105. (Visited on 11/14/2024).

[175] K. J. Van Meter and N. B. Basu. "Time Lags in Watershed-Scale Nutrient Transport: An Exploration of Dominant Controls". In: *Environmental Research Letters* 12.8 (Aug. 2017), p. 084017. ISSN: 1748-9326. DOI: 10.1088/1748-9326/aa7bf4. (Visited on 11/18/2021).

[176] Neil Dubrovsky et al. "The Quality of Our Nation's Waters—Nutrients in the Nation's Streams and Groundwater, 1992–2004". In: *The quality of our Nation's waters-nutrients in the Nation's streams and groundwater* (Jan. 2010).

[177] A. L. Heathwaite, P. F. Quinn, and C. J. M. Hewett. "Modelling and Managing Critical Source Areas of Diffuse Pollution from Agricultural Land Using Flow Connectivity Simulation". In: *Journal of Hydrology*. Nutirent Mobility within River Basins: A European Perspective 304.1 (Mar. 2005), pp. 446–461. ISSN: 0022-1694. DOI: 10.1016/j.jhydrol.2004.07.043. (Visited on 10/07/2024).

[178] Y. van der Velde et al. “Nitrate Response of a Lowland Catchment: On the Relation between Stream Concentration and Travel Time Distribution Dynamics”. In: *Water Resources Research* 46.11 (2010). ISSN: 1944-7973. DOI: 10.1029/2010WR009105. (Visited on 11/15/2024).

[179] Andreas Musolff et al. “Forest Dieback Alters Nutrient Pathways in a Temperate Headwater Catchment”. In: *Hydrological Processes* 38.10 (2024), e15308. ISSN: 1099-1085. DOI: 10.1002/hyp.15308. (Visited on 02/14/2025).

[180] Louise J. Bracken et al. “Sediment Connectivity: A Framework for Understanding Sediment Transfer at Multiple Scales”. In: *Earth Surface Processes and Landforms* 40.2 (2015), pp. 177–188. ISSN: 1096-9837. DOI: 10.1002/esp.3635. (Visited on 10/07/2024).

[181] Jeffrey J. McDonnell. “Where Does Water Go When It Rains? Moving beyond the Variable Source Area Concept of Rainfall-Runoff Response”. In: *Hydrological Processes* 17.9 (2003), pp. 1869–1875. ISSN: 1099-1085. DOI: 10.1002/hyp.5132. (Visited on 02/14/2025).

[182] Tailin Li et al. “Assessing Spatial Soil Moisture Patterns at a Small Agricultural Catchment”. In: *2021 IEEE International Workshop on Metrology for Agriculture and Forestry (MetroAgriFor)*. Nov. 2021, pp. 279–284. DOI: 10.1109/MetroAgriFor52389.2021.9628588. (Visited on 10/14/2024).

[183] E. Racchetti et al. “Influence of Hydrological Connectivity of Riverine Wetlands on Nitrogen Removal via Denitrification”. In: *Biogeochemistry* 103.1 (Apr. 2011), pp. 335–354. ISSN: 1573-515X. DOI: 10.1007/s10533-010-9477-7. (Visited on 10/10/2024).

[184] N. R. Finkler et al. “Riparian Land Use and Hydrological Connectivity Influence Nutrient Retention in Tropical Rivers Receiving Wastewater Treatment Plant Discharge”. In: *Frontiers in Environmental Science* 9 (Sept. 2021). ISSN: 2296-665X. DOI: 10.3389/fenvs.2021.709922. (Visited on 10/10/2024).

[185] Catherine M. Pringle. “Hydrologic Connectivity and the Management of Biological Reserves: A Global Perspective”. In: *Ecological Applications* 11.4 (2001), pp. 981–998. ISSN: 1939-5582. DOI: 10.1890/1051-0761(2001)011[0981:HCATMO]2.0.CO;2. (Visited on 10/10/2024).

[186] Günter Blöschl et al. “Twenty-Three Unsolved Problems in Hydrology (UPH) – a Community Perspective”. In: *Hydrological Sciences Journal/Journal des Sciences Hydrologiques* 64 (June 2019), pp. 1141–1158. DOI: 10.1080/02626667.2019.1620507.

[187] Felipe A. Saavedra et al. “Disentangling Scatter in Long-Term Concentration–Discharge Relationships: The Role of Event Types”. In: *Hydrology and Earth System Sciences* 26.23 (Dec. 2022), pp. 6227–6245. ISSN: 1027-5606. DOI: 10.5194/hess-26-6227-2022. (Visited on 12/15/2022).

[188] Shannon L. Speir et al. “Catchment Concentration–Discharge Relationships across Temporal Scales: A Review”. In: *WIREs Water* 11.2 (2024), e1702. ISSN: 2049-1948. DOI: 10.1002/wat2.1702. (Visited on 11/18/2024).

[189] H. J. Tromp-van Meerveld and J. J. McDonnell. "On the Interrelations between Topography, Soil Depth, Soil Moisture, Transpiration Rates and Species Distribution at the Hillslope Scale". In: *Advances in Water Resources*. Experimental Hydrology: A Bright Future 29.2 (Feb. 2006), pp. 293–310. ISSN: 0309-1708. DOI: 10.1016/j.advwatres.2005.02.016. (Visited on 12/05/2024).

[190] Rodger Grayson and Andrew Western. "Terrain and the Distribution of Soil Moisture". In: *Hydrological Processes* 15.13 (2001), pp. 2689–2690. ISSN: 1099-1085. DOI: 10.1002/hyp.479. (Visited on 12/05/2024).

[191] Dara Entekhabi et al. "The Soil Moisture Active Passive (SMAP) Mission". In: *Proceedings of the IEEE* 98.5 (May 2010), pp. 704–716. ISSN: 1558-2256. DOI: 10.1109/JPROC.2010.2043918. (Visited on 01/20/2025).

[192] Karianne J. Bergen et al. "Machine Learning for Data-Driven Discovery in Solid Earth Geoscience". In: *Science* 363.6433 (Mar. 2019), eaau0323. DOI: 10.1126/science.aau0323. (Visited on 10/07/2024).

[193] Zhenyu Wang et al. "Filling in Missing Pieces in the Co-Development of Artificial Intelligence and Environmental Science". In: *The Innovation Geoscience* 1.1 (Sun May 28 00:00:00 CST 2023), pp. 100007–2. ISSN: 2959-8753. DOI: 10.59717/j.xinngeo.2023.100007. (Visited on 09/14/2023).

[194] Shijie Jiang et al. "How Interpretable Machine Learning Can Benefit Process Understanding in the Geosciences". In: *Earth's Future* 12.7 (2024), e2024EF004540. ISSN: 2328-4277. DOI: 10.1029/2024EF004540. (Visited on 07/19/2024).

[195] Pia Ebeling et al. "Archetypes and Controls of Riverine Nutrient Export Across German Catchments". In: *Water Resources Research* 57.4 (2021), e2020WR028134. ISSN: 1944-7973. DOI: 10.1029/2020WR028134. (Visited on 07/15/2021).

[196] Kayalvizhi Sadayappan et al. "Nitrate Concentrations Predominantly Driven by Human, Climate, and Soil Properties in US Rivers". In: *Water Research* 226 (Nov. 2022), p. 119295. ISSN: 0043-1354. DOI: 10.1016/j.watres.2022.119295. (Visited on 10/08/2024).

[197] Gourab Kumer Saha et al. "A Deep Learning-Based Novel Approach to Generate Continuous Daily Stream Nitrate Concentration for Nitrate Data-Sparse Watersheds". In: *Science of The Total Environment* 878 (June 2023), p. 162930. ISSN: 0048-9697. DOI: 10.1016/j.scitotenv.2023.162930. (Visited on 07/05/2023).

[198] Gourab Saha et al. "Performance Evaluation of Deep Learning Based Stream Nitrate Concentration Prediction Model to Fill Stream Nitrate Data Gaps at Low-Frequency Nitrate Monitoring Basins". In: *Journal of Environmental Management* 357 (Apr. 2024), p. 120721. ISSN: 0301-4797. DOI: 10.1016/j.jenvman.2024.120721. (Visited on 10/08/2024).

[199] T. Blume, E. Zehe, and A. Bronstert. "Use of Soil Moisture Dynamics and Patterns at Different Spatio-Temporal Scales for the Investigation of Subsurface Flow Processes". In: *Hydrology and Earth System Sciences* 13.7 (July 2009), pp. 1215–1233. ISSN: 1607-7938. DOI: 10.5194/hess-13-1215-2009. (Visited on 11/18/2024).

[200] Noemi Vergopolan et al. “SMAP-HydroBlocks, a 30-m Satellite-Based Soil Moisture Dataset for the Conterminous US”. In: *Scientific Data* 8.1 (Oct. 2021), p. 264. ISSN: 2052-4463. DOI: 10.1038/s41597-021-01050-2. (Visited on 02/28/2023).

[201] Magdalena Bieroza et al. “Advances in Catchment Science, Hydrochemistry, and Aquatic Ecology Enabled by High-Frequency Water Quality Measurements”. In: *Environmental Science & Technology* 57.12 (Mar. 2023), pp. 4701–4719. ISSN: 0013-936X. DOI: 10.1021/acs.est.2c07798. (Visited on 03/30/2023).

[202] Noemi Vergopolan et al. “Combining Hyper-Resolution Land Surface Modeling with SMAP Brightness Temperatures to Obtain 30-m Soil Moisture Estimates”. In: *Remote Sensing of Environment* 242 (June 2020), p. 111740. ISSN: 0034-4257. DOI: 10.1016/j.rse.2020.111740. (Visited on 02/15/2025).

[203] Sriram Balasubramanian and Soheil Feizi. “Towards Improved Input Masking for Convolutional Neural Networks”. In: *2023 IEEE/CVF International Conference on Computer Vision (ICCV)*. Paris, France: IEEE, Oct. 2023, pp. 1855–1865. ISBN: 9798350307184. DOI: 10.1109/ICCV51070.2023.00178. (Visited on 10/08/2024).

[204] Hyesook Son and Yun Jang. “Partial Convolutional LSTM for Spatiotemporal Prediction of Incomplete Data”. In: *IEEE Access* 8 (2020), pp. 164762–164774. ISSN: 2169-3536. DOI: 10.1109/ACCESS.2020.3022774.

[205] Bilal Alsallakh et al. *Mind the Pad – CNNs Can Develop Blind Spots*. Oct. 2020. DOI: 10.48550/arXiv.2010.02178. arXiv: 2010.02178 [cs]. (Visited on 02/15/2025).

[206] Camilo Daleles Rennó et al. “HAND, a New Terrain Descriptor Using SRTM-DEM: Mapping Terra-Firme Rainforest Environments in Amazonia”. In: *Remote Sensing of Environment* 112.9 (Sept. 2008), pp. 3469–3481. ISSN: 0034-4257. DOI: 10.1016/j.rse.2008.03.018. (Visited on 10/08/2024).

[207] S. Gharari et al. “Hydrological Landscape Classification: Investigating the Performance of HAND Based Landscape Classifications in a Central European Meso-Scale Catchment”. In: *Hydrology and Earth System Sciences* 15.11 (Nov. 2011), pp. 3275–3291. ISSN: 1027-5606. DOI: 10.5194/hess-15-3275-2011. (Visited on 10/08/2024).

[208] Ralf Loritz et al. “A Topographic Index Explaining Hydrological Similarity by Accounting for the Joint Controls of Runoff Formation”. In: *Hydrology and Earth System Sciences* 23.9 (Sept. 2019), pp. 3807–3821. ISSN: 1027-5606. DOI: 10.5194/hess-23-3807-2019. (Visited on 10/08/2024).

[209] Richard Barnes. *RichDEM: Terrain Analysis Software*. 2016. URL: http://github.com/r-barnes/richdem.

[210] James A. Falcone. *GAGES-II: Geospatial Attributes of Gages for Evaluating Streamflow*. Tech. rep. U.S. Geological Survey, 2011. DOI: 10.3133/70046617. (Visited on 02/15/2025).

[211] Xingjian Shi et al. *Convolutional LSTM Network: A Machine Learning Approach for Precipitation Nowcasting*. https://arxiv.org/abs/1506.04214v2. June 2015. (Visited on 10/08/2024).

[212] Sepp Hochreiter and Jürgen Schmidhuber. "Long Short-Term Memory". In: *Neural Computation* 9.8 (1997), pp. 1735–1780. ISSN: 1530-888X. DOI: 10.1162/neco.1997.9.8.1735.

[213] Kumar Puran Tripathy and Ashok K. Mishra. "Deep Learning in Hydrology and Water Resources Disciplines: Concepts, Methods, Applications, and Research Directions". In: *Journal of Hydrology* 628 (Jan. 2024), p. 130458. ISSN: 0022-1694. DOI: 10.1016/j.jhydrol.2023.130458. (Visited on 10/08/2024).

[214] Frederik Kratzert et al. "Towards Learning Universal, Regional, and Local Hydrological Behaviors via Machine Learning Applied to Large-Sample Datasets". In: *Hydrology and Earth System Sciences* 23.12 (Dec. 2019), pp. 5089–5110. ISSN: 1027-5606. DOI: 10.5194/hess-23-5089-2019. (Visited on 03/20/2024).

[215] Rizgar Zebari et al. "A Comprehensive Review of Dimensionality Reduction Techniques for Feature Selection and Feature Extraction". In: *Journal of Applied Science and Technology Trends* 1.1 (May 2020), pp. 56–70. ISSN: 2708-0757. DOI: 10.38094/jastt1224. (Visited on 01/21/2025).

[216] Robert Tibshirani. "Regression Shrinkage and Selection via the Lasso". In: *Journal of the Royal Statistical Society. Series B (Methodological)* 58.1 (1996), pp. 267–288. ISSN: 0035-9246. JSTOR: 2346178. (Visited on 02/15/2025).

[217] G. E. P. Box and D. R. Cox. "An Analysis of Transformations". In: *Journal of the Royal Statistical Society: Series B (Methodological)* 26.2 (1964), pp. 211–243. ISSN: 2517-6161. DOI: 10.1111/j.2517-6161.1964.tb00553.x. (Visited on 10/08/2024).

[218] Amerah Alabrah. "Scientific Elegance in NIDS: Unveiling Cardinality Reduction, Box-Cox Transformation, and ADASYN for Enhanced Intrusion Detection". In: *Computers, Materials & Continua* 79.3 (2024), pp. 3897–3912. ISSN: 1546-2226. DOI: 10.32604/cmc.2024.048528. (Visited on 10/08/2024).

[219] Luca Blum, Mohamed Elgendi, and Carlo Menon. "Impact of Box-Cox Transformation on Machine-Learning Algorithms". In: *Frontiers in Artificial Intelligence* 5 (Apr. 2022). ISSN: 2624-8212. DOI: 10.3389/frai.2022.877569. (Visited on 02/15/2025).

[220] Hoshin V. Gupta et al. "Decomposition of the Mean Squared Error and NSE Performance Criteria: Implications for Improving Hydrological Modelling". In: *Journal of Hydrology* 377.1 (Oct. 2009), pp. 80–91. ISSN: 0022-1694. DOI: 10.1016/j.jhydrol.2009.08.003. (Visited on 12/05/2024).

[221] Lutz Prechelt. "Automatic Early Stopping Using Cross Validation: Quantifying the Criteria". In: *Neural Networks* 11.4 (June 1998), pp. 761–767. ISSN: 0893-6080. DOI: 10.1016/S0893-6080(98)00010-0. (Visited on 02/15/2025).

[222] Larisa Tarasova et al. "The Value of Large-Scale Climatic Indices for Monthly Forecasting Severity of Widespread Flooding Using Dilated Convolutional Neural Networks". In: *Earth's Future* 12.2 (2024), e2023EF003680. ISSN: 2328-4277. DOI: 10.1029/2023EF003680. (Visited on 02/15/2025).

[223] P Jonathon Phillips et al. *Four Principles of Explainable Artificial Intelligence*. Tech. rep. NIST IR 8312. Gaithersburg, MD: National Institute of Standards and Technology (U.S.), Sept. 2021. DOI: 10.6028/NIST.IR.8312. (Visited on 11/22/2024).

[224] Cynthia Rudin et al. *Interpretable Machine Learning: Fundamental Principles and 10 Grand Challenges*. July 2021. DOI: 10.48550/arXiv.2103.11251. arXiv: 2103.11251 [cs]. (Visited on 02/15/2025).

[225] Lloyd S. Shapley. *Notes on the N-Person Game — II: The Value of an N-Person Game*. Tech. rep. RAND Corporation, Aug. 1951. (Visited on 02/15/2025).

[226] Scott M. Lundberg and Su-In Lee. "A Unified Approach to Interpreting Model Predictions". In: *Proceedings of the 31st International Conference on Neural Information Processing Systems*. NIPS'17. Red Hook, NY, USA: Curran Associates Inc., Dec. 2017, pp. 4768–4777. ISBN: 978-1-5108-6096-4. (Visited on 10/08/2024).

[227] Antonios Mamalakis, Elizabeth A. Barnes, and Imme Ebert-Uphoff. "Carefully Choose the Baseline: Lessons Learned from Applying XAI Attribution Methods for Regression Tasks in Geoscience". In: *Artificial Intelligence for the Earth Systems* 2.1 (Jan. 2023). ISSN: 2769-7525. DOI: 10.1175/AIES-D-22-0058.1. (Visited on 10/08/2024).

[228] Karen Simonyan, Andrea Vedaldi, and Andrew Zisserman. *Deep Inside Convolutional Networks: Visualising Image Classification Models and Saliency Maps*. Apr. 2014. DOI: 10.48550/arXiv.1312.6034. arXiv: 1312.6034 [cs]. (Visited on 11/22/2024).

[229] Fu-Jun Yue et al. "Source Availability and Hydrological Connectivity Determined Nitrate-Discharge Relationships during Rainfall Events in Karst Catchment as Revealed by High-Frequency Nitrate Sensing". In: *Water Research* 231 (Mar. 2023), p. 119616. ISSN: 00431354. DOI: 10.1016/j.watres.2023.119616. (Visited on 10/10/2024).

[230] Li Li et al. "River Water Quality Shaped by Land–River Connectivity in a Changing Climate". In: *Nature Climate Change* 14.3 (Mar. 2024), pp. 225–237. ISSN: 1758-6798. DOI: 10.1038/s41558-023-01923-x. (Visited on 04/09/2024).

[231] Caroline A. Davis et al. "Antecedent Moisture Controls on Stream Nitrate Flux in an Agricultural Watershed". In: *Journal of Environmental Quality* 43.4 (2014), pp. 1494–1503. ISSN: 1537-2537. DOI: 10.2134/jeq2013.11.0438. (Visited on 09/23/2021).

[232] Wei Zhi and Li Li. "The Shallow and Deep Hypothesis: Subsurface Vertical Chemical Contrasts Shape Nitrate Export Patterns from Different Land Uses". In: *Environmental Science & Technology* 54.19 (Oct. 2020), pp. 11915–11928. ISSN: 0013-936X. DOI: 10.1021/acs.est.0c01340. (Visited on 04/29/2022).

[233] Felipe Saavedra et al. "Winter Post-Droughts Amplify Extreme Nitrate Concentrations in German Rivers". In: *Environmental Research Letters* 19.2 (Jan. 2024), p. 024007. ISSN: 1748-9326. DOI: 10.1088/1748-9326/ad19ed. (Visited on 02/12/2024).

[234] Rémi Dupas et al. "Landscape Spatial Configuration Influences Phosphorus but Not Nitrate Concentrations in Agricultural Headwater Catchments". In: *Hydrological Processes* 37.2 (2023), e14816. ISSN: 1099-1085. DOI: 10.1002/hyp.14816. (Visited on 02/27/2023).

[235] Aleix Calsamiglia et al. "Evaluating Functional Connectivity in a Small Agricultural Catchment under Contrasting Flood Events by Using UAV". In: *Earth Surface Processes and Landforms* 45.4 (2020), pp. 800–815. ISSN: 1096-9837. DOI: 10.1002/esp.4769. (Visited on 10/10/2024).

[236] Daniel Rasche et al. "Towards Disentangling Heterogeneous Soil Moisture Patterns in Cosmic-Ray Neutron Sensor Footprints". In: *Hydrology and Earth System Sciences* 25.12 (Dec. 2021), pp. 6547–6566. ISSN: 1027-5606. DOI: 10.5194/hess-25-6547-2021. (Visited on 12/05/2024).

[237] M. Köhli et al. "Footprint Characteristics Revised for Field-Scale Soil Moisture Monitoring with Cosmic-Ray Neutrons". In: *Water Resources Research* 51.7 (2015), pp. 5772–5790. ISSN: 1944-7973. DOI: 10.1002/2015WR017169. (Visited on 12/05/2024).

[238] Joel Hestness, Newsha Ardalani, and Greg Diamos. *Beyond Human-Level Accuracy: Computational Challenges in Deep Learning*. Sept. 2019. DOI: 10.48550/arXiv.1909.01736. arXiv: 1909.01736 [cs]. (Visited on 01/23/2025).

[239] Zeyad Emam et al. *On The State of Data In Computer Vision: Human Annotations Remain Indispensable for Developing Deep Learning Models*. July 2021. DOI: 10.48550/arXiv.2108.00114. arXiv: 2108.00114 [cs]. (Visited on 01/23/2025).

[240] Jennifer W. Edmonds et al. "Using Large, Open Datasets to Understand Spatial and Temporal Patterns in Lotic Ecosystems: NEON Case Studies". In: *Ecosphere* 13.5 (2022), e4102. ISSN: 2150-8925. DOI: 10.1002/ecs2.4102. (Visited on 02/19/2025).

[241] Wei Zhi et al. "Deep Learning for Water Quality". In: *Nature Water* 2.3 (Mar. 2024), pp. 228–241. ISSN: 2731-6084. DOI: 10.1038/s44221-024-00202-z. (Visited on 04/09/2024).

[242] Wulahati Adalibieke et al. "Global Crop-Specific Nitrogen Fertilization Dataset in 1961–2020". In: *Scientific Data* 10.1 (Sept. 2023), p. 617. ISSN: 2052-4463. DOI: 10.1038/s41597-023-02526-z. (Visited on 02/19/2025).

[243] Junguo Liu et al. "A High-Resolution Assessment on Global Nitrogen Flows in Cropland". In: *Proceedings of the National Academy of Sciences of the United States of America* 107.17 (Apr. 2010), pp. 8035–8040. ISSN: 0027-8424. DOI: 10.1073/pnas.0913658107. (Visited on 02/19/2025).

[244] Noemi Vergopolan et al. *SMAP-HydroBlocks: Hyper-resolution Satellite-Based Soil Moisture over the Continental United States*. Aug. 2021. DOI: 10.5281/zenodo.5206725. (Visited on 02/19/2025).

[245] James Wickham et al. "Thematic Accuracy Assessment of the NLCD 2016 Land Cover for the Conterminous United States". In: *Remote Sensing of Environment* 257 (May 2021), p. 112357. ISSN: 00344257. DOI: 10.1016/j.rse.2021.112357. (Visited on 02/19/2025).

[246] A. Borriero et al. "The Value of Instream Stable Water Isotope and Nitrate Concentration Data for Calibrating a Travel Time-Based Water Quality Model". In: *Hydrological Processes* 38.5 (2024), e15154. ISSN: 1099-1085. DOI: 10.1002/hyp.15154. (Visited on 06/10/2025).

[247] Wei Zhi et al. “Temperature Outweighs Light and Flow as the Predominant Driver of Dissolved Oxygen in US Rivers”. In: *Nature Water* 1.3 (Mar. 2023), pp. 249–260. ISSN: 2731-6084. DOI: 10.1038/s44221-023-00038-z. (Visited on 06/10/2025).

[248] G. Gorski et al. “Stream Nitrate Dynamics Driven Primarily by Discharge and Watershed Physical and Soil Characteristics at Intensively Monitored Sites: Insights From Deep Learning”. In: *Water Resources Research* 60.9 (2024), e2023WR036591. ISSN: 1944-7973. DOI: 10.1029/2023WR036591. (Visited on 06/10/2025).